真菌由来エンド-1,4-β-キシラナーゼに関する生化学および分子遺伝学的研究

Studies on Biochemical and Molecular Characterization of Fungal Endo-1,4-β-xylanases

（真菌由来エンド-1,4-β-キシラナーゼに関する生化学および分子遺伝学的研究）

Hidenori Tanaka

2006

Contents

Acknowledgments

This research has been performed in the Laboratory of Applied and Molecular Microbiology, Department of Biochemistry and Applied Biosciences, University of Miyazaki, Miyazaki City, Japan.

I acknowledge all those who contributed to the accomplishment of this research, especially the following:

I wish to express my sincerest thanks and gratitude to my supervisor Professor Dr. Kazuyoshi Ohta for his proper guidance during my research period. I would like to have this opportunity to thank him for giving me the chance to accomplish my study. I want to thank him for his educational and technical assistance throughout the course of my graduate study. My sincerest thanks and gratitude to Professor Dr. Michio Muguruma at Department of Biochemistry and Applied Biosciences, University of Miyazaki, for his various assistances. Many thanks go to Professor Dr. Fumio Kato at Department of Applied Biological Sciences, Saga University. I would also like to thank Professor Dr. Jun-ichi Abe at Department of Biochemical Science and Technology, Kagoshima University, and Professor Dr. Sachio Hayashi at Department of Applied Chemistry, University of Miyazaki, and Associate Professor Dr. Naoto Yoshida at Department of Biochemistry and Applied Biosciences, University of Miyazaki, for their valuable advices and discussions during the study.

I am grateful to Professor Dr. Tatsuo Nakayama at Miyazaki Medical College for the N-terminal amino acid sequencing. A special thank goes to Dr. Masil Khan, JSPS Research Fellow at the Laboratory of Applied and Molecular Microbiology, University of Miyazaki, for his critical reading and grammatical correction of my dissertation.

I also wish to express my deep appreciation to Dr. Hidetoshi Akimoto, Dr. Satoshi Moriyama and Mr. Norio Suetsugu for their kindness and useful advices regarding my research, and for their friendly environment facilitated daily in the laboratory. Special thanks are given to Mr. Masato Uwataki, Mr. Takato Shige, Ms. Tomoko Okuno, Mr. Motoki Wakiyama, Mr. Toshihide Nakamura and Mr. Daisuke Yamakawa for their kind support. All members of the Laboratory of Applied and Molecular Microbiology are also gratefully acknowledged.

Last, but not least, I am deeply indebted to all my family members and relatives, especially my father Shinmei and mother Atsuko, for their constant attention and encouragement.

Abbreviations

3D	three-dimensional
A_{600}	absorbance at 600 nm
AOX1	alcohol oxidase I
DIG	digoxigenin
DP	degree of polymerization
GH	glycoside hydrolase
HIS	histidiol dehydrogenase
HPLC	high-performance liquid chromatography
IEF	isoelectric focusing
IPTG	isopropylthio-β-D-galactoside
LB	Luria-Bertani
M_r	relative molecular mass
ORF	open reading frame
PHO1	acid phosphatase
PIPES	piperazine-*N*,*N'*-bis(2-ethanesulfonic acid)
RACE	rapid amplification of cDNA ends
RBB	Remazol Brilliant Blue
RT-PCR	reverse transcription-PCR
SDS	sodium dodecyl sulfate
SDS–PAGE	sodium dodecyl sulfate–polyacrylamide gel electrophoresis
TAE	tris-acetate/EDTA electrophoresis buffer
TLC	thin-layer chromatography
YNB	yeast nitrogen base
nt	nucleotide
p*I*	isoelectric point
*p*NP	*p*-nitrophenyl
α-MF	α-mating factor

Strains and plasmids used in this study

Strain or plasmid	Relevant characteristics	Reference or source
Strains		
Escherichia coli		
INVαF'	F' *end*A1 *rec*A1 *hsd*R17 (r_k^-, m_k^+) *sup*E44 *thi*-1 *gyr*A96 *rel*A1 Φ80*lac*ZΔM15 Δ(*lac*ZYA-*arg*F)U169 λ^-	Invitrogen
TOP10	F^- *mcr*A Δ(*mrr-hsd*RMS-*mcr*BC) Φ80*lac*ZΔM15Δ*lac*X74 *rec*A1 *deo*R *ara*D139 Δ(*ara-leu*)7697 *gal*U *gal*K *rps*L (Str^R) *end*A1 *nup*G	Invitrogen
JM109	F' *rec*A1 *end*A1 *gyr*A96 *thi*-1 *hsd*R17 (r_k^-, m_k^+) $e14^-$ ($mcrA^-$) *sup*E44 *rel*A1 Δ(*lac-proAB*) [*traD*36 $proAB^+$ $lacI^q$ *lacZ*ΔM15]	Takara Bio
KO11	*E. coli* B – Δ*frd pfl*::pdc_{Zm} $adhB_{Zm}$ *cat*	Ohta *et al.* 1991
Saccharomyces cerevisiae		
INVScI	*MAT*a *his3*Δ*1 leu2 trp1*-289 *ura3*-52/*MAT*α *his3*Δ1 *leu2 trp1*-289 *ura3*-52	Invitrogen
Pichia pasotirs		
GS115	*his4*	Invitrogen
Plasmids		
pUC18	Cloning vector under the control of *lac* promoter, Ap^r	Takara Bio
pCR2.1-TOPO	TA cloning vector under the control of *lac* promoter, Ap^r, Km^r	Invitrogen
pYES2	*E. coli-S. cerevisiae* shuttle vector under the control of *GAL1* promoter, *URA3*, Ap^r	Invitrogen
pHIL-S1	Expression vector with *PHO1* secretory signal sequence in *P. pastoris* under the control of *AOX1* promoter, *HIS4*, Ap^r	Invitrogen
pPIC9	Expression vector with α-MF secretory signal sequence in *P. pastoris* under the control of *AOX1* promoter, *HIS4*, Ap^r	Invitrogen
pPIC3.5	Expression vector without secretory signal sequence in *P. pastoris* under the control of *AOX1* promoter, *HIS4*, Ap^r	Invitrogen
pXYN102	pUC18::2.7-kbp *Hin*dIII fragment carrying *xynI*	This study
pXYN117	pYES2::0.7-kbp *Eco*RI-*Xba*I fragment carrying *xynI* with its own secretory signal sequence	This study
pXYN118	pHIL-S1::0.7-kbp *Eco*RI-*Sma*I fragment carrying *xynI* with *PHO1* secretory signal sequence	This study
pXYN119	pPIC3.5::0.7-kbp *Eco*RI fragment carrying *xynI* with its own secretory signal sequence	This study
pXYN120	pPIC9::0.7-kbp *Eco*RI fragment carrying *xynI* with α-MF secretory signal sequence	This study
pXYN123	pPIC3.5::0.7-kbp *Eco*RI fragment carrying *xynI* without its own secretory pro-signal sequence	This study
pXYN128	pPIC3.5::0.7-kbp *Eco*RI fragment carrying *xynI* with its own secretory signal sequence (D73N)	This study

(Continued on the next page)

pXYN129	pPIC3.5::0.7-kbp *Eco*RI fragment carrying *xynI* with its own secretory signal sequence (V141C/C150Y)	This study
pXYN131	pPIC3.5::0.7-kbp *Eco*RI fragment carrying *xynI* with its own secretory signal sequence (E153T)	This study
pXYN132	pPIC3.5::0.7-kbp *Eco*RI fragment carrying *xynI* with its own secretory signal sequence (E157Q)	This study
pXYN204	pUC18::9.0-kbp *Eco*RI fragment carrying *xynII*	This study
pXYN205	pUC18::3.5-kbp *Xba*I-*Kpn*I fragment carrying *xynII*	This study
pXYN207	pPIC3.5::1.1-kbp *Eco*RI fragment carrying *xynII* with its own secretory signal sequence	This study
pXYN302	pUC18::5.0-kbp *Bam*HI fragment carrying *xynA*	This study
pXYN303	pPIC3.5::0.6-kbp *Bam*HI fragment carrying *xynA* with its own secretory signal sequence	This study
pEXN101	pUC18::0.6-kbp *Eco*RI-*Sma*I fragment carrying *xynI* without its own secretory signal sequence	This study
pEXN102	pUC18::0.6-kbp *Eco*RI-*Sma*I fragment carrying *xynI* with its own secretory signal sequence	This study
pEXN301	pUC18::0.6-kbp *Kpn*I-*Xba*I fragment carrying *xynA* with its own secretory signal sequence	This study
pEXN401	pUC18::0.6-kbp *Kpn*I-*Xba*I fragment carrying *xynA* mature protein coding region with *xynI* secretory signal sequence	This study

General introduction

The explosive increase in the human population, which will reach 9-10 billion by the middle of the 21st century, and the anticipated depletion of fossil fuels may cause serious food and energy shortages. Furthermore, the indiscriminate use of natural resources such as fossil fuels burning for energy purpose will further increase greenhouse gases production. Greenhouse gases are one of the main factors of global warming. Accordingly, new technologies to more effectively utilize our sustainable resources must be developed to provide us and left for further generations with sufficient amounts of natural resources.

The Kyoto Protocol in 1997 calls on major industrialized countries to reduce emissions of carbon dioxides and other global warming gases in accordance with the United Nations Framework Convention on Climate Change. The protocol was adopted at the Conference of Parties to the Convention III (COP3) held in Kyoto. This international accord requests Japan to reduce the emission levels of greenhouse gases in 1990 by 6% during the period of the year 2008 to 2012.

Nevertheless, the emission of greenhouse gases in 2002 has already reached the level that is 7% higher than that in 1990. This means that Japan's greenhouse gas emissions were around 13% higher than the required level in the protocol. Hence, Japanese government decided "Biomass Nippon Strategy" at the cabinet meeting in December 2002. The strategy presents the developmental direction of, and the technology for, biomass utilization. It aims for the time being at the target year 2010, which corresponds to the midpoint of the first commitment period of the Kyoto Protocol. The strategy encourages untapped-resource usage for fuel production called biomass fuels.

Biomass fuels are produced by conversion of agricultural/forestry products using microorganisms such as *Saccharomyces* spp., *Zymomonas mobilis*, and *Rhodobacter sphaeroides*. Such fuels are gaining increasing attention as an effective tool to curb global warming or emissions of greenhouse gases. These biomass fuels are not responsible for an accumulation of carbon dioxide, because carbon dioxide generated by combustion of the fuels stem from fixed carbon (carbon neutral).

In the United States, about 6 million kiloliters of fuel ethanol, which is equivalent to 3% of total gasoline consumption, are mainly made from corn and used annually by mixing with gasoline to give its content of 10% (E10). Brazil is the world's largest producer of ethanol, with an annual output of 16 million kiloliters. Brazilian ethanol is made from sugar cane, and the country aims to start exporting fuel ethanol. Japanese government has allowed up to 3% blending of ethanol into gasoline.

However, in Japan where there are no surplus farm products, such as corn and sugar cane, it is inevitable to produce ethanol from alternative sources of biomass. Since about two thirds of total area in Japan is a forest and there are a lot of wooden buildings, it is important to use these abundant ligneous resources for biomass fuel production. The major components of ligneous biomasses are cellulose, hemicellulose and lignin. A typical hardwood biomass contains on average 40% cellulose, 33% hemicellulose and 23% lignin by dry weight basis. Cellulose is a homopolysaccharide composed of β-1,4-linked D-glucosyl residues, whereas hemicellulose is composed of heteropolysaccharides.

Heteropolysaccharides, collectively referred to as the β-1,4-D-xylans based on a backbone structure of β-1,4-linked D-xylosyl residues, constitute the main polymeric component of the hemicellulose fraction of plant cell walls. The β-1,3-linked xylans are found only in marine algae (Dekker and Richards 1976), while those containing a mixture of β-1,3 and β-1,4 linkages are found in seaweeds. On the other hand, the β-1,4-linked xylans are commonly found in hardwoods, softwoods, and grasses (Barry and Dillon 1940). Hardwood xylan, which may account for up to 10-35% of dry weight, is acetyl-4-*O*-methylglucuronoxylan with a degree of polymerization (DP) of about 200 (Puls and Schuseil 1993). The β-D-xylopyranosyl units are substituted at C-2 with a 4-*O*-metyl-α-D-glucuronic acid residue to the extent of about 10%, acetylated to the extent of 70% at C-2, C-3 or both (Puls and Schuseil 1993; Fig. 1A). In addition, most hardwood xylans contain small amounts of rhamnosyl and galacturonyl residues as integral components of the main chain (Coughlan and Hazlewood 1993).

The xylan of grasses, such as oat spelt, is arabino-(4-*O*-methyl-glucurono) xylan with a DP of 70. It has less 1,2-linked 4-*O*-methyl-α-D-glucuronic acid residues than does hard wood xylan but does have a large content of L-arabinofuranosyl side chains (Puls and Schuseil 1993; Fig. 1B). These are linked to C-2, C-3, or both, of the β-D-xylanopyranosyl residues of the main chain. In addition, such xylans contain 2-5% (w/w) of *O*-acetyl groups linked to C-2 or C-3 of the xylopyranose units. Moreover, the arabinosyl side chains are substituted at C-5 with feruloyl groups and *p*-coumaroyl residues to the extents of 6% and 3%, respectively (Coughlan and Hazlewood 1993). Thus, complete hydrolysis of these natural xylan requires a number of main-chain- and side-chain-cleaving enzymes to use these renewable resources.

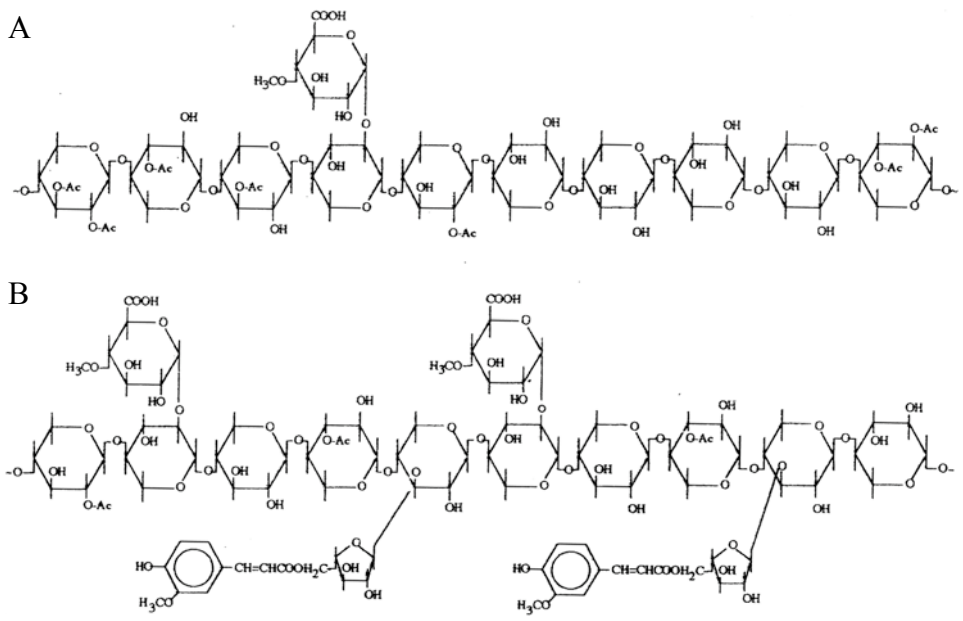

Fig. 1. Typical xylan structure. (A) *O*-acetyl-(4-*O*-methyl-glucurono) xylan and (B) arabino-(4-*O*-methyl-glucurono) xylan. (Coughlan and Hazlewood 1993)

Endo-β-1,4-xylanases (β-1,4-D-xylan xylanohydrolase; EC 3.2.1.8) and β-1,4-xylosidases (β-1,4-D-xyloside xylohydrolase; EC 3.2.1.37) degrade the main-chain in natural xylans, while α-L-arabinofuranosidases (α-L-arabinofuranoside arabinofuranohydrolase; EC 3.2.1.55) and α-D-glucuronidases (α-D-glucosiduronate glucuronohydrolase; EC 3.2.1.139) degrade the side-chain. Concerted effect of these enzymes leads to quick and efficient degradation of xylan to xylose and liberate acetyl, coumaroyl and feruloyl substituents.

In recent years, many nucleotide sequences of glycoside hydrolase genes, which include xylan-degrading enzymes, have been identified. Although glycoside hydrolases are categorized by the Enzyme Nomenclature Committee of the International Union of Biochemistry and Molecular Biology (IUBMB; formerly the International Union of Biochemistry, IUB) based on the type of reaction that enzyme catalyze and on their substrate specificity, the category dose not reflect the structural features of these enzymes. Henrissat

(1991) classified these glycoside hydrolases (GH) based on their amino acid sequence similarities, as there is direct relationship between sequence and folding similarities (Coutinho and Henrissat 1999, the web site available at http:// afmb.cnrs-mrs.fr/CAZY/).

GH family has expanded into about 100 families. It has been reported that GH families contained several Enzyme Commission (EC) entries in IUBMB and enzymes with similar substrate-specificities belonged to non-related families. The classification would be a convenient tool for the assessment of the evolutionary relationships between these enzymes and the consideration of the modes of action. For this reason, it is necessary to clarify a variety of nucleotide sequences and to analyze their functions.

Endo-1,4-β-xylanases fall into several families, mainly GH family 10 (formerly F) and 11 (formerly G). Family 11 consists of xylanases with a relatively low M_r ranging from 19,000 to 25,000, whereas family 10 comprises xylanases with a higher M_r of >30,000. A hierarchy among the family-11 and -10 xylanases was proposed for microbial degradation of plant cell wall xylan to xylose (Pell *et al*. 2004). Therefore, a molecular characterization of such multiple xylanases produced by a single microorganism will allow us to better understand their physiological roles in xylan degradation process. Moreover, it is useful for the exploitation of untapped hemicellulose to acquire many gene resources involved in xylan degradation enzymes.

These xylan-degrading enzymes occur in a wide variety of microorganisms, including gram-positive bacteria such as *Clostridium* spp. and eubacteria *Streptomyces* spp., and filamentous fungi *Aspergillus* spp. and *Trichoderma* spp., and non-*Saccharomyces* yeast (Strauss *et al.* 2001).

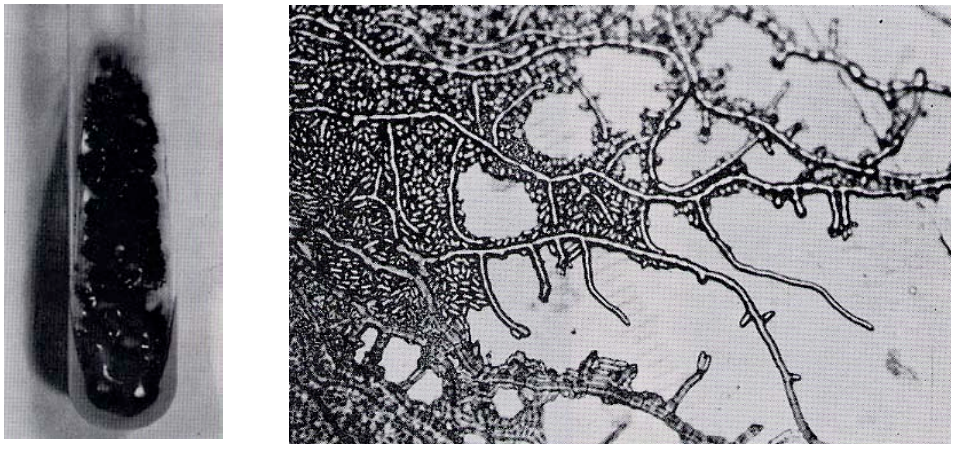

Fig. 2. Colony morphology (left panel) and microscopic observation (right panel) of *Aureobasidium pullulans* ATCC 20524. (Fujii and Shinohara 1987)

Aureobasidium pullulans is a ubiquitous saprophyte that occurs commonly in the leaf surfaces of many crop plants and on various tropical fruits (Domsch *et al.* 1980). *A. pullulans* was previously classified under fungi imperfecti. DeHoog and McGinnis (1987) classified it into ascomycetes, although a perfect stage had not been found in it. *A. pullulans* (De Bary) Arnaud is presently accepted as terminology. The organism shows polymorphism in the imperfect stage wherein it can grow as a budding-yeast or as a mycelium, depending on environmental conditions (Fig. 2). *A. pullulans* typically produces a black pigment, whereas natural color variants of *A. pullulans* that exhibit brilliant pigments of red, yellow, orange, or purple, were isolated from tropical regions (Hermanides-Nijhof 1977).

A. pullulans has been employed in industries to produce many useful extracellular polysaccharides, organic acids, and enzymes, because a culture of *A. pullulans* is designated as General Recognized as Safe (GRAS) of the Food and Drug Administration (FDA) in USA. For example, *A. pullulans* produces pullulans (Hayashibara Shoji, Inc., Okayama), gluconic acid or L-malic acid (Deshpande *et al.* 1992). The most extensively studied enzymes are fructofuranosidase, xylanase, and glucoamylase. Ljungdahl and his colleagues (Li *et al.* 1993;

Li and Ljungdahl 1994, 1996) reported that two extracellular xylanases have been purified from color variant *A. pullulans* NRRL Y-2311-1, from which the encoding gene was cloned and sequenced, and its cDNA was expressed in the yeast *Saccharomyces cerevisiae*.

Penicillium species occur abundantly in soil, decaying vegetation, foods, textiles, and other materials undergoing biodegradation (Pitt 1979). Penicillia are notable and well studied for the diversity of their secondary-metabolite production, such as penicillin from *Penicillium notatum* and the citrinin from *P. citrinum*. The research on the xylanase is less than the one that concerns the mycotoxin. To date, *Penicillium* xylanase genes have been described for *P. chrysogenum* (Haas *et al.* 1993), *P. canescens* (GenBank accession number AY756109), *P. funiculosum* (Alcocer *et al.* 2002), *P. purpurogenum* (Díaz *et al.* 1997; Chaves *et al.* 2001), *P. simplicissimum* (Schmidt *et al.* 1998), and *Penicillium* sp. strain 40 (Kimura *et al.* 2000).

However, there have been no reports of the xylanase from *A. pullulans*, which produces a black pigment, and *P. citrinum*. Therefore, the author aimed at biochemical and molecular characterization of endo-1,4-β-xylanases from two fungi, *A. pullulans* var. *melanigenum* ATCC 20524 and *P. citrinum* FERM P-1594 and these characterized xylanases were undertaken to use for biomass utilization.

Chapters I and III described purification and enzymatic properties of two extracellular xylanases XynI and XynII that were classified into GH family 10 and 11, respectively, from *A. pullulans* ATCC 20524. For comparison, a GH family-11 xylanase XynA from *P. citrinum* was purified and characterizaed in Chapter IV. Subsequently, all the three fugal xylanase genes (*xynI*, *xynII*, and *xynA*) were cloned and sequenced to define their phylogenetic

positions among homologous xylanases, and expressed in the methylotrophic yeast *Pichia pastoris*.

In Chapter II, the author generated a plausible three-dimensional (3D) model for the *A. pullulans* XynI protein. The 3D model and mutational analysis identified key amino acid residues responsible for low pH optimum of the acidophilic xylanase (XynI) from *A. pullulans*. Then, the XynI signal peptide was compared with other two conventional yeast signal peptides for the secretion efficiency of XynI mature protein expressed in *P. pastoris*.

Chapter III evaluated the pH responsiveness of the expression of the GH family-10 xylanase gene (*xynII*) from *A. pullulans* using quantitative real-time PCR.

Finally, in Chapter V, in an attempt to construct the direct xylan-fermentable strain, the author expressed the xylanase XynA from *P. citrinum* in ethanologenic strain *Escherichia coli* KO11 (Ohta *et al.* 1991) and secreted the XynA by using the secretory signal peptide from the acidophilic xylanase XynI.

Chapter I

Purification and characterization of an acidophilic family-11 xylanase from *Aureobasidium pullulans* and sequence analysis of the encoding gene

1-1. Introduction

Endo-1,4-β-xylanases (EC 3.2.1.8) hydrolyze the internal β-1,4-xylosidic linkages in the xylan backbone, and have received considerable attention because of their practical value, such as bio-breeching of pulps. The endo-xylanases were formerly classified into four types on the basis of their enzymatic properties (Reilly 1981). Recently, they are reclassified as GH family based on their amino acid sequence similarities. The majority of xylanases fall into GH families 10 and 11, whereas some other xylanases are classified into GH families 5, 8, and 43 (http://afmb.cnrs-mrs.fr/CAZY/). Xylanases of GH family 11, which show relatively low M_rs ranging from 19,000 to 25,000, generally play an important role in an initial step of xylan hydrolysis.

Two extracellular xylanases, APX-I and APX-II, have been purified from the natural color variant of *A. pullulans* NRRL Y-2311-1 (Leathers 1989; Li *et al.* 1993). The gene (*xynA*) encoding APX-II with an optimum pH of 4.8 was cloned and sequenced (Li and Ljungdahl 1994). The APX-II was expressed in the yeast *Saccharomyces cerevisiae* (Li and Ljungdahl 1996). The majority of xylanases are classified into GH family-11 on the basis of its deduced amino acid sequence and have optimum pH near the neutral, but some genes encoding acidophilic xylanases were cloned and sequenced from *Aspergillus kawachii* XynC (pH 2.0) (Ito *et al.* 1992), *Aspergillus niger* XynI (pH 3.0) (Krengel and Dijkstra 1996), *Penicillium* sp. strain 40 XynA (pH 2.0) (Kimura *et al.* 2000) and *Cryptococcus* sp. S-2

Xyn-CS2 (pH 2.0) (Iefuji *et al.* 1996). There is no report of acidophilic xylanase from *A. pullulans*.

Fujii and Shinohara (1987) previously isolated and identified a typically pigmented strain as *A. pullulans* var. *melanigenum* ATCC 20524. Here, the author found that the *A. pullulans* ATCC 20524 showed high levels of extracellular xylanase activity when grown in the presence of xylan. In this chapter, the purification and characterization of an acidophilic xylanase from the *A. pullulans* as well as the cloning and sequencing of a genomic DNA and cDNAs encoding the enzyme are described. In addition, available sequence data of the homologous xylanases reported so far and presented in this work enables us to perform phylogenetic analysis.

1-2. Materials and methods

1-2-1. Strain and culture conditions

A wild-type strain *A. pullulans* ATCC 20524 was used in this study. Growth medium (initial pH of 5.0) contained 6.7 g/*l* of yeast nitrogen base (YNB; Difco Laboratories, Detroit, MI, USA) and 10 g/*l* of oat-spelt xylan (Sigma Chemical Co., St. Louis, MO, USA) as the carbon source. For the comparative study of xylanase production using different carbon sources, various carbohydrates described in the text were substituted for xylan at the same concentration in the synthetic medium. Liquid cultures were grown on a rotary shaker (140 rpm) in 500-ml Erlenmeyer flasks containing 100 ml of medium at 30ºC for the length of time specified in the text.

1-2-2. Enzyme and protein assays

The reaction mixture consisted of 0.5 ml of a 1.0% (w/v) suspension of oat-spelt xylan in deionized water and 0.5 ml of a suitably diluted enzyme solution in 0.1 M sodium acetate-HCl buffer (pH 2.0). After incubation at 45ºC for 30 min, reducing sugars were determined by the dinitrosalicylic acid method (Miller 1959). One unit (U) of xylanase activity was defined as the amount of enzyme that liberated 1.0 μmol of xylose equivalents from xylan per min. The purified xylanase (0.13 U/ml) was assayed for hydrolytic activity toward birch-wood xylan (Sigma), Avicel (Asahi Kasei Co., Tokyo) and carboxymethyl cellulose (Wako Pure Chemical Industries, Osaka) under the conditions described above. The β-xylosidase activity was assayed by detecting the fluorescence of umbelliferone released from the synthetic substrate 4-methylumbelliferyl 7-β-D-xyloside (Sigma). Protein concentrations were measured by the method of Lowry *et al*. (1951), using bovine serum albumin (Sigma) as the standard.

1-2-3. Enzyme purification

All purification procedures were carried out at 4ºC. A 5-days-old submerged culture of *A*. *pullulans* was centrifuged at 2,000 × *g* for 30 min. The supernatant (800 ml) was concentrated to 70 ml by ultrafiltration through a 3×10^3 molecular-weight cut-off membrane (Diaflo YM3; Amicon Inc., Beverly, MA, USA) in a stirred cell. The concentrated sample was loaded to anion-exchange column of a DEAE-Cellulofine A-500 (Seikagaku Kogyo, Tokyo) column (2.6 × 45 cm) that was equilibrated with 20 mM Tris-HCl buffer (pH 8.5). The adsorbed enzyme was eluted at a flow rate of 1.5 ml/min with a linear gradient of 0 to 0.5 M NaCl in the same buffer. The fractions exhibiting the enzyme activity were pooled and then

chromatographed on a Sephacryl S-200 HR (Amersham Biosciences, Piscataway, NJ, USA) column (1.6 × 60 cm) at a flow rate of 0.5 ml/min with 20 mM Tris-HCl buffer (pH 8.5) containing 0.15 M NaCl. Xylanase was eluted as a single protein peak that coincided with the peak of enzyme activity.

1-2-4. SDS–PAGE, N-terminal amino acid sequencing, and IEF

SDS–polyacrylamide gel electrophoresis (SDS–PAGE) was carried out with a 4.5% stacking gel and a 12.5% separating gel as described by Laemmli (1970). The electrophoresis was run at a constant current of 25 mA. Gels were stained for protein with Coomassie Brilliant Blue R-250 and for carbohydrate by using the Schiff's reagent (Gerard 1990). The protein bands on SDS–polyacrylamide gels were electroblotted onto a polyvinylidene difluoride membrane (Bio-Rad Laboratories, Hercules, CA, USA) using Mini Trans-Blot Cell system (Bio-Rad), and the N-terminal amino acid sequence was identified using a 476A gas-phase protein sequencer (Applied Biosystems Inc., Foster City, CA, USA).

Analytical isoelectric focusing (IEF) was performed with a Multiphor II electrophoresis system (Amersham Biosciences) using Ampholine PAGplate (pH 3.5 to 9.5) according to the manufacturer's instructions. An IEF calibration kit (Amersham Biosciences) was used to determine the p*I* value.

1-2-5. Effect of pH and temperature on enzyme activity and stability

The optimal pH for xylanase activity was determined under the standard assay conditions except that the reaction mixture was prepared with the following buffers: 0.1 M acetate–HCl (pH 1.0 to 4.5), 0.1 M acetate (pH 4.5 to 6.0), and 0.1 M phosphate (pH 6.0 to

8.0). Enzyme stability at different pH values was measured by the residual activity after the enzyme was incubated at 30ºC for 24 h with following buffers: 0.1 M acetate–HCl (pH 1.0 to 4.0), 0.1 M acetate (pH 4.0 to 6.0), 0.1 M phosphate (pH 6.0 to 8.0), and 0.1 M glycine–NaOH (pH 9.0 to 13.0). The optimal temperature for xylanase activity was found under the standard assay conditions except that the reaction mixture was incubated at temperatures from 10ºC to 70ºC. Thermal stability was measured in terms of the residual activity after the enzyme was incubated in acetate–HCl buffer (pH 2.0) at temperatures from 10ºC to 80ºC for 30 min.

1-2-6. HPLC analysis of hydrolysis products

The reaction mixture consisting of equal volumes of a 5.0% (w/v) suspension of birch-wood xylan and the enzyme solution (11.5 U/ml) was incubated at 45ºC for 24 h. The hydrolysis products were analyzed using a high-performance liquid chromatography (HPLC) system (Tosoh Co., Tokyo) equipped with a dual pump (model CCPM), a column oven (CO-8010) and a differential refractive index detector (RI-8010). The TSKgel NH-60 column (4.6 × 250 mm; Tosoh) was maintained at 36ºC. The mobile phase was an acetonitrile-water mixture (63:37, v/v) at a flow rate of 1.0 ml/min. Sugars were identified using xylose, xylobiose, and xylotriose (Wako) as authentic standards.

1-2-7. DNA manipulations and analyses

Genomic DNA of *A. pullulans* was extracted and purified from 72-h-grown mycelia using an ISOPLANT DNA extraction kit (Wako) according to the manufacturer's instructions. Plasmid pUC18 was used for the construction of the fungal genomic library and subcloning in

Escherichia coli JM109 (Yanisch-Perron *et al*. 1985). Restriction endonucleases and DNA-modifying enzymes were used as recommended by the supplier (Nippon Gene, Tokyo). Standard molecular cloning techniques were carried out as described by Sambrook and Russel (2001). PCRs were done in a thermal cycler (GeneAmp PCR system 2400; Applied Biosystems). Plasmid pCR2.1 was used for TA cloning of amplified DNA fragments in *E. coli* INVαF' (Invitrogen Co., San Diego, CA, USA). The nucleotide sequences of both strands were determined with an ABI Prism 310 genetic analyzer (Applied Biosystems) using an ABI Prism BigDye Terminator Sequencing Ready Kit version 1.0 (Applied Biosystems). The nucleotide sequence data were analyzed using GENETYX-MAC software package (Software Development Co. Ltd., Tokyo). Homology search in DNA or Protein databases was carried out with the BLAST program (Altschul *et al.* 1997). Multiple sequence alignments were generated by using the CLASTALW program with BLOSUM matrix (Thompson *et al.* 1994). A neighbor-joining tree (Saitou and Nei 1987) was constructed from the aligned amino acid sequences using the TREECON software package (Van de Peer and De Wachter 1994). The reliability of the tree was assessed by the bootstrap method (Felsenstein 1985) with 1,000 replications.

1-2-8. Construction of the xylanase-specific DNA probe

A pair of 21-mer oligonucleotides was designed from the known nucleotide sequence of the *A. pullulans* NRRL Y-2311-1 xylanase gene (*xynA*) (Li and Ljungdahl 1994); P1-1 (forward; 5′-GGC ATC AAC TAC GTC CAG AAC-3′) and P1-2 (reverse; 5′-CCA ACC GAG ACC AAC GAC GAA-3′). The primers amplified a 126-bp internal fragment of the coding region of the potential xylanase gene, designated as *xynI*, from the *A. pullulans* ATCC

20524 genomic DNA. The PCR-amplified fragment was excised from the gel, and purified with QIAquick Gel Extraction Kit (Qiagen, Valencia, CA, USA). The fragment was cloned into pCR2.1 vector with the TA Cloning Kit (Invitrogen), and sequenced to confirm its identity. The amplified 126-bp fragment was labeled with digoxigenin (DIG)-11-dUTP by the random primed method using a DIG DNA labeling and detection kit (Roche Diagnostics, Mannheim, Germany) for use as a hybridization probe.

1-2-9. Southern blot and DNA hybridization

The *A. pullulans* genomic DNA was digested with several restriction enzymes, and the resulting fragments were separated by electrophoresis on a 1.0% (w/v) agarose gel using Tris-acetate/EDTA (TAE) buffer. The DNA was blotted from the gel onto a positively charged nylon membrane (Hybond-N+; Amersham International plc, Amersham, UK) by capillary transfer using 0.4 M NaOH as the transfer solution. Blots were hybridized with the xylanase-specific probe for overnight at 68ºC in a buffer containing 0.5 M Na_2HPO_4 (pH 7.2) and 1% SDS at 68ºC. Hybridized DIG-labeled probes on the membranes were detected colorimetrically with alkaline-phosphatase labeled antibody to DIG using the above-mentioned kit.

1-2-10. Construction and screening of the A. pullulans genomic library

*Hin*dIII-digests of genomic DNA were fractionated by electrophoresis on a 1.0% (w/v) agarose gel. Fractions that contained DNA fragment of approximate size 2.7 kbp was excised from the gel, and the fragments were eluted and ligated into the *Hin*dIII site of pUC18, generating a plasmid pXYN102. *E. coli* JM109 competent cells (Takara Bio, Otsu, Japan)

were transformed with each of these ligation mixtures to make DNA libraries that were enriched for each of the potential xylanase gene. Transformants were transferred to Hybond-N+ nylon membranes and screened for hybridization with the DIG-labeled DNA probe as described above for Southern hybridization.

1-2-11. Isolation of poly(A)$^+$ RNA and cDNA cloning

Mycelia were harvested from 72-h-old cultures by filtration, and total RNA was isolated using an ISOGEN RNA isolation kit (Wako). Poly(A)$^+$ RNA was obtained from total RNA by oligo-dT-cellulose column (Stratagene, La Jolla, CA, USA).

To obtain the full-length cDNA sequences, we employed a 5′ and 3′ rapid amplification of cDNA ends (RACE) system (SMART RACE cDNA amplification kit; Clontech, Palo Alto, CA, USA). First-strand cDNA was synthesized and used as the template in the two-step nested-PCR. For 5′ RACE, P1-3 (forward; UPM provided in the kit) and P1-4 (reverse; 5′-AGG TAG CGC CAT CGC TGA CGA CGG-3′ complementary to nt 475 to 498; see nt sequence in Fig. 1-6) were used in the first-round PCR. The amplified fragment served as the template for the second-round PCR in which P1-5 (forward; NUP provided in the kit) and P1-6 (reverse; 5′-TAC CGA GCT GAG TGA CAC CGG AC-3′ complementary to nt 451 to 474) were used. For 3′ RACE, P1-7 (forward; 5′-TCG TCG GTC TCG GTT GGT CGA CTG-3′ corresponding to nt 283 to 306; see Fig. 1-6) and P1-3 (reverse; see above) were used in the first-round PCR. The amplified fragment served as the template for the second-round PCR in which P1-8 (forward; 5′-GTG CTG CTC GCT CCA TCA CCT ACT-3′ corresponding to nt 307 to 330) and P1-5 (reverse; see above) were used. The partially overlapping 5′ and 3′ RACE products were cloned into pCRII and sequenced.

1-2-12. Expression of xynI cDNA in Saccharomyces cerevisiae

To amplify the *xynI* coding region from the first-strand cDNA template, a pair of primers was designed from the genomic sequence (see *1-3-5*): P1-9 (forward; 5′-CGG AAT TCC GAA C**AT GAA GTT CTT CGC CAC TAT T**-3′) and P1-10 (reverse; 5′-GCT CTA GAG CTG ACA T**CT AAG AGA CAG TAA CGC T**-3′) (letters in bold type indicate the coding sequence). The primers contained additional sequences at their 5′ ends to generate *Eco*RI and *Xba*I sites (underlined in the sequences above) in the amplified fragment at the 5′ and 3′ ends, respectively.

A *xynI* cDNA was cloned and expressed in *S. cerevisiae* INVSc1 using the vector pYES2 according to the manufacturer's instructions (Invitrogen). The amplified 700-bp cDNA fragment was inserted into pYES2 at the *Eco*RI-*Xba*I sites in the orientation of transcription from the *GAL1* promoter to generate pXYN117. The *S. cerevisiae* strain was transformed with the resulting pXYN117 by the lithium acetate method (Kaiser *et al.* 1994). The recombinant strain, *S. cerevisiae* (pXYN117), was grown at 30ºC for 90 h on the agar plate of uracil-deficient synthetic complete medium supplemented with 0.2% (w/v) Remazol Brilliant Blue (RBB)-xylan (Sigma) and 2% (w/v) galactose. The plate was then washed with 70% (v/v) ethanol to destain the digested RBB-xylan.

1-2-13. Nucleotide sequence accession number

The nucleotide sequence of the 2703-bp fragment containing the *xynI* gene has been deposited in the DDBJ/EMBL/GenBank nucleotide sequence databases with the accession number AB053298.

1-3. Results

1-3-1. Effect of carbon sources on xylanase production

Xylanase production by *A. pullulans* ATCC 20524 was compared for carbon sources using medium (initial pH of 5.0) containing 1.0% (w/v) xylan, carboxymethyl cellulose, inulin, dextrin, soluble starch, sucrose, lactose, maltose, xylose, or fructose. Of the sugars tested, only the xylan-grown culture showed extracellular xylanase activity that reached 8.0 U/ml after the 5-day incubation, and the final pH of this culture was as low as 2.7. In contrast, xylanase activity in *A. pullulans* Y-2311-1 was induced by xylose as well as by xylan (Li and Ljungdahl 1994). Induction of the synthesis of xylan-degrading enzymes by xylanolytic organisms cultured with xylan as carbon source is well documented (Coughlan and Hazlewood 1993).

1-3-2. Purification and properties of an extracellular xylanase

Table 1-1 summarizes the procedure for the purification of extracellular xylanase from *A. pullulans* ATCC 20524. This protocol afforded a 4.2-fold purification of the xylanase from the culture supernatant with a yield of 62.2%. The enzyme was homogeneous as judged by SDS–PAGE and IEF, which showed an apparent M_r of 24,000 and a p*I* of 6.7, respectively (Fig. 1-1). Schiff staining of the protein band showed that it was glycosylated. The purified enzyme showed relatively high activity under acidic conditions with an optimum of pH 2.0 (Fig. 1-2A), lower than the optimum of pH 4.8 for the APX-II (Li and Ljungdahl 1994). The enzyme retained greater than 80% of the original activity between pH 2.0 and 10.0 after 24-hour incubation (Fig. 1-2B). Thus, the xylanase was acidophilic and stable over a wide pH range. The optimal temperature for the enzyme activity was determined to be 50ºC (Fig.

1-3A). The enzyme remained stable up to 50ºC, but it lost activity at 80ºC (Fig. 1-3B).

The effect of metal cations and *p*-chloromercuribenzoate on xylanase activity was determined at a final concentration of 1 mM. The enzyme activity was promoted by Fe^{3+} (288%), Cu^{2+} (274%), or Co^{2+} (257%). Mn^{2+}, Mg^{2+}, Zn^{2+}, Cd^{2+}, or Ni^{2+} showed no or slightly stimulatory effects, whereas *p*-chloromercuribenzoate strongly inhibited the enzyme activity (17%).

The xylanase hydrolyzed xylans from oat-spelt and birch-wood at similar rates, but it had no detectable activity toward Avicel or carboxymethyl cellulose. In addition, no β-xylosidase activity was detected with 4-methylumbelliferyl 7-β-D-xyloside. HPLC analysis showed that the enzyme released mainly xylose, xylobiose and xylotriose from birch-wood xylan (Fig. 1-4).

1-3-3. N-terminal amino acid sequencing

N-terminal amino acid sequencing of the enzyme identified the first 20 residues: A-G-P-G-G-I-N-Y-V-Q-N-Y-N-G-N-L-G-Q-F-T. The N-terminal amino acid sequence was identical to that of the APX-II (M_r 25,000, p*I* 9.4) from *A. pullulans* Y-2311-1 (Li and Ljungdahl 1994) despite the different p*I* values between the two enzymes.

Table 1-1. Purification of extracellular GH family-11 xylanase from *A. pullulans* ATCC 20524.

Step	Total activity (U)	Total protein (mg)	Specific activity (U/mg)	Purification (fold)	Yield (%)
Culture supernatant	6370	52.5	121	1.0	100.0
Ultrafiltration	5090	39.5	129	1.1	80.0
DEAE-Cellulofine	4660	25.8	181	1.5	73.2
Sephacryl S-200	3960	7.74	512	4.2	62.2

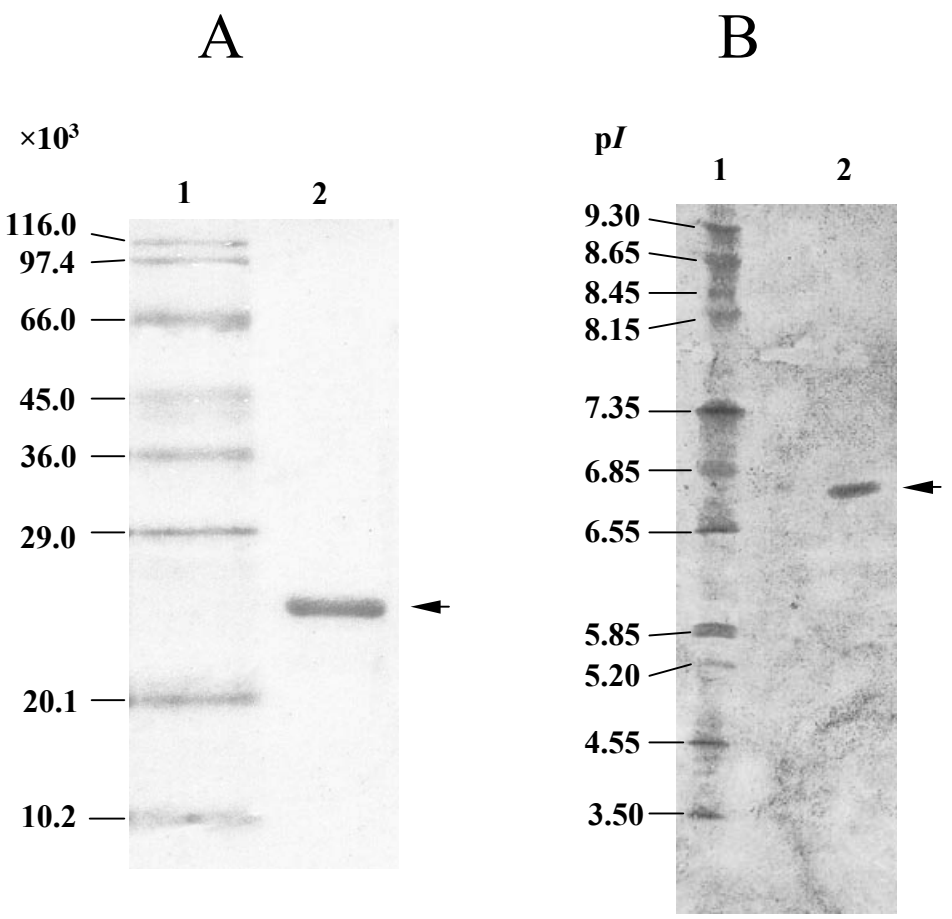

Fig. 1-1. SDS-PAGE (A) and IEF (B) of purified xylanase from *A. pullulans* ATCC 20524.

Protein was visualized by Coomassie Brilliant Blue R-250 staining. Lanes: 1, standard proteins; 2, purified xylanase.

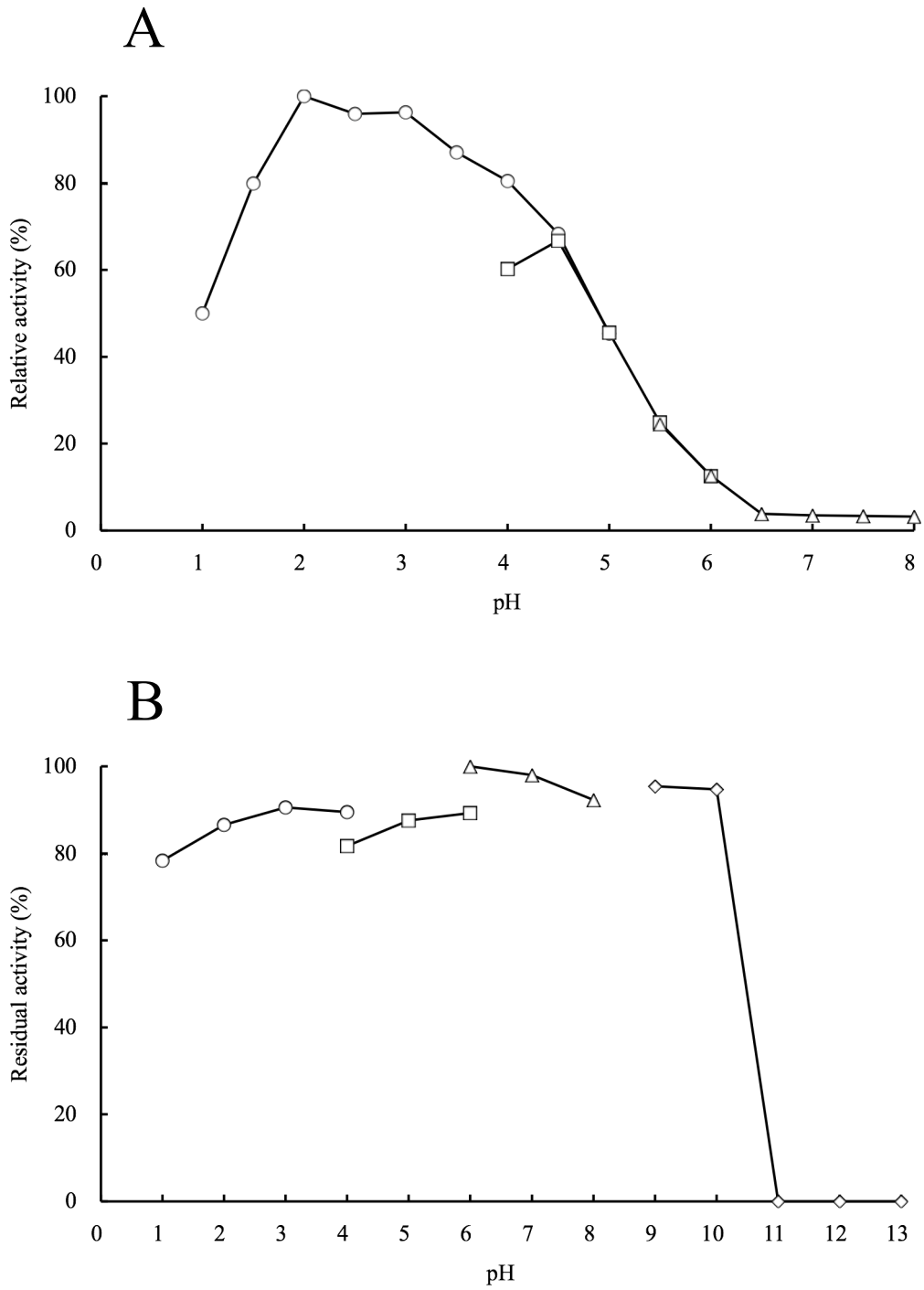

Fig. 1-2. Effect of pH on activity (A) and stability (B) of purified xylanase from *A. pullulans* ATCC 20524.

The reaction conditions are described in the text (see *1-2-5*). Relative and residual activities were expressed as percentage of the highest activity and the initial activity, respectively. Symbols: circles, sodium acetate-HCl buffer; squares, acetate buffer; triangles, phosphate buffer; diamonds, glycine-NaOH buffer.

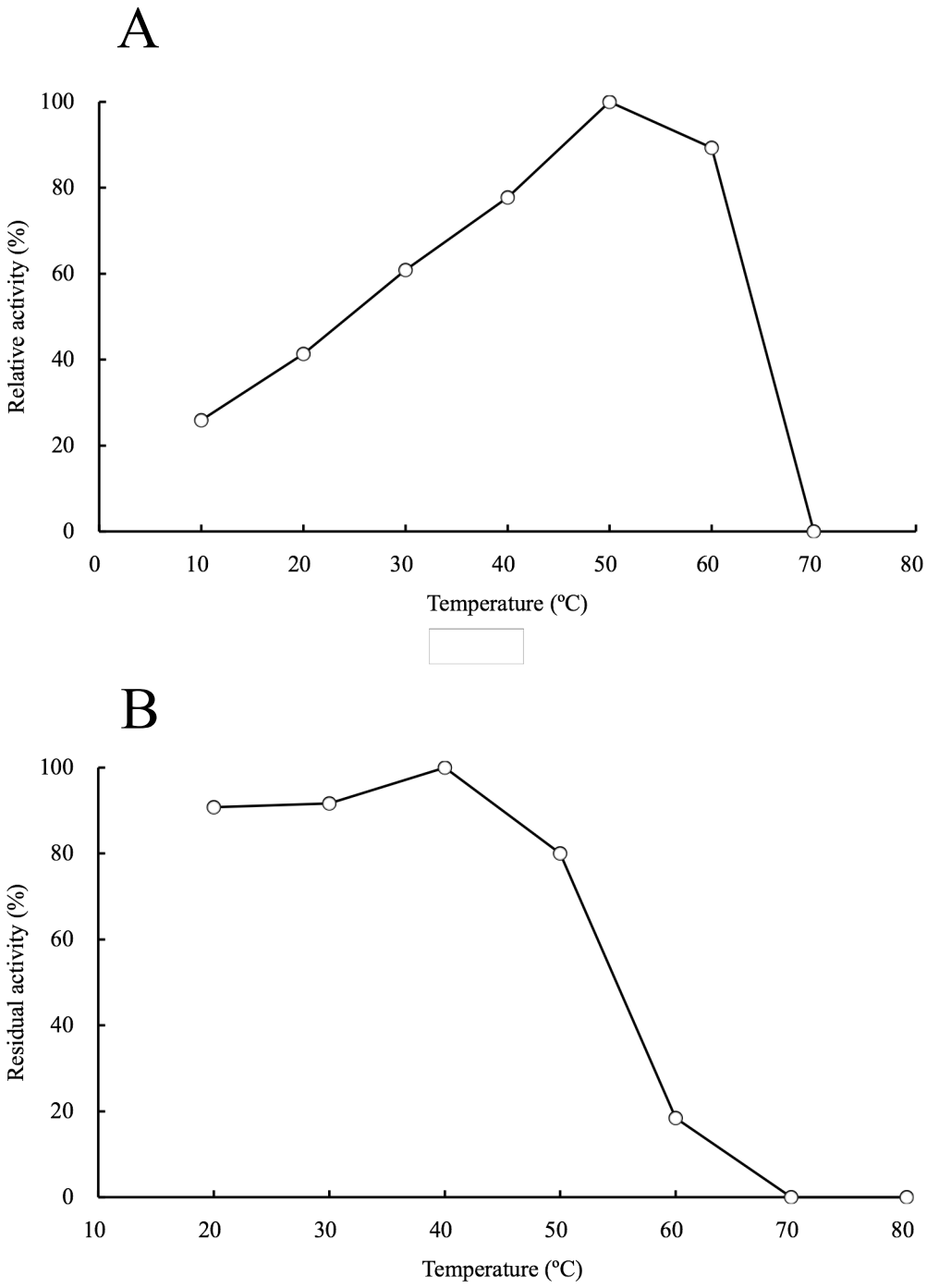

Fig. 1-3. Effect of temperature on activity (A) and stability (B) of purified xylanase from *A. pullulans* ATCC 20524.

The reaction conditions are described in the text (see *1-2-5*). Relative and residual activities were expressed as percentage of the highest activity and the initial activity, respectively.

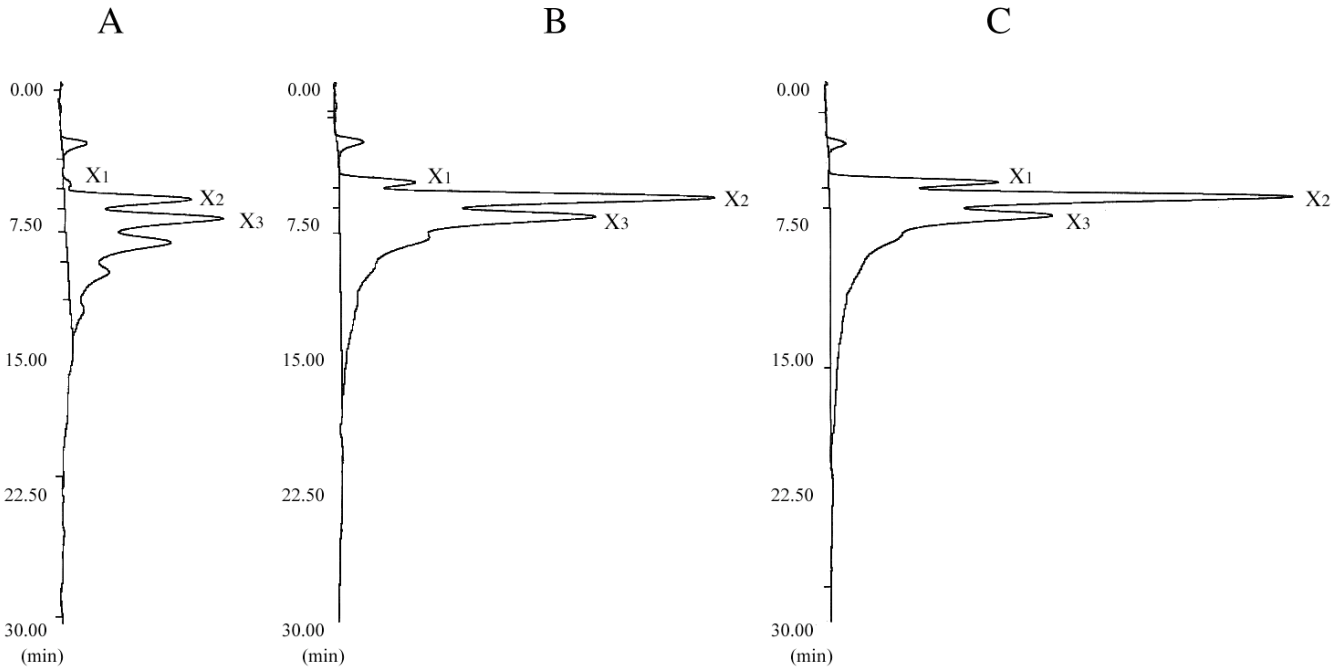

Fig. 1-4. HPLC analysis for hydrolysis products of birch-wood xylan by purified xylanase from *A. pullulans* ATCC 20524.

X1, Xylose; X2, Xylobiose; X3, Xylotriose. A, 0.5 h of incubation; B, 6.0 h of incubation; C, 24 h of incubation. Reaction and analytical conditions are described in the text (see *1-2-6*).

1-3-4. Cloning of the xylanase gene

The nucleotide sequence of the 126-bp fragment amplified from the *A. pullulans* ATCC 20524 genomic DNA (see *1-2-8*) was 94% identical to the region between nt 174 and 299 of the *A. pullulans* Y-2311-1 *xynA* coding sequence (Li and Ljungdahl 1994). The deduced amino acid residues of one of the reading flames of this fragment matched the N-terminal amino acid residues 5 to 20 of the xylanase purified from *A. pullulans* ATCC 20524. Southern blots of the genomic DNA digested with various restriction enzymes were probed with the 126-bp DIG-labeled fragment. A single hybridizing band was observed following *Eco*RI (10 kbp), *Bam*HI (8.0 kbp), *Sal*I (6.0 kbp), *Pst*I (2.7 kbp), or *Hin*dIII (2.7 kbp) digestion (Fig. 1-5). These data indicate that the *xynI* gene exists as a single copy in the *A. pullulans* ATCC 20524 genome. The 2.7-kbp *Hin*dIII fragment containing the *xynI* gene was ligated into pUC18. *E. coli* JM109 cells were transformed with the ligation mixture to make DNA libraries that were enriched for potential xylanase gene. The resultant transformants were screened by colony hybridization using the DIG-labeled 126-bp probe to obtain positive colonies harboring the xylanase gene.

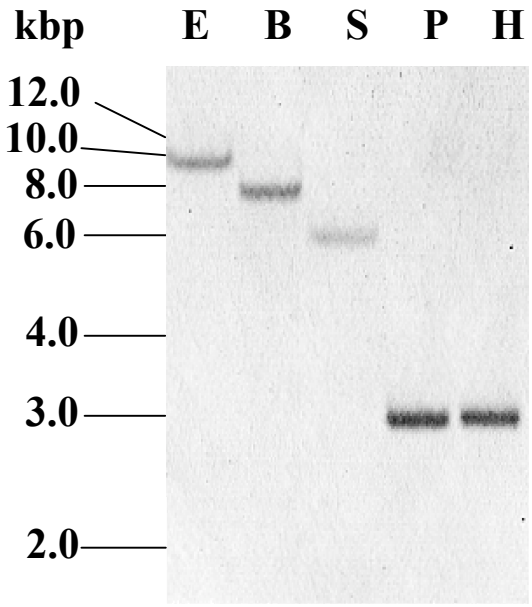

Fig. 1-5. Southern blot analysis of genomic DNA from *A. pullulans* ATCC 20524.

Genomic DNA was digested with *Eco*RI (lane E), *Bam*HI (lane B), *Sal*I (lane S), *Pst*I (lane P), or *Hin*dIII (lane H). The resultant fragments were separated with the 126-bp DIG-labeled *xynI*-specific probe (see *1-2-8*). Hybridization signals were detected with DIG labeling and detection kit. The numbers on the left margin indicate the positions of size markers.

1-3-5. Nucleotide sequences of the xynI gene and its cDNAs

Nucleotide sequence analysis revealed that the 2.7-kbp fragment contained a complete *xynI* open reading frame (ORF) and its flanking regions (Fig. 1-6). The molar G+C content in the *xynI* coding sequence was 59.9%. The deduced ATG start codon had a consensus A residue at the –3 position (Kozak 1989). A comparison of the xynI genomic and cDNA sequences showed that the coding region was interrupted by a single intron of 59 bp. This intron fitted the GT/AG rule for 5′ and 3′ splice sites (Gurr *et al.* 1987).

The *xynI* 5′-noncoding region included promoter elements of a putative TATA box at nt –91 (TATATAA) and two putative CCAAT boxes at nt –247 (CAAT) and –283 (CCAAT) from the start codon. Consensus binding sites for the CREA repressor (5′-SYGGRG-3′), which mediates carbon catabolite repression in *Aspergillus nidulans* (Cubero and Scazzocchio 1994), were present further upstream in the *xynI* promoter region at nt –626 (GTGGGG), –618 (CTGGAG), –419 (CCCCAC), and –414 (CCCCAC).

Sequence analysis of a total of 15 independent cDNA clones of 5′ RACE products showed that a single transcription start point of the *xynI* gene was present at nt –46 (A) from the start codon. Of the 53 different cDNA clones of 3′ RACE products, 13 and 40 cDNA clones were polyadenylated 79 and 176 bp downstream of the stop codon, respectively.

1-3-6. Deduced amino acid sequence and enzymatic activity of the xynI gene product

The *xynI* ORF encoded a precursor protein (XynI) of 221 amino acids with a calculated M_r of 23,373. The N-terminal amino acid sequence of the mature protein purified from the culture filtrate matched the deduced sequence of Ala-35 to Thr-54 in the XynI. The

XynI mature protein consisted of 187 amino acids with a calculated M_r of 19,929 and a deduced p*I* of 5.05. The calculated M_r was smaller than 24,000 as measured by SDS–PAGE, probably because decreased binding of SDS to the glycoprotein reduced the electrophoretic mobility. The deduced p*I* was lower than the p*I* of 6.7 determined by IEF. The difference in p*I* may be due to a particular configuration of this protein. Since there was no Asn-X-Ser/Thr sequence required for *N*-linked glycosylation in the XynI protein, the secreted enzyme may be glycosylated by *O*-linked oligosaccharides.

The *xynI* gene used only 41 out of possible 61 sense codons. The percentages of A, T, G, and C at the third position of each codon were 2.3, 20.4, 15.8, and 61.5%, respectively, indicating a marked preference for C at the third position and a tendency to avoid codons ending in A.

To prove the identity of the *xynI* as a xylanase gene, the expression of the *xynI* cDNA in *S. cerevisiae* INVSc1 was studied using the agar plate containing RBB–xylan (Fig. 1-7). Large halos developed around the colonies of the recombinant strain, *S. cerevisiae* (pXYN117). This is indicative of radial diffusion of the active xylanase that was synthesized and secreted by the recombinant yeast. The control strain, *S. cerevisiae* (pYES2), had no detectable xylanase activity.

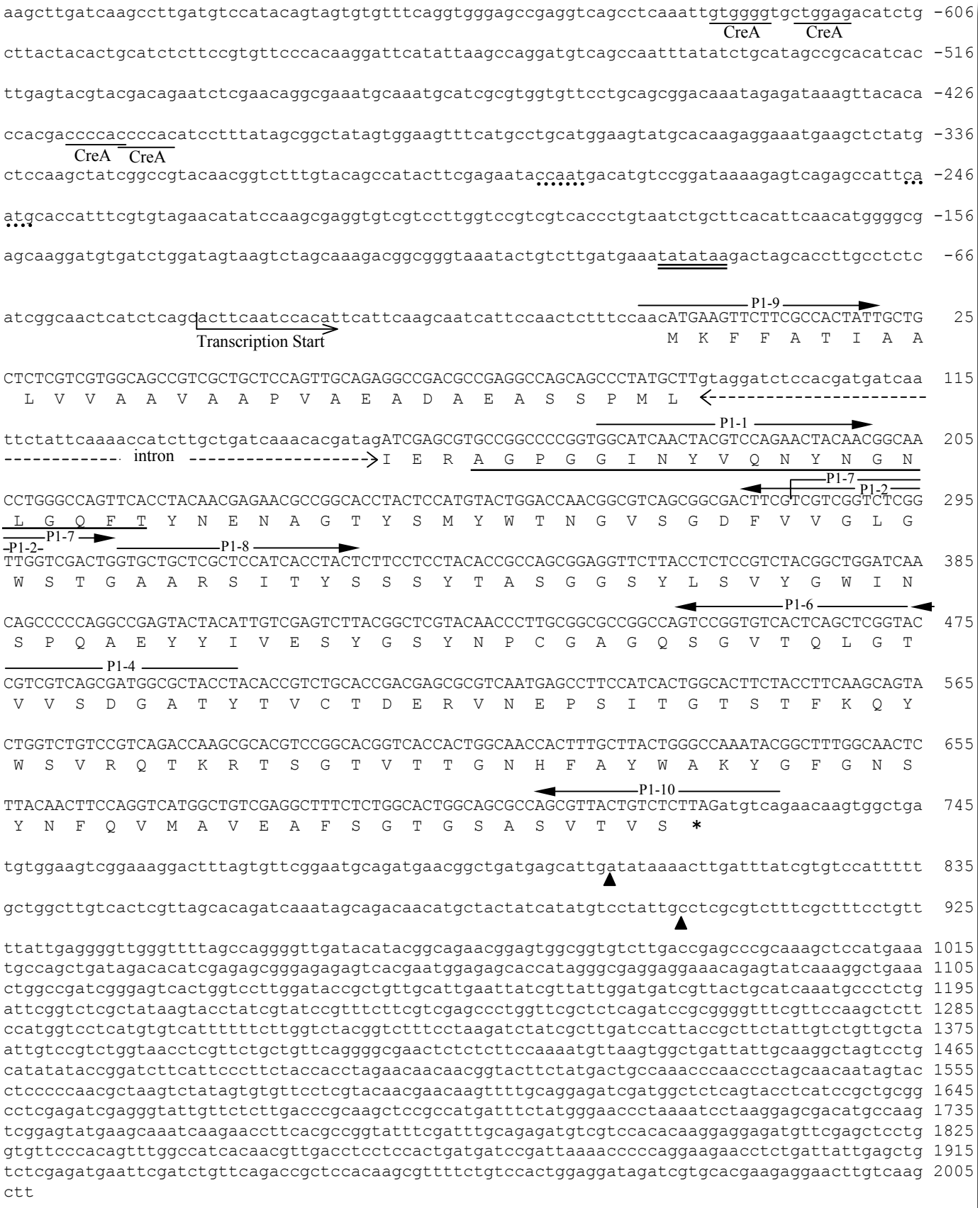

Fig. 1-6. Nucleotide sequence of *A. pullulans* ATCC 20524 *xynI* gene and flanking regions and deduced amino acid sequence.

The N-Terminal amino acid sequence determined for the mature protein is underlined.The TATA box is doubly underlined, and the two CCAAT boxes are shown by a dotted line. Two polyadenylation sites are indicated by solid allowheads. The positions of gene-specific primers, P1-1 to P1-10 (excluding the universal primers), are indicated.

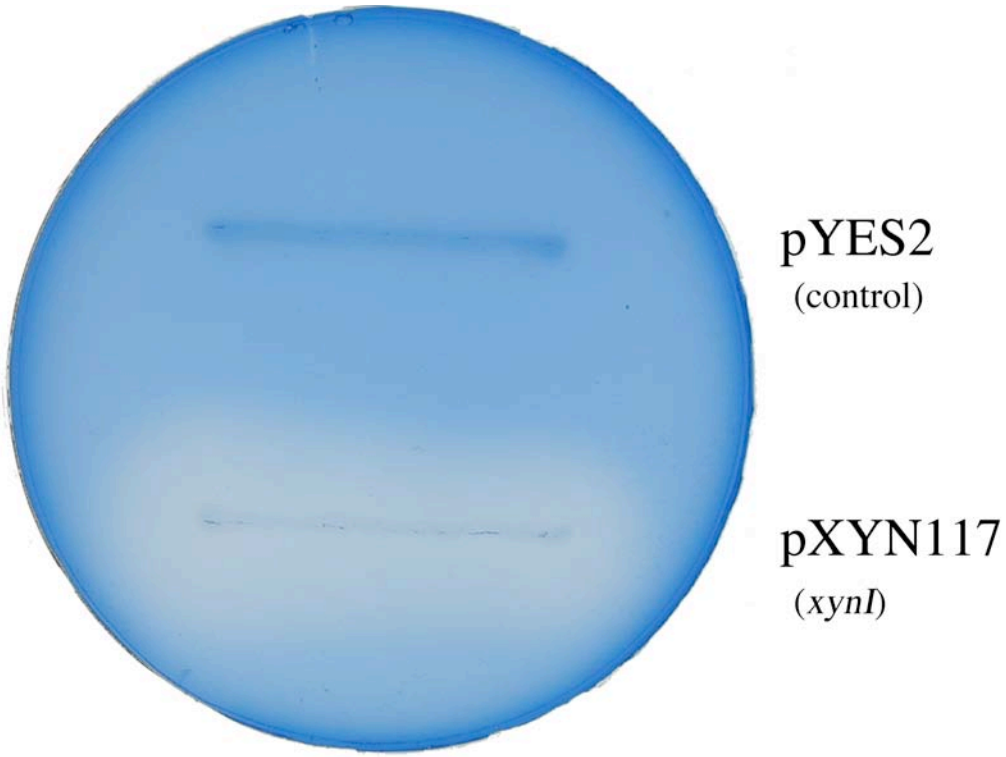

Fig. 1-7. Functional expression of *A. pullulans* ATCC 20524 *xynI* cDNA in *S. cerevisiae* INVScI.

A 700-bp cDNA fragment containg the *xynI* ORF was inserted into the expression vector pYES2 to generate pXYN117. *S. cerevisiae* (pXYN117) and the control strain, *S. cerevisiae* (pYES2), were both streaked on the agar plate containing 0.2% (w/v) RBB-xylan and grown at 30ºC for 90 h. A colony degrading RBB-xylan is surrounded by pale clearing zones.

1-3-7. Sequence comparisons with other xylanases

A BLAST search of *A. pullulans* ATCC 20524 XynI in the protein sequence databases found significant degrees of identity to the following xylanases from filamentous fungi and a basidiomycetous yeast (pH optima for enzyme activities are shown in parentheses): 94% for *A. pullulans* XynA (pH 4.8) (Li and Ljungdahl 1994); 70% for *Penicillium purpurogenum* XynB (pH 3.5) (Belancic *et al.* 1995; Díaz *et al.* 1997); 65 to 66% for *Aspergillus awamori* ExlA (Hessing *et al.* 1994), *A. niger* xylanase I (pH 3.0) (Krengel and Dijkstra 1996), *A. kawachii* XynC (pH 2.0) (Ito *et al.* 1992), and *Aspergillus tubigensis* XlnA (de Graaff *et al.* 1994); 52% for the yeast *Cryptococcus* sp. S-2 xyn-CS2 (pH 2.0) (Iefuji *et al.* 1996), 45 and 48% for *A. nidulans* XlnA (pH 5.5) and XlnB (pH 5.5), respectively (Pérez-González *et al.* 1996; Fernándex-Espinar *et al.* 1993, 1996); and 44% for *Penicillium* sp. 40 XynA (pH 2.0) (Kimura *et al.* 2000). All of these homologous xylanases have relatively low M_r ranging from 19,000 to 25,000, and belong to family 11 in the numerical classification of glycoside hydrolases. The alignment of these homologous sequences is given in Fig. 1-8. The NYVQNYNGN sequence is conserved in the N-terminal regions of the homologous enzymes except in those of the *A. nidulans* and *Penicillium* sp. 40 enzymes.

1-3-8. Phylogenetic positions of Aureobasidium xylanases

To assess the evolutionary relationships between the *Aureobasidium* xylanases XynI and XynA and the other fungal and yeast xylanases shown in Fig. 1-8, an unrooted phylogenetic tree was constructed on the basis of their full-length amino acid sequences (Fig. 1-9). Since xylanases from four black aspergilli (*A. awamori*, *A. niger*, *A. kawachii*, and *A.*

tubigensis) were highly homologous, *A. kawachii* XynC and *A. tubigensis* XlnA were shown as their representatives. Evolutionary distance among the enzymes showed that the *Aureobasidium* xylanases are closely related to those from the black aspergilli and *P. purpurogenum* and that the acidophilic xylanase from *Penicillium* sp. 40 forms a cluster with the *A. nidulans* XlnA and XlnB with optimum pH 5.5. The yeast xylanase from *Cryptococcus* sp. S-2 is distant from both clusters of the fungal enzymes.

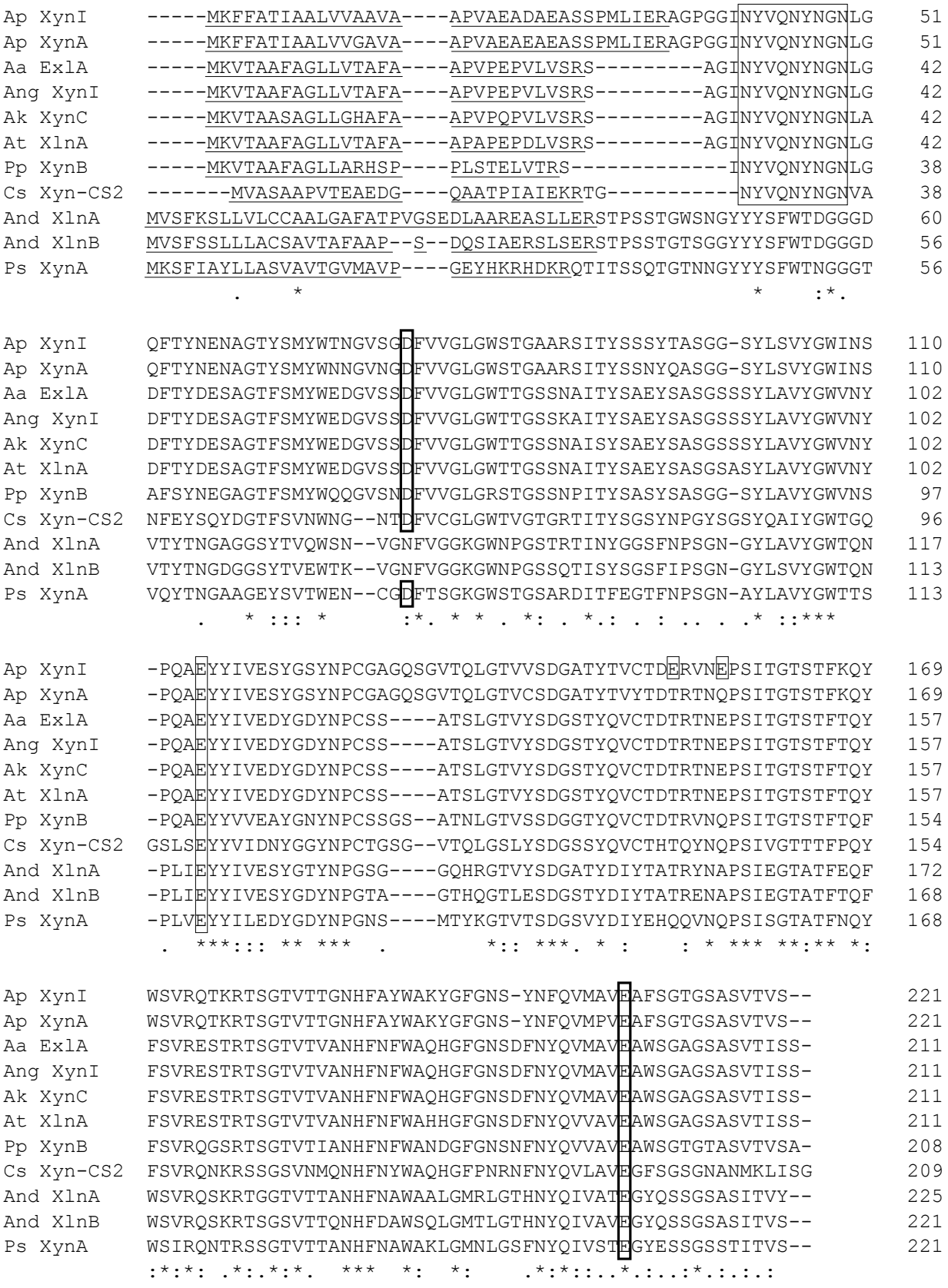

Fig. 1-8. Alignment of amino acid sequences of *A. pullulans* ATCC 20524 and homologus xylanases.

Ap, *A. pullulans*; Aa, *A. awamori*; Ang, *A. niger*; Ak, *A. kawachii*; At, *A. tubigensis*; Pp, *P. purpurogenum*; Cs, *Cryptococcus* sp. S-2; And, *A. nidulans*; Ps, *Penicillium* sp. 40. The alignment was done using the CLUSTAL W program. Dashes indicate gaps introduced during the alignment process. Asterisks indicate identity, and single and double dots indicate semiconservative and conservative replacements, respectively. Numbering of the amino acids starts at the N-termini of the proteins. The presumed prepropeptides are underlined. The boxed amino acid residues are discussed in the text.

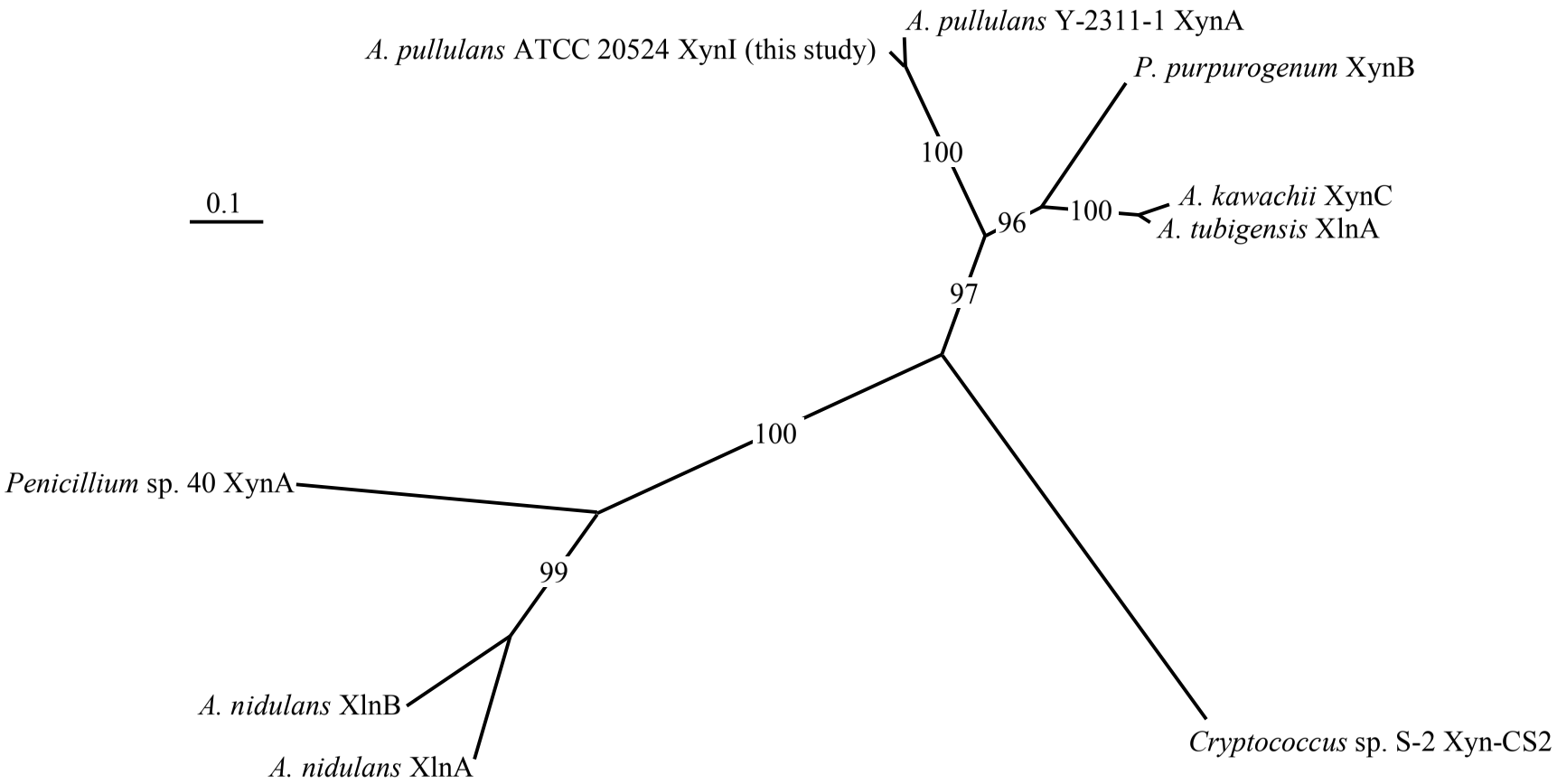

Fig. 1-9. Unrooted tree showing phylogenetic relationships between *Aureobasidium* xylanases and homologous xylanases.

The phylogenetic tree is drawn on the basis of the deduced amino acid sequences. The values represent the percentage of 1,000 bootstrap replication. The scale bar corresponds to 0.1 amino acid substitution per site. Sources of sequence data (the numbers in parentheses are accession numbers for the reference sequences): *A. pullulans* ATCC 20524 *xynI* (this study), *A. pullulans xynA* (U10298), *A. kawachii xynC* (D14848), *A. tubigensis xlnA* (L26988), *P. purpurogenum xynB* (Z50050), *Cryptococcus* sp. S-2 xyn-CS2 (D63382), *A. nidulans xlnA* (Z49892) and *xlnB* (Z49893), and *Penicillium* sp. 40 *xynA* (AB035540).

1-4. Discussion

The acidophilic xylanase from *A. pullulans* ATCC 20524 initially hydrolyzed xylan to yield xylooligosaccharides and it had no β-xylosidase activity. These findings confirmed that the enzyme was an endo-1,4-β-xylanase. The heavily substituted soluble xylans are too large to be transported into the cells. Accordingly, it is assumed that the xylanase (XynI) plays an important role in an initial step of xylan degradation.

The *xynI* coding sequence showed 91% identity to that of the *A. pullulans xynA* gene (Li and Ljungdahl 1994), while the *xynI* 5′-noncoding sequence showed much lower identity of 76% to the 380-bp 5′-noncoding sequence reported for the *A. pullulans xynA* gene (Wymelenberg *et al.* 1999). These results show that the typically pigmented *A. pullulans* var. *melanigenum* ATCC 20524 is closely related to but distinct from the color variant *A. pullulans* Y-2311-1, which can probably be designated an *A. pullulans* var. *pullulans* strain (Hermanides-Nijhof 1977) based on its pale pink colonies (Wickerham and Kurtzman 1975). van Peij *et al.* (1998) have shown that the sequence 5′-GGCTAA-3′ is the binding site for a transcriptional activator XlnR of the xylanolytic system in *A. niger*. A potential XlnR-binding site was found in the *A. pullulans xynA* promoter region at nt −125 from the start codon (Li and Ljungdahl 1994), but absent in the *A. pullulans xynI* gene. This observation may account for the lack of xylose inducibility of xylanase activity in the *A. pullulans* ATCC 20524.

The N-terminal amino acid sequence of the purified protein revealed that the XynI had a presumed signal peptide of 34 amino acids and a mature protein of 187 amino acids in the deduced amino acid sequence. However, a signal peptide cleavage site in the XynI is predicted between Ala-16 and -17 on the basis of the parameters described by von Heijne (1986) for known signal peptides. In addition to the removal of the signal peptide, the

resulting 18-amino acid putative propeptide preceding the N-terminus of the mature protein could be removed by a secondary cleavage after Arg-34. Such two-step proteolytic processing of the presumed prepropeptide was postulated for *A. niger* glucoamylase (Innis *et al.* 1985). The Glu-114 and -208 (boxed with thin and thick lines in Fig. 1-8, respectively) in *A. pullulans* ATCC 20524 XynI are conserved in the family-11 xylanases, and could be involved in catalysis as a nucleophile and as a proton donor to the glycosidic oxygen, respectively.

X-ray crystallographic and site-directed mutagenesis studies suggested the importance of an Asp residue in the *A. niger* xylanase I (Krengel and Dijkstra 1996) and *A. kawachii* XynC (Fushinobu *et al.* 1998) for their low pH optima; the Asp (boxed with thick line in Fig. 1-8) forms a hydrogen bond with the Glu (boxed with thick line in Fig. 1-8) at high pH, while both the acidic residues are protonated only at low pH and the available proton of Glu-197 enables xylan hydrolysis. A similar catalytic mechanism could probably be expected for the corresponding Asp-73 and Glu-208 in the XynI. The Asp residue was conserved in these homologous xylanases except in the *A. nidulans* enzymes with higher pH optima where the Asp residue was replaced by Asn. A comparison of the deduced amino acid sequences between *A. pullulans* XynI (this study) and *A. pullulans* XynA (Li and Ljungdahl 1994) showed substitutions of 2 out of 34 residues in the prepropeptide sequences and 10 out of 187 residues in the mature proteins. It was noticed that Thr-153 and Gln-157 in the *A. pullulans* XynA with optima of pH 4.8 (Li *et al.* 1993; Li and Ljungdahl 1994) were both replaced by Glu residues in the XynI with optima of pH 2.0. Thus, spatially biased distribution of Asp-152 and the additional acidic residues, Glu-153 and -157, in the XynI may be responsible for its lower pH optimum and p*I* value, without affecting the temperature optimum. The acidophilic nature of the XynI is subsequently studied in Chapter II.

Chapter II

Efficient expression and secretion of an acidophilic xylanase in *Pichia pastoris* and mutational analysis

2-1. Introduction

The yeast-like fungus *A. pullulans* ATCC 20524 produces an acidophilic xylanase with an optimum pH of 2.0 extracellularly as described in Chapter I. The *A. pullulans* enzyme is a family-11 xylanase with a M_r of 24,000. The xylanase gene (*xynI*) encoded a precursor protein (XynI) composed of a putative prepro-peptide of 34 amino acids and a mature protein of 187 amino acids. The *xynI* cDNA was expressed in the yeast *S. cerevisiae* and its product was secreted by its own signal peptide into the culture medium. Li and Ljungdahl (1996) demonstrated that the signal peptide of the equivalent xylanase XynA from *A. pullulans* strain Y-2311-1 was more efficient than the pre-signal peptides of *S. cerevisiae* invertase and α-mating factor (α-MF) in secreting the heterologous xylanase from *S. cerevisiae*.

The methylotrophic yeast *Pichia pastoris* has several advantages over *S. cerevisiae* as a host system for heterologous expression of xylanases because of its high secretion efficiency, high cell densities attained in inexpensive culture media, and the relative ease of scale-up to industrial processes (Cregg 1999). Berrin *et al*. (2000) reported that an *Aspergillus niger* family-11 xylanase was efficiently secreted from *P. pastoris* using the *S. cerevisiae* invertase signal peptide. The author describes here the functional expression of the *A. pullulans* XynI in *P. pastoris* and the high-level secretion directed by the XynI signal peptide. Furthermore, the 3D model and mutational analysis of the acidophilic xylanase have facilitated identification of key amino acid residues responsible for its low pH optimum, along

with their locations.

2-2. Materials and methods

2-2-1. Yeast strain and plasmids

The yeast *P. pastoris* strain GS115 (*his4*) and the integrative expression vectors pPIC3.5, pHIL-S1, and pPIC9 were obtained from Invitrogen. These yeast expression vectors contain the promoter and terminator of the alcohol oxidase I gene (*AOX1*) as an expression cassette and the *HIS4* selectable marker. Vectors pHIL-S1 and pPIC9 have a secretory signal from *P. pastoris* acid phosphatase (PHO1) and *S. cerevisiae* α-MF, respectively, while pPIC3.5 does not contain a secretory signal.

2-2-2. DNA manipulations and analyses

DNA manipulations and analyses were carried out as described in *1-2-7*.

2-2-3. Construction of yeast expression plasmids

A full-length cDNA of the xylanase gene *xynI* from *A. pullulans* strain ATCC 20524 was cloned into pUC18 as described in Chapter I. The *xynI* cDNA was used for construction of the following series of yeast expression plasmids.

Plasmids containing the three different secretory signals On the basis of the nucleotide sequence of *xynI* (see *1-3-5*), the following PCR primers were designed to amplify the precursor or mature protein region of *xynI* cDNA (letters in bold type indicate the *xynI* coding sequence): 5′-CGG AAT TCC GAA C**AT GAA GTT CTT CGC CAC TAT T**-3′

(P2-1; forward) and 5′-CGG AAT TCC GTG ACA TCT A**AG AGA CAG TAA CGC T**-3′ (P2-2; reverse) containing *Eco*RI sites (underlined) for expression of the precursor protein with its own signal sequence using pPIC3.5; 5′-CCG GAA TTC **GCC GGC CCC GGT GGC ATC AAC TAC**-3′ (P2-3; forward) and 5′-TCC CCC GGG GGA TGA CAT CTA **AGA GAC AGT AAC GCT**-3′ (P2-4; reverse) containing *Eco*RI and *Sma*I sites (underlined) for fusion of the PHO1 signal peptide encoded in pHIL-S1 to the mature protein; and the P2-3 (forward) and P2-2 (reverse) primers for fusion of the α-MF signal peptide encoded in pPIC9 to the mature protein. These three amplified *xynI* cDNA fragments were digested with the appropriate endonucleases and cloned into pPIC3.5, pHIL-S1, and pPIC9 to yield pXYN119, pXYN118, and pXYN120, respectively.

Mutant plasmids Site-directed mutagenesis was performed using the overlap extension PCR method (Ho *et al.* 1989). The following internal mutagenic primers were designed to incorporate mutations (in bold type): D73N (forward), 5′-CAG CGG C**A**A CTT CGT CGT CG-3′; D73N (reverse), 5′-GT**T** GCC GCT GAC GCC GTT GG-3′; E153T (forward), 5′-CAC CGA C**AC T**CG CGT CAA TG-3′; E153T (reverse), 5′-**AGT** GTC GGT GCA GAC GGT GTA-3′; E157Q (forward), 5′-CGC GTC AAT **C**AG CCT TCC AT-3′; E157Q (reverse), 5′-**G**AT TGA CGC GCT CGT CGG TG-3′; V141C (forward), 5′-TAC CGT C**TG** CAG CGA TGG CG-3′; V141C (reverse), 5′-CAT CGC TG**C A**GA CGG TAC CG-3′; C150Y (forward), 5′-CAC CGT CT**A** CAC CGA CGA GC-3′; and C150Y (reverse), 5′-CGT CGG TG**T** AGA CGG TGT AG-3′.

For the first-round PCR, the P2-1 (forward) or P2-2 (reverse) external primer (see above) was used along with equimolar amounts of reverse or forward internal mutagenic primer, respectively. Mutated fragments were amplified using *xynI* cDNA as a template, DNA

polymerase (KOD -Plus-; Toyobo, Osaka) and dNTPs through 25 cycles of denaturation (15 s at 94ºC), annealing (30 s at 56ºC), and extension (1 min at 68ºC). Two amplified fragments having overlapping ends were precipitated by ethanol, redissolved, and combined. Subsequent 3′ extension of the complementary strand consisted of a denaturation step at 94˚C for 2 min and 5 cycles of the following steps: denaturation (15 s at 94˚C), annealing of the denatured fragments at the overlap (30 s at 60˚C), and extension (1 min at 68˚C). The mutant fusion product was gel-purified using the QIAquick gel extraction kit (Qiagen). Each purified product was amplified further by the second-round PCR using the P2-1 (forward) and P2-2 (reverse) primers. The amplified fragments, each carrying mutation that corresponded to D73N, V141C/C150Y, E153T, and E157Q, were digested with *Eco*RI and cloned into pPIC3.5 to yield pXYN128, pXYN129, pXYN131, and pXYN132, respectively. Sequences of the mutant plasmids were verified by DNA sequence analysis of the entire inserts.

Plasmid containing XynI pre-signal sequence To delete the 18-amino acid pro-region from the XynI prepro-signal sequence (Fig. 2-1), overlap extension was performed using the following internal primers: P2-5 (forward; 5′-AGC CGT CGC TGC CGG CCC CG-3′) and P2-6 (reverse; 5′-CGG GGC CGG CAG CGA CGG CT-3′) that are complementary to each other and correspond to the sequence at the pre-region (underlined) and mature XynI boundary. The amplified fragment was cloned into pPIC3.5 to yield pXYN123.

2-2-4. Transformation of P. pastoris

The resulting plasmids were linearized by digestion with *Sac*I to favor integration via homologous recombination at the *AOX1* locus. These DNA segments were used to transform

the yeast *P. pastoris* strain GS115 by electroporation pulsed at 6.25 kV/cm, 25 μF, and 200 Ohms using a Gene Pulser II with Pulse Controller (Bio-Rad) according to the manufacturer's instructions. As the corresponding controls, yeast cells were also transformed with the vector pPIC3.5, pHIL-S1, or pPIC9 using the same method. After pulsing, one ml of cold 1 M sorbitol was added to the cuvettes immediately, and His^+ transformants were recovered on MD plates (13.4 g/*l* of YNB w/o amino acids [Sigma], 4 μg/*l* of biotin, 20 g of dextrose, 15 g/*l* of agar). A representative transformant for each construct was selected for xylanase production in shake-flask cultures.

2-2-5. Media and culture conditions for P. pastoris transformants

P. pastoris transformants were inoculated into 20 ml of BMG medium (13.4 g/*l* of YNB, 4 μg/*l* of biotin, 10 g/*l* of glycerol, 100 mM potassium phosphate buffer [pH 6.0]) in 100-ml Erlenmeyer flasks. The pre-cultures were grown on an orbital shaker (150 rpm) at 30°C to an A_{600} of 1.3 to 1.6. The cells were harvested by centrifugation at 1,500 × *g* for 10 min and resuspended in 100 ml of BMMY medium (the same as BMG, except that glycerol was replaced by methanol [5 ml/*l*] and the medium was supplemented with yeast extract [10 g/*l*] and peptone [20 g/*l*]) in 500-ml Erlenmeyer flasks. The cultures were grown at 30°C under the same aerobic conditions. 0.5 ml of methanol was fed every 24 h during the culture period to enable methanol induction of the *AOX1* promoter. The growth of transformants was monitored by measuring the A_{600} periodically. Culture aliquots (1 ml) were collected daily and cells were removed by centrifugation at 10,000 × *g* for 10 min. The supernatant fluids were assayed for the xylanase activity as described below.

2-2-6. Enzyme and protein assays

Enzyme and protein assays used in this chapter are described in *1-2-2*.

2-2-7. Enzyme purification

The transformant cultures grown for 5 days were centrifuged at 4,000 × *g* for 25 min at 4ºC. Clear supernatant (200 ml) was concentrated to 35 ml by ultrafiltration through a 3×10^3 molecular-weight cut-off membrane (Diaflo YM3; Amicon) in a stirred cell. The concentrated sample was loaded to anion-exchange column of a Q-Sepharose HP (Amersham Biosciences) column (1.6 × 20 cm) that was equilibrated with 20 mM acetate buffer (pH 6.0). The adsorbed enzyme was eluted at a flow rate of 1.0 ml/min with a linear gradient of 0 to 0.5 M NaCl in the same buffer. The fractions exhibiting enzyme activity were pooled and then chromatographed on a Superdex 75 pg (Amersham Biosciences) column (1.6 × 60 cm) at a flow rate of 1.0 ml/min with 10 mM acetate buffer (pH 6.0) containing 0.15 M NaCl. The recombinant xylanase was eluted as a single protein peak that coincided with the peak of enzyme activity.

2-2-8. Effect of pH and temperature

The effects of pH and temperature on the xylanase activity of the recombinant enzyme and its variants were determined as described in *1-2-5*.

2-2-9. SDS–PAGE and N-terminal amino acid sequencing

SDS–PAGE and membrane transfer methods used in this chapter is described in *1-2-4*. N-terminal amino acid sequence was identified using a G1005A Hewlett-Packard protein

sequencer (Palo Alto, CA, USA).

2-2-10. Amino acid numbering

The standard amino acid numbering used in the text starts at the N-termini of the precursor proteins (see Fig. 2-1).

2-3. Results

2-3-1. Effect of signal sequences on secretion levels of recombinant xylanase from P. pastoris

The efficiency of xylanase secretion directed by the XynI signal peptide in *P. pastoris* was compared with those directed by the two yeast signal peptides from *P. pastoris* PHO1 and *S. cerevisiae* α-MF that were fused to the mature XynI protein. The 34 amino acid prepro-signal peptide of the *A. pullulans* XynI contains a putative recognition site for a signal peptidase in the endoplasmic reticulum and a processing site for a *KEX2*-like endopeptidase in the Golgi apparatus (Fig. 2-1A). The 89 amino acid prepro leader of *S. cerevisiae* α-MF consists of a 19 amino acid pre-signal sequence, a 66 amino acid pro-sequence and the repeats of spacer peptide (EAEA). However, the 22 amino acid signal peptide of the PHO1 lacks the pro-region. Three transformants showed similar growth curves, independent of the secretory signal contained (Fig. 2-2A). The three transformants secreted recombinant xylanases by signal peptides of *A. pullulans* XynI, *P. pastoris* PHO1, and *S. cerevisiae* α-MF during the 5 days of induction by methanol, and xylanase activities in the culture supernatants were 38, 15, and 38 U/ml, respectively (Fig. 2-2B). Control cells transformed with the corresponding

vector plasmids were devoid of the extracellular enzyme activity. On the basis of their specific activities of the purified enzymes (see *2-3-2*), the estimated concentrations of the recombinant xylanases in the culture medium were 178 mg/*l* for XynI, 180 mg/*l* for α-MF, and 100 mg/*l* for PHO1. Thus, the amount of recombinant xylanase secreted into the medium by the XynI signal peptide was comparable to that by the prepro leader of α-MF and two-fold higher than that by the PHO1 pre-type signal peptide, and was also higher than 60 mg/*l* previously reported for the *A. niger* xylanase secreted from *P. pastoris* using the 19 amino acid signal peptide of the *S. cerevisiae* invertase (Berrin *et al.* 2000).

2-3-2. Purification and properties of recombinant xylanase

Recombinant enzyme was purified from the culture supernatant after the *P. pastoris* transformant bearing the XynI signal peptide was grown for 5 days. The recovery yield was as high as 27.9%, and the specific activity was 213 U/mg, which was lower than that of the native enzyme (512 U/mg) (see *1-3-2*), probably because of slight miss folding. The specific activities of the other two recombinant xylanases purified for comparison were 210 U/mg for α-MF and 150 U/mg for PHO1. Analysis by SDS–PAGE of the purified recombinant xylanase revealed a single band with a M_r of 24,000, which was similar to that of the native enzyme purified from the culture filtrate of *A. pullulans* (Fig. 2-3). It is probable that the recombinant enzyme is *O*-linked glycosylated since there was no putative *N*-linked glycosylation site in the deduced amino acid sequence of *A. pullulans* XynI (see *1-3-6*). To confirm the two-step processing of the XynI prepro-signal sequence, the XynI without the pro-sequence was also expressed in the pXYN123 transformant. The N-terminal amino acid sequences of recombinant enzymes secreted from *P. pastoris* transformants bearing the XynI

prepro-signal sequence and only the pre-signal sequence were both determined to be A-G-P-G-G-I-N, which is identical to that of the native enzyme (see *1-3-3*). The results show that both the pre- and pro-signal peptides of *A. pulllulans* XynI were correctly recognized and processed by the *P. pastoris* secretory pathway.

The recombinant enzyme showed maximal activity at pH 2.5, and the pH-activity profile was similar to that of the native enzyme with an optimum pH of 2.0 (Fig. 2-4A). The temperature-activity profile of the recombinant enzyme shifted from that of the native enzyme to a temperature lower by 10 units, and the optimum temperature of the recombinant enzyme was 40˚C (Fig. 2-4B).

A

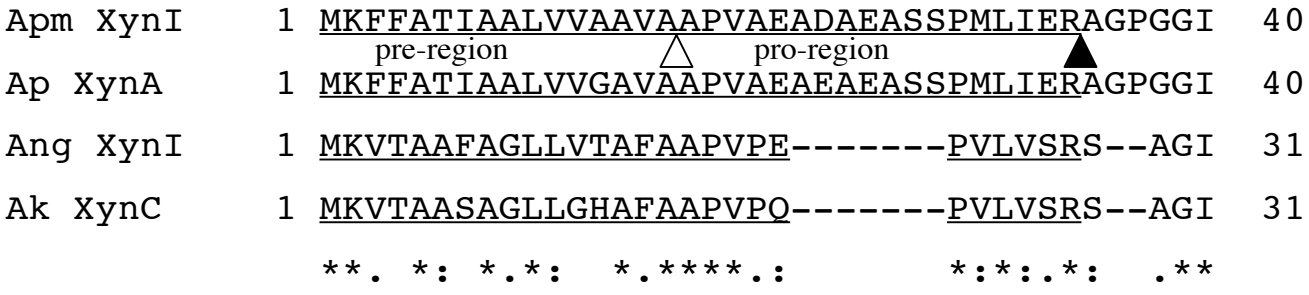

B

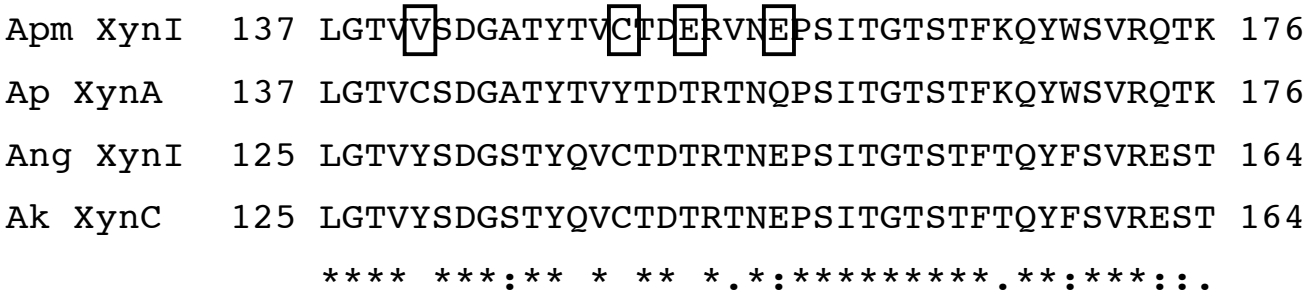

Fig. 2-1. Alignment of N-terminal (A) and internal (B) amino acid sequences of *A. pullulans* ATCC 20524 XynI and homologous xylanases.

Apm, *A. pullulans* var. *melanigenum* ATCC 20524; Ap, *A. pullulans*; Ang, *A. niger*; Ak, *A. kawachii*. The alignment was done using the CLUSTAL W program. Dashes indicate gaps introduced during the alignment process. Asterisks indicate identity, and single and double dots indicate semiconservative and conservative replacements, respectively. The signal peptides are underlined. Putative recognition sites for the signal peptidase and *KEX2*-like endopeptidase in the XynI signal peptide are shown by open and solid arrowheads, respectively. The boxed residues in XynI indicate the sites for targeted mutagenesis to be used in this study.

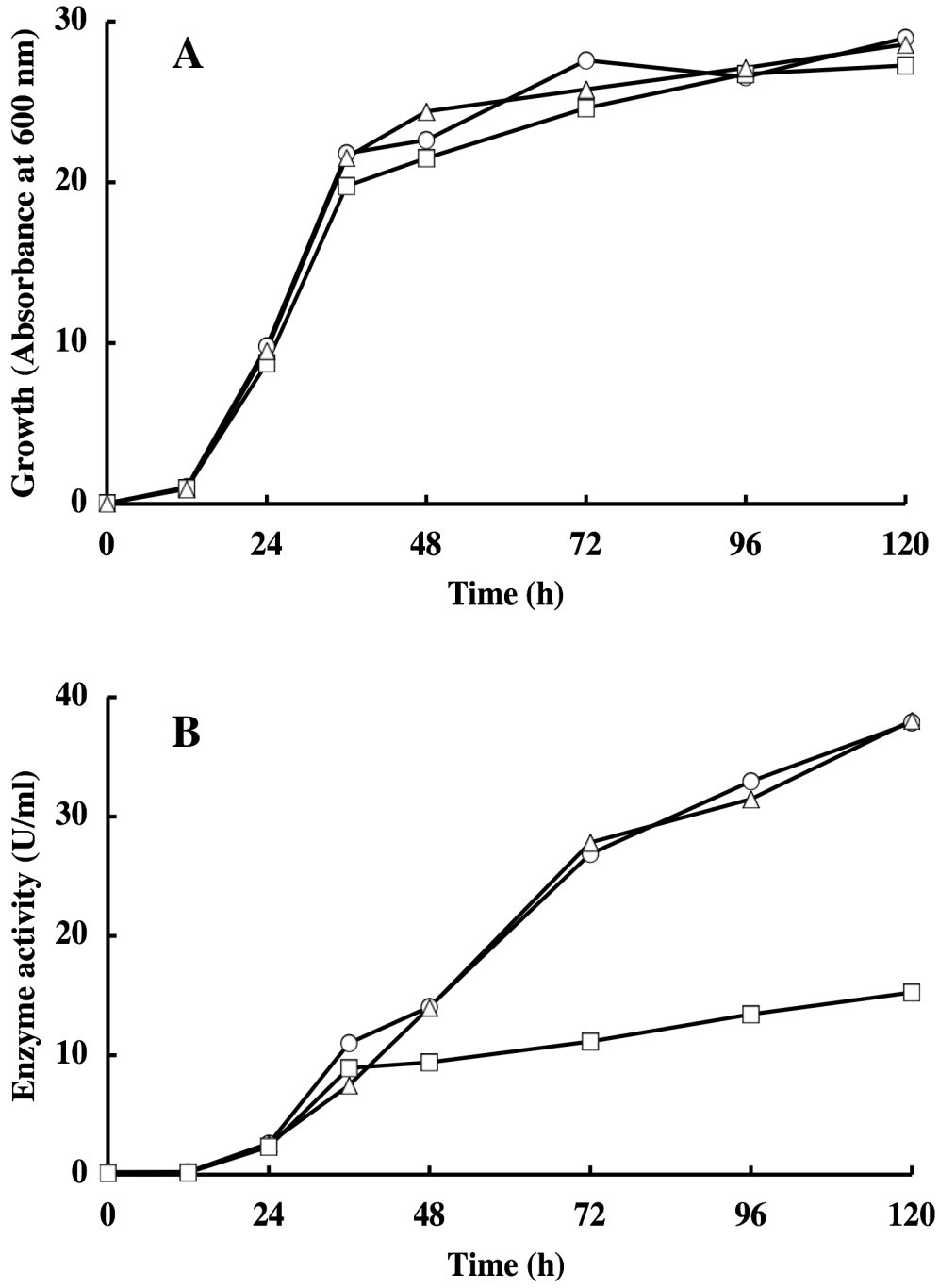

Fig. 2-2. Growth (A) and extracellular enzyme production (B) in shake-flask cultures of *P. pastoris* transformants.

The *P. pastoris* transformants were grown at 30ºC in the buffered methanol complex medium. The values represent the means of three independent experiments. Symbols: circles, XynI signal peptide; squares, PHO1 signal peptide; triangles, α-MF signal peptide.

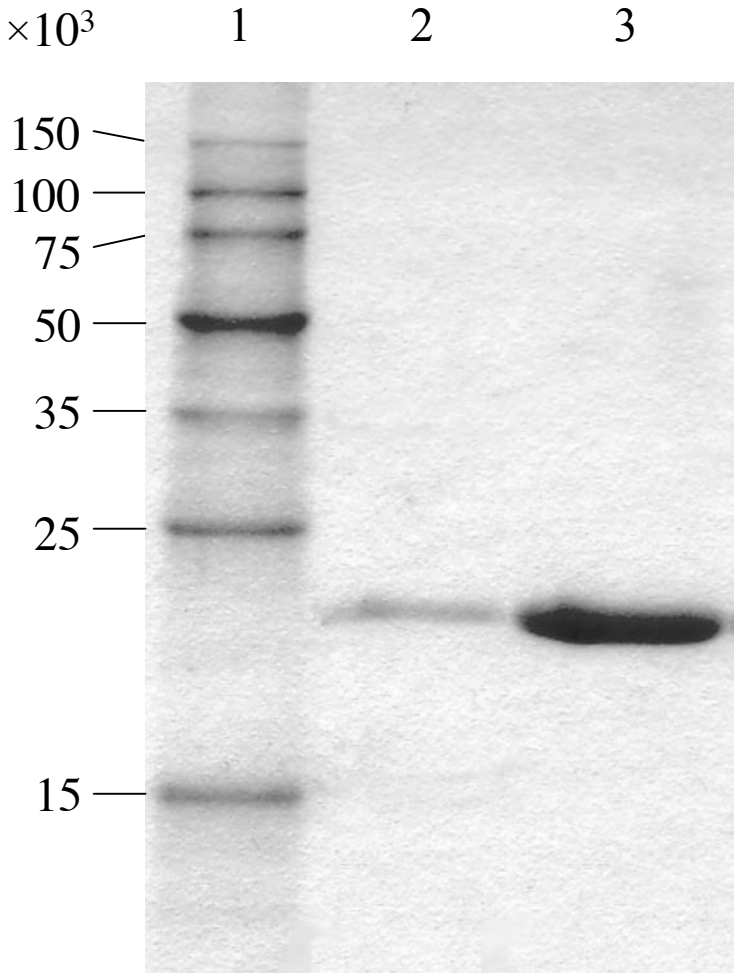

Fig. 2-3. SDS–PAGE analysis of purified native and recombinant xylanases.

SDS–PAGE was done using a 12.5% (w/v) polyacrylamide slab gel. Protein was stained by Coomassie Brilliant Blue R-250. Lanes: 1, standard proteins; 2, the native xylanase; 3, the recombinant xylanase.

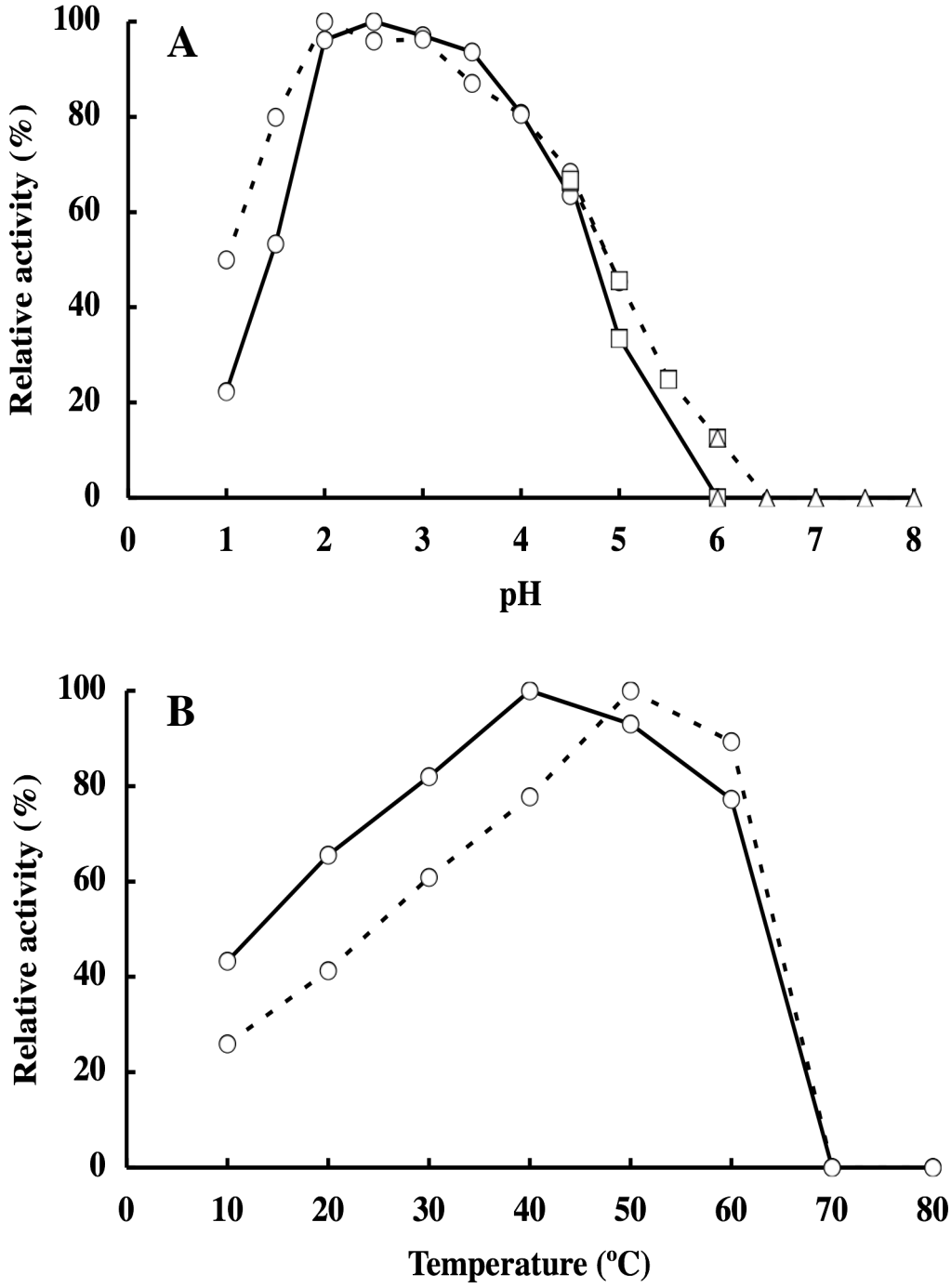

Fig. 2-4. Effect of pH (A) and temperature (B) on the enzyme activity of recombinant xylanase.

The broken lines indicate the previous data of the native enzyme (see Chapter I). Relative activity was expressed as percentage of the highest activity. The values represent the means of three measurements. (A) The enzyme activity was determined using 0.1 M sodium acetate–HCl (pH 1.0 to 4.5), 0.1 M acetate (pH 4.5 to 6.0), and 0.1 M phosphate (pH 6.0 to 8.0) buffers. (B) The enzyme activity was determined using various temperatures at pH 2.0. Symbols: circles, sodium acetate-HCl buffer; squares, acetate buffer; triangles, phosphate buffer.

2-3-3. Structural prediction of XynI

A. pullulans XynI showed 66% sequence identity to acidophilic xylanases, *A. niger* xylanase I and *Aspergillus kawachii* xylanase C (XynC), for which 3D structures were available (Krengel and Dijkstra 1996; Fushinobu *et al.* 1998). Based on the common sequence pattern between *A. pullulans* XynI and the *Aspergillus* enzymes, the author generated a plausible 3D model for the *A. pullulans* XynI protein using Swiss-Model (Peitsch 1995; Guex and Peitsch 1997; Schwede *et al.* 2003) (Fig. 2-5). The overall structure of the XynI has the shape of a "right hand" in common with family-11 xylanases (Krengel and Dijkstra 1996; Fushinobu *et al.* 1998; Törrönen *et al.* 1994) and is composed of the "fingers" at the top, the "palm" at the right-hand side, and the "thumb" at the bottom of the molecule. The active site was located within an extended open cleft, which is lined with many aromatic residues and is large enough to accommodate the xylan polymers. The two conserved glutamate residues, Glu-114 and -208, which could be involved in catalysis as a nucleophile and an acid-base catalyst, respectively, extend their side chains to the bottom of the cleft from the opposite sides. Some aromatic residues forming subsites were also suggested to be structural features among acidophilic xylanases (Fushinobu *et al.* 1998).

2-3-4. Mutational analyses of amino acid residues potentially responsible for the low pH optimum of xylanase

Conserved Asp residue in xylanases with low pH optima An Asp-64 residue of the *A. niger* xylanase I is suggested to be critical for its low pH optimum of 3.0 (Krengel and Dijkstra 1996). Subsequent studies of the *A. kawachii* XynC by X-ray crystallography and

site-directed mutagenesis showed the importance of the equivalent Asp-64 residue in the low pH optimum of 2.0 (Fushinobu *et al.* 1998). Availability of the *P. pastoris* expression system and the 3D structure of the *A. pullulans* xylanase allowed to determine whether the corresponding Asp-73 residue is responsible for the acidophilicity by means of site-directed mutagenesis and to map its position at the upper edge of the active site cleft (Fig. 2-5). The activity of the D73N variant decreased to about 19% of that of the wild-type XynI and its optimum pH shifted upward (Fig. 2-6).

Amino acid residues substituted between A. pullulans XynI and XynA The amino acid sequences of XynI (see *1-3-6*) and the equivalent xylanase XynA from *A. pullulans* strain Y-2311-1 (Li and Ljungdahl 1994) differ in 10 out of 187 residues. Despite the high identity of these sequences, the *A. pullulans* XynA has an optimal pH of 4.8 (Li *et al.* 1993). Among the 10 amino acid substitutions in XynI *ver* XynA, the four residues at positions 141 (Val *ver* Cys), 150 (Cys *ver* Tyr), 153 (Glu *ver* Thr), and 157 (Glu *ver* Gln) (Fig. 2-1B) were hypothesized to be responsible for its lower pH optimum on the basis of their positions in the predicted 3D structure. Accordingly, the author constructed three mutant plasmids, pXYN129 (V141C/C150Y), pXYN131 (E153T), and pXYN132 (E157Q). The E153T and E157Q variants secreted from *P. pastoris* were enzymatically active, but not the double mutant V141C/C150Y probably due to misfolding and aggregation (data not shown). The optimum pH of the E157Q variant shifted to 3.5, the variant retained the activity of the wild-type enzyme (Fig. 2-6).

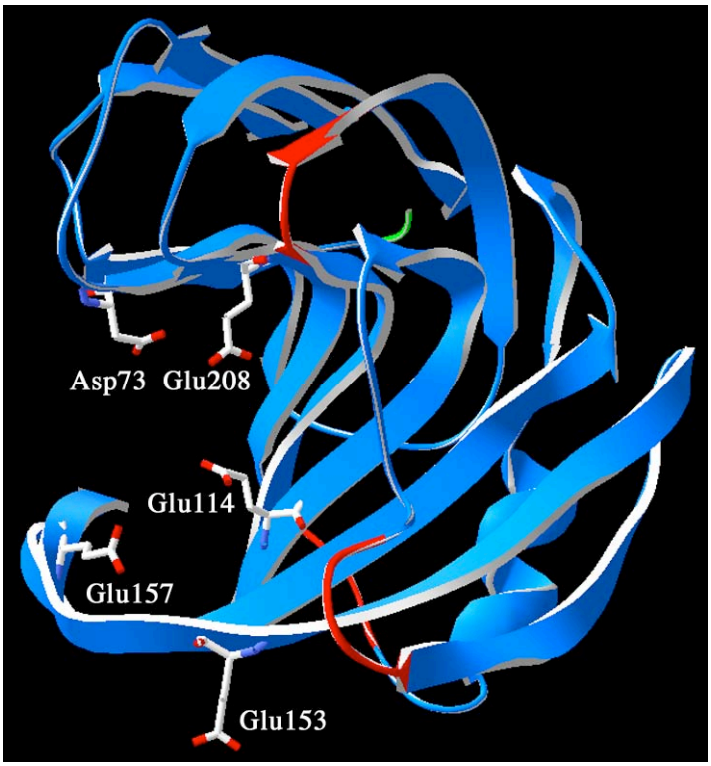

Fig. 2-5. Hypothetical 3D structure proposed for *A. pullulans* XynI protein.

The ribbon diagram was created on the basis of its homology with the structures of *Aspergillus* xylanases using the Swiss-Model server and DeepView software.

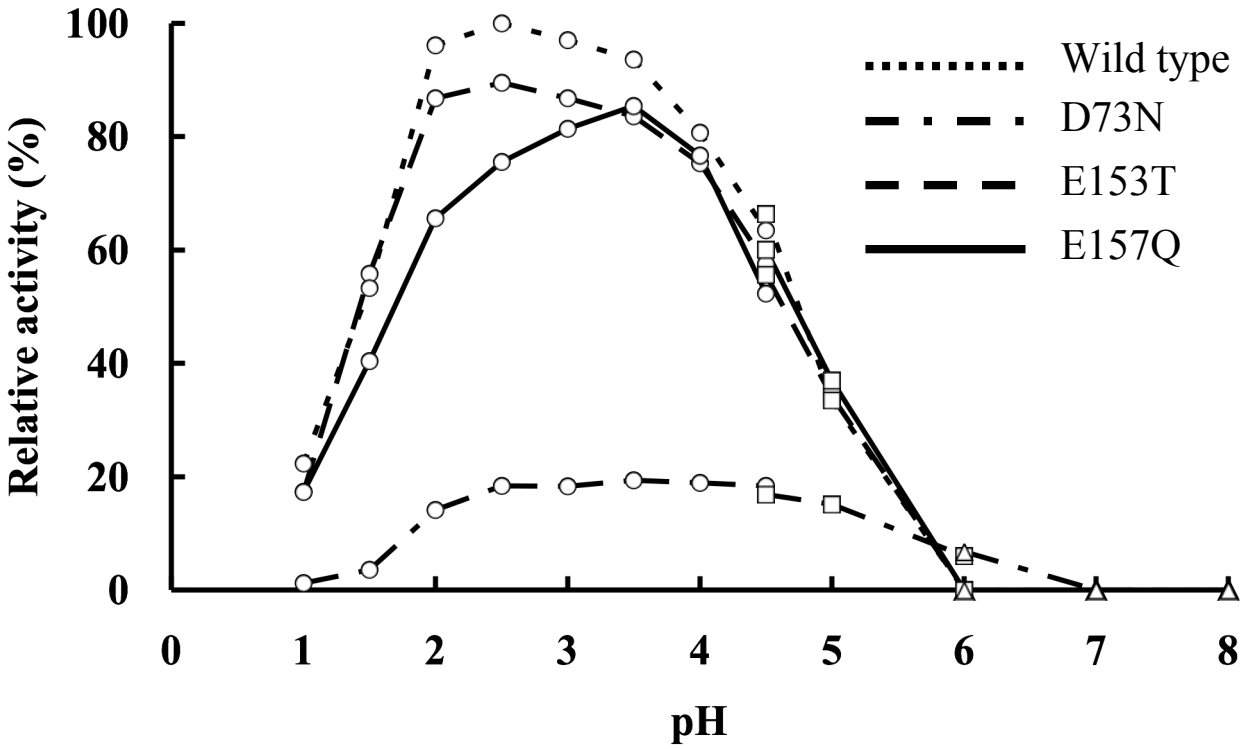

Fig. 2-6. Effect of pH on the enzyme activities of the mutant xylanases.

The values correspond to the averages of three measurements. Relative activity was expressed as a percentage of the highest activity of the recombinant wild-type enzyme (see Fig. 2-4A). Symbols: circles, sodium acetate-HCl buffer; squares, acetate buffer; triangles, phosphate buffer.

2-4. Discussion

The deletion analysis of signal peptide and N-terminal amino acid sequence of secreted xylanases in *P. pastoris* revealed that the secretory signal sequence of XynI from *A. pullulans* (see Chapter I) had two potential cleavage sites. Accordingly, it seemed the signal sequence is prepro-type signal peptide. And the amount of expressed xylanase by the XynI secretory signal was the same as the level of α-MF. These results showed that the signal of XynI could lead to secreting a large amount of protein in culture medium and could be probably useful for industrial application.

The mutational analysis of Asp-73 and Glu-157 showed the higher optimum pH than the wild type. Additively, the D73N variant decreased to about 19% of the xylanase activity; it is likely that the asparagine residue of the variant maintains the hydrogen bond with the acid-base catalyst Glu-208 and this interaction prevents the proton of Glu-208 from dissociating as described for the *A. kawachii* XynC (Fushinobu *et al.* 1998). The E157Q variant shifted the optimum pH to 3.5 without decrease in the xylanase activity. These results showed that Glu-157 partially determines the pH dependence of activity by a different mechanism from that of Asp-73; the Glu-157 residue located in the thumb at the bottom and pointing into the active site is protonated at low pH, so that electrostatic repulsion would disappear between the cleft and the xylan that exhibits a certain degree of negative charge due to glucuronic acid substituents. The E157Q variant showed enzyme activity in the higher pH range, probably because the Gln-157 residue in the variant suppressed the repulsion at a higher pH than glutamate. Although a number of threonine residues were highly conserved in the same region of several family-11 xylanases of fungal origin and have their side chains

highly solvent-exposed (Tahir *et al.* 2002), one of the conserved residues was replaced with Glu-153 in XynI (Fig. 2-1B). Unlike Glu-157, the carboxyl group of a closely neighboring residue Glu-153 in the thumb region protrudes into the solvent (Fig. 2-5). The E153T variant did not differ from the wild type in xylanase activity or pH optimum, suggesting that the Glu-153 residue was not related to optimum pH (Fig. 2-6).

In conclusion, this is the first description of the functional expression of *A. pullulans* xylanase in *P. pastoris* and the high secretion level using its own signal sequence. The mutational analysis of the recombinant xylanase based on the structural comparison of related xylanases suggested that Glu-157 as well as Asp-73 at the edge of the active site cleft play a significant role in its acidophilicity.

Chapter III

Purification and characterization of a family-10 xylanase from *Aureobasidium pullulans* and sequence analysis of the encoding gene

3-1. Introduction

Endo-1,4-β-xylanases have been classified into two GH families, family 10 (formerly F) and 11 (formerly G), on the basis of amino acid sequence similarities (Henrissat 1991; Henrissat and Bairoch 1993). Family 11 consists of xylanases with a relatively low M_r ranging from 19,000 to 25,000, whereas the family 10 comprises xylanases with a higher M_r of >30,000. A hierarchy among the family-11 and -10 xylanases was proposed for microbial degradation of plant cell wall xylan to xylose (Pell *et al*. 2004). In *A. pullulans*, several xylanases were purified and the encoding genes were cloned. To date, however, there have been no reports of family-10 xylanases from *A. pullulans*.

This chapter describes the purification and properties of an extracellular family-10 xylanase from the fungal strain and the cloning and sequencing of a genomic DNA and cDNAs encoding the enzyme. Moreover, the author defined the phylogenetic position of the *A. pullulans* xylanase among homologous xylanases belonging to family 10.

3-2. Materials and methods

3-2-1. Strain and culture conditions

A wild-type strain *A. pullulans* var. *melanigenum* ATCC 20524 was used in this study. Growth medium contained 6.7 g/*l* of YNB (Difco) and 10 g/*l* of oat-spelt xylan (Sigma) as the

sole carbon source in 0.1 M phosphate buffer (pH 6.0) unless otherwise stated. Liquid cultures were grown on a rotary shaker (150 rpm) in 500-ml Erlenmeyer flasks containing 100 ml of medium at 30ºC for the time specified in the text.

3-2-2. Enzyme and protein assays

The reaction mixture consisted of 0.2 ml of a 1.0% (w/v) suspension of oat-spelt xylan in deionized water and 0.2 ml of a suitably diluted enzyme solution in 0.1 M sodium acetate-HCl buffer (pH 6.0). After incubation at 45°C for 30 min, reducing sugars were determined by the method of Somogyi and Nelson (Somogyi 1952; Nelson 1955). The unit definition of xylanase activity is described in *1-2-2*. To study the substrate specificity, the reaction mixture consisting of 0.5 ml of the enzyme solution and 0.5 ml of 10 mM *p*-nitrophenyl (*p*NP) glycosides (*p*NP-β-D-cellobioside, *p*NP-β-D-xylopyranoside, and *p*NP-α-L-arabinofuranoside; Sigma) was incubated at 45ºC for 10 min. The reaction was terminated by the addition 1.0 ml of 1 M Na_2CO_3, and A_{410} was measured. One unit (U) of enzyme activities toward *p*-nitrophenyl glycosides was defined as the amount of enzyme that liberated 1 μmol of *p*-nitrophenol per min from each substrate. Protein concentrations were measured as described in *1-2-2*.

3-2-3. Enzyme purification

The submerged cultures grown for 5 days were centrifuged for 30 min at 6,000 × *g* at 4°C. The culture supernatant (1,900 ml) was concentrated to about one-tenth of its original volume in dialysis tubing surrounded by a thick layer of dry polyethylene glycol 20,000 (Wako). The sample was further concentrated in an ultrafiltration cell by passage through a 3

× 10^3 molecular-weight cut-off membrane (Diaflo YM3; Amicon). The concentrate was subjected to cation exchange chromatography on a CM-Cellulofine C-500 (Seikagaku Kogyo) column (2.6 × 45 cm) that had been equilibrated with 20 mM acetate buffer (pH 6.0). The adsorbed proteins were eluted at a flow rate of 1.0 ml/min with a linear gradient of 0 to 1.0 M NaCl in the same buffer. The fractions exhibiting the enzyme activity were pooled and further purified by gel-permeation chromatography on a Superdex 75 pg (Amersham Biosciences) column (1.6 × 60 cm) at a flow rate of 0.5 ml/min with 10 mM acetate buffer (pH 6.0) containing 0.15 M NaCl.

3-2-4. SDS–PAGE, N-terminal amino acid sequencing, and IEF

SDS–PAGE, IEF, and membrane transfer methods used in this chapter are described in *1-2-4*. For the internal sequencing, the purified enzyme was cleaved by protease from *Staphylococcus aureus* V8 (Wako) using Cleveland method (Cleveland *et al.* 1977). The resulting peptide fragments were separated by SDS–PAGE. N-terminal amino acid sequence was identified using a Procise 492 protein sequencing system (Applied Biosystems).

3-2-5. TLC analysis

The reaction mixture (50 μl) consisting of equal volumes of a 1% (w/v) solution of xylooligosaccharides (Megazyme, Wicklow, Ireland) or 3% (w/v) suspension of birch-wood xylan (Sigma) and the enzyme solution (20 mU/ml) in 50 mM phosphate buffer (pH 6.0) was incubated at 45ºC. Hydrolysis was stopped by boiling for 10 min, and the hydrolysis products were analyzed for TLC on silica gel plates (Merck AG, Darmstadt, Germany). The TLC plates were developed twice at room temperature with a solvent system of 1-butanol, pyridine,

and water (3:2:1, v/v). Spots were stained by spraying the plates with orcinol-sulfuric acid reagent and then heating at 120ºC for 5 min.

3-2-6. DNA manipulations and analyses

DNA manipulations and analyses were carried out as described in *1-2-7*, except that the reaction ready mixture and PCR instrument were replaced by the BigDye Terminator, version 3.1, cycle sequencing kit (Applied Biosystems) and the Thermal Cycler Dice (Takara Bio), respectively.

3-2-7. Construction of xylanase-specific DNA probe

A pair of degenerate 20-mer oligonucleotides was designed and synthesized according to the N-terminal amino acid sequence G-L-A-Q-A-W-T and the internal amino acid sequence M-K-W-E-S-T-E of the purified enzyme (see *3-3-1*): P3-1 (forward; 5′-GGY CTY GCY CAG GCY TGG AC-3′) and P3-2 (reverse; 5′-TCR GTR SWY TCC CAY TTC AT -3′). The primers amplified a 152-bp internal coding region of the potential xylanase gene, designated as *xynII*, from the *A. pullulans* genomic DNA as the template. The amplified fragment was cloned into pCR2.1-TOPO with the TOPO TA cloning kit (Invitrogen) and sequenced to confirm its identity. The DNA fragment was then labeled with DIG by the random-primed method using DIG DNA labeling and detection kit (Roche Diagnostics) for use as hybridization probe using the methods described in *1-2-8* to *-10*.

3-2-8. Isolation of poly(A)$^+$ RNA and cDNA cloning

Mycelia were harvested from 72-h-old cultures by centrifugation, and total RNA was isolated using an ISOGEN RNA isolation kit (Wako). Poly(A)$^+$ RNA was obtained from total RNA by PolyATract mRNA Isolation System IV (Promega, Madison, WI, USA). The 5′ and 3′ ends of *xynII* transcripts were determined by 5′ and 3′ RACE using a SMART RACE cDNA amplification kit (Clontech) as described in *1-2-11*. For 5′ RACE, P1-5 (NUP provided in the kit, see *1-2-11*) and P3-3 (5′-TCG GTA GAC TCC CAC TTC AT-3′ complementary to nt 285 to 304 relative to the A of the ATG start codon [see Fig. 3-5]) were used. For 3′ RACE, P3-4 (5′-AGA ATG CCA TGA AGT GGG A-3′ corresponding to nt 277 to 295) and P1-5 (see above) were used. The 5′ and 3′ RACE products were cloned into pCR2.1-TOPO and sequenced.

3-2-9. Quantitative real-time PCR

Mycelia were harvested from 72-h-old culture grown with pH control at pH 6.0 or 8.0 by 0.1 M phosphate buffer or without pH control (initial pH of 6.0). Total RNA was extracted from each mycelium as described in *3-2-8*. First-strand cDNA was synthesized using total RNA as template and oligo-dT primers by reverse transcriptase (ReverTra Ace; Toyobo). The *xynII* transcripts were quantified by real-time PCR with an ABI Prism 7000 (Applied Biosystems) using the first-strand cDNA as the template and SYBR *Premix Ex Taq* (Takara Bio) according to the manufacturer's instructions. Quantification was based on 104-bp amplicons generated using the following gene-specific primers: P3-5 (forward; 5′-CCA CTG ACG CGA AGC TCA A-3′) and P3-6 (reverse; 5′-GGA AAC ACC CCA GAC AGT GAT AC-3′; the coding region interrupted by intron) for the *xynII*, and P3-7 (forward; 5′-AGG

CCA GCA GCC CTA TGC-3′) and P3-8 (reverse; 5′-GGC GTT CTC GTT GTA GGT GAA-3′) for the *xynI*. The expression of a housekeeping 18S rRNA gene of *A. pullulans* (Li *et al*. 1996) as an endogenous reference was measured in parallel PCR runs using P3-9 (forward; 5′-TTG TCT GCT TAA TTG CGA TAA CGA-3′) and P3-10 (reverse; 5′-GCT TGA GCC GAT AGT CCC TCT AA-3′). The thermal cycle program consisted of an initial step of 95ºC for 10 s and 50 cycles of 95ºC for 5 s and 60ºC for 31 s. After determining amplifications, the target specificity was examined by the melting-point analysis of RT-PCR products using a dissociation protocol in which the temperature was raised linearly from 60ºC. Each dissociation curve of the amplicons was observed as a single peak. In addition, amplicons of the expected size were confirmed by agarose gel electrophoresis. Real-time PCR data were processed using the relative quantitative method based on simulation of PCR kinetics (Liu and Saint 2002). Amplification efficiencies were calculated for each sample as

$$E = \left(\frac{R_{n,A}}{R_{n,B}} \right)^{\frac{1}{C_{T,A} - C_{T,B}}} - 1$$

where R_n is reporter fluorescence at cycle n, $R_{n,A}$ and $R_{n,B}$ are R_n at arbitrary thresholds A and B in an individual curve, respectively, and $C_{T,A}$ and $C_{T,B}$ are the threshold cycles at these arbitrary thresholds. Normalization of *xynII* expression level to that of the *rRNA* gene was presented as

$$\frac{R_{0,xynII}}{R_{0,rRNA}} = \frac{(1 + E_{rRNA})^{C_{T,rRNA}}}{(1 + E_{xynII})^{C_{T,xynII}}}$$

where $R_{0,xynII}$ and $R_{0,rRNA}$ are the initial copy numbers and $C_{T,rRNA}$ and $C_{T,xynII}$ are threshold cycles at the arbitrary thresholds. In this experiment, the *xynII* transcript level observed in *A. pullulans* grown without pH control was treated as the basal expression level.

3-2-10. Construction of yeast expression plasmid and P. pastoris transformation

The *xynII* cDNA encoding the precursor protein that includes a secretory signal sequence was amplified from the first strand cDNA as the template with a pair of primers P3-11 (5′-GGA ATT CC**A TGC ACT TCT CCA CAA TCA C**-3′; forward) and P-3-12 (5′-GGA ATT CCT GAA TAC AAC TTG ATA CAT T-3′; reverse) (letters in bold type indicate the *xynII* coding sequence) containing *Eco*RI sites (underlined). The PCR product was cloned into the integrative yeast expression vector pPIC3.5 (Invitrogen) at *Eco*RI site in the orientation of transcription from *AOX1* promoter, yielding pXYN207. The pXYN207 was linearlized with *Sac*I, and the yeast *P. pastoris* GS115 (Invitrogen) was transformed with the DNA fragment by electroporation as described in *2-2-4*.

3-2-11. Culture conditions for P. pastoris transformants and purification of recombinant enzyme

P. pastoris transformants were grown in 500-ml Erlenmeyer flasks on an orbital shaker (150 rpm) at 30ºC for 3 days. Each flask contained 100 ml of the buffered methanol-complex medium as described in *2-2-5*. Additional methanol was supplied every 24 h to give a final concentration of 0.5% (v/v) during the culture period. Clear supernatant obtained from the contents of duplicate flasks was dialyzed against deionized water and lyophilized. The lyophilized sample was dissolved in 5 ml of 20 mM acetate buffer (pH 6.0) and subjected to purification by SP-Sepharose (Amersham Biosciences) and Superdex 75 pg column chromatographies.

3-2-12. Nucleotide sequence accession number

The nucleotide sequence of the 3,293-bp region containing the *xynII* gene has been deposited in the DDBJ/EMBL/GenBank nucleotide sequence databases with the accession number AB201542.

3-3. Results

3-3-1. Purification and properties of the xylanase

Table 3-1 summarizes the procedure for the purification of family-10 xylanase from *A. pullulans*. Cation exchange chromatography of the adsorbed proteins on a CM-Cellulofine column resulted in one major peak of xylanase with activity measured at pH 6.0. The family-10 xylanase was eluted from a Superdex 75 pg column as a single protein peak that coincided with the peak of enzyme activity. This protocol afforded a 48-fold purification of the xylanase from the culture supernatant with a yield of 27%. The enzyme was homogeneous as judged by SDS–PAGE and IEF (Fig. 3-1A, B), which showed an apparent M_r of 39,000 and a p*I* of 8.9, respectively. The purified enzyme had a specific activity of 29.5 U/mg. The N-terminal amino acid sequencing identified the first 17 residues: S-Y-S-K-N-Q-G-L-A-Q-A-W-T-S-K-G-R. Internal sequences were identified for the two peptide fragments recovered after cleavage by V8 protease: N-A-M-K-W-E-S-T-E-P and L-D-V-R-F-T-T-P-A-T.

The xylanase activity was optimal at pH 6.0 and 70ºC (Figs. 3-2A and 3-3A). The enzyme retained greater than 80% of the original activity between pH 4.0 to 10.0 (Fig. 3-2B). The enzyme remained stable up to 70ºC, but it lost the activity at 80ºC (Fig. 3-3B). The

xylanase activity was not influenced by EDTA (112%), guanidine hydrochloride (110%), and *p*-chloromercuribenzoate (109%) at a final concentration of 1 mM, suggesting that any metal ions and sulfhydryl groups in the enzyme were not essential for the enzymatic activity.

The purified xylanase was studied for its substrate specificity. The xylanase hydrolyzed birch-wood xylan (Sigma) with a similar activity toward oat-spelt xylan (Table 3-2). This enzyme also showed weak activities toward *p*NP-β-D-cellobioside and *p*NP-β-D-xylopyranoside, but no detectable activity toward carboxymethyl cellulose and *p*NP-α-L-arabinofuranoside. TLC analysis indicated that initial hydrolysis of birch-wood xylan by the xylanase yielded a series of oligosaccharides with a DP of two and above (Fig. 3-4A). Xylotriose was produced as an intermediate that was eventually cleaved to xylobiose and xylose. The enzyme hydrolyzed xylotriose, xylotetraose, and xylopentaose, but not xylobiose (Fig. 3-4B).

Table 3-1. Purification of extracellular GH family-10 xylanase from *A. pullulans*.

Step	Total activity (U)	Total protein (mg)	Specific activity (U/mg)	Purification (fold)	Yield (%)
Culture supernatant	186	301	0.6	1.0	100
Ultrafiltration	175	145	1.2	2.0	94
CM-Cellulofine	98.3	11.0	8.9	14.5	53
Superdex 75 pg	50.3	1.7	29.5	47.7	27

Table 3-2. Substrate specificity of GH family-10 xylanase from *A. pullulans*.

Substrate	Specific activity (U/mg)
Oat-spelt xylan	29.5
Birch-wood xylan	35.0
Carboxymethyl cellulose	ND
*p*NP-β-D-cellobioside	0.23
*p*NP-β-D-xylopyranoside	0.02
*p*NP-α-L-arabinofuranoside	< 0.01

Experimental conditions are described in the text (see *3-2-2*).

ND, Not detected.

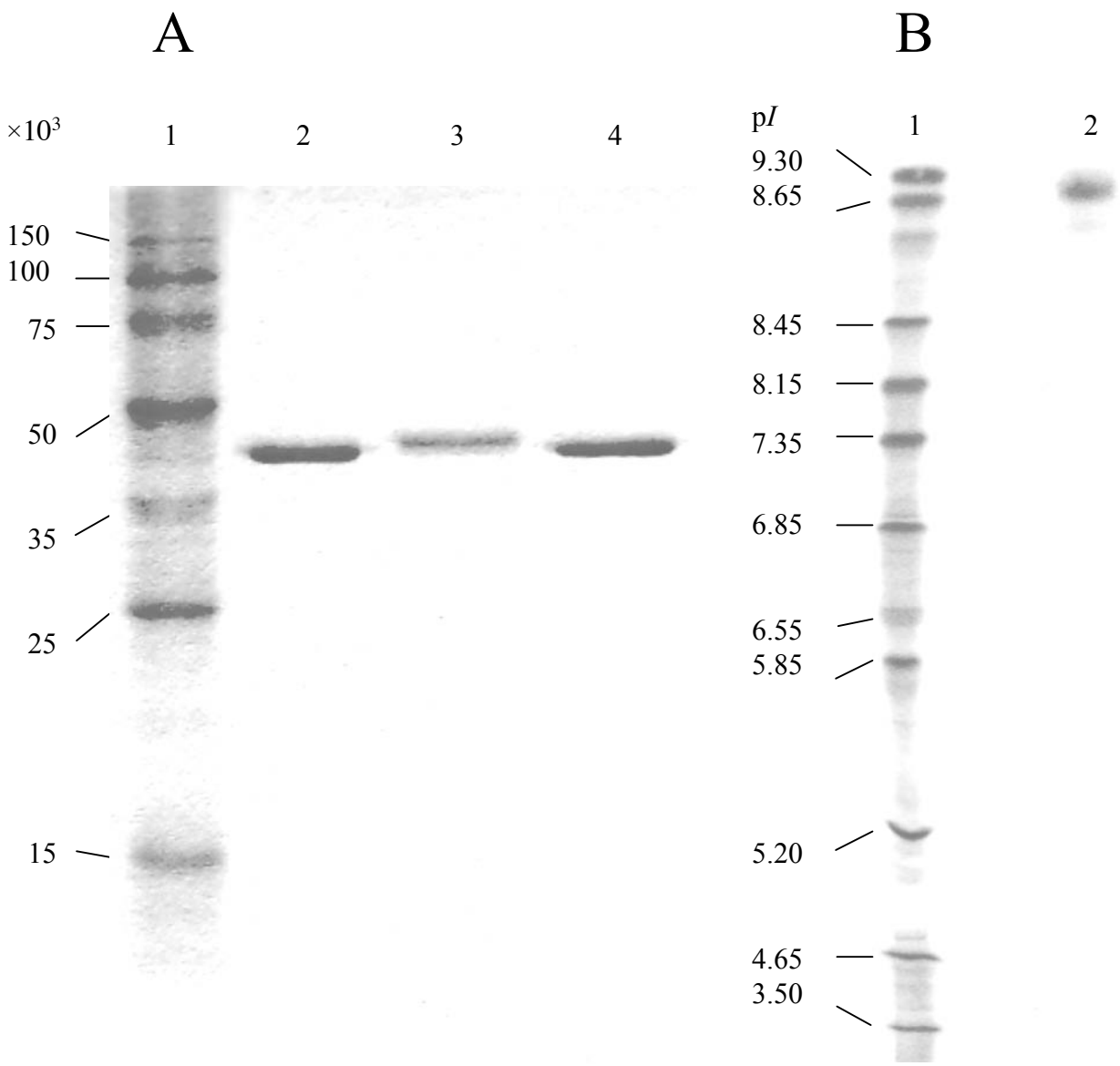

Fig. 3-1. SDS-PAGE (A) and IEF (B) of purified native xylanase from *A. pullulans* ATCC 20524 and the recombinant xylanases expressed in *P. pastoris*.

Protein was visualized by Coomassie Brilliant Blue R-250 staining. Lanes: 1, standard proteins; 2, the native xylanase; 3, the recombinant xylanase P-1; and 4, the recombinant xylanase P-II.

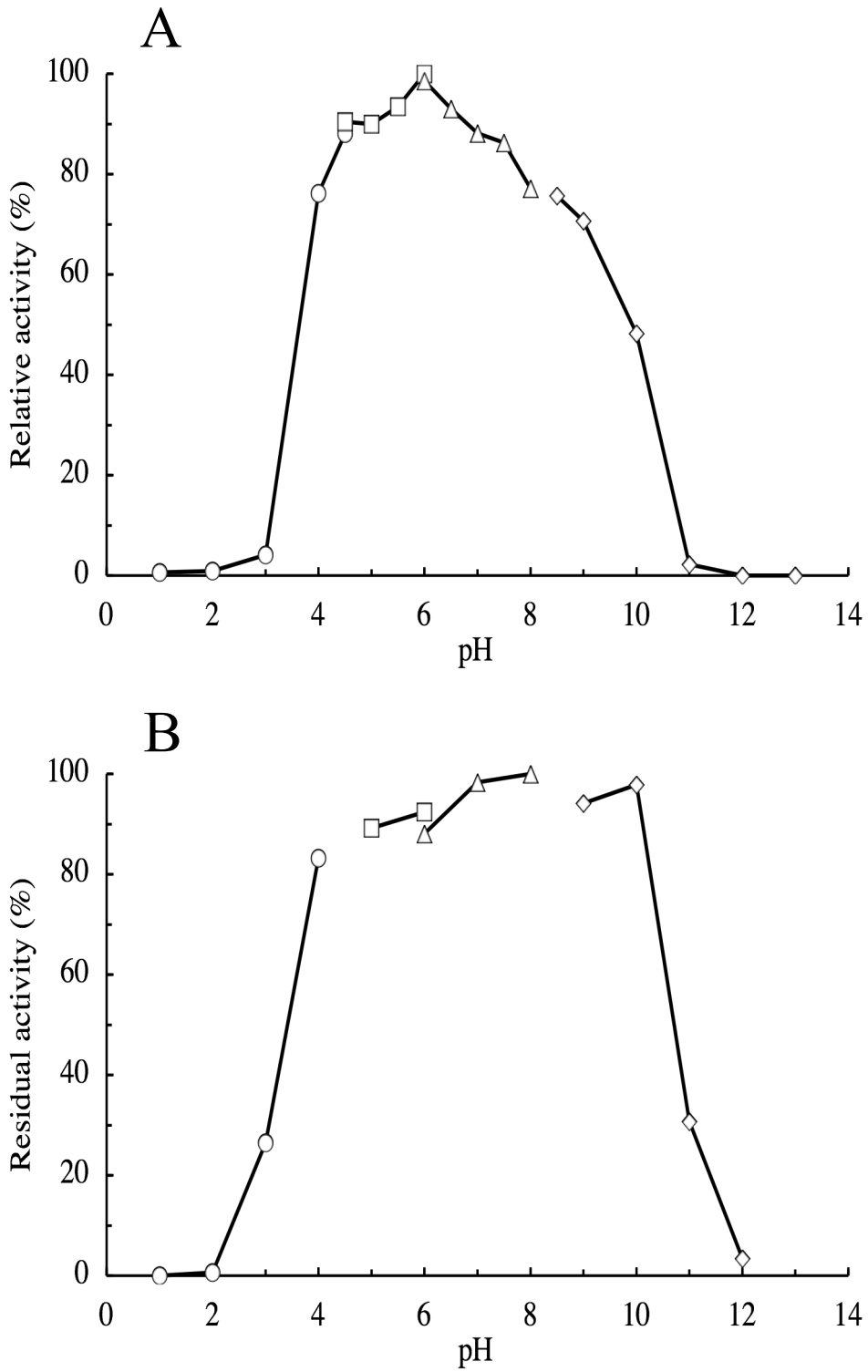

Fig. 3-2. Effect of pH on activity (A) and stability (B) of purified xylanase from *A. pullulans* ATCC 20524.

The reaction conditions are described in the text (see *1-2-5*). Relative and residual activities were expressed as percentage of the highest activity and the initial activity, respectively. Symbols: circles, sodium acetate-HCl buffer; squares, acetate buffer; triangles, phosphate buffer; diamonds, glycine-NaOH buffer.

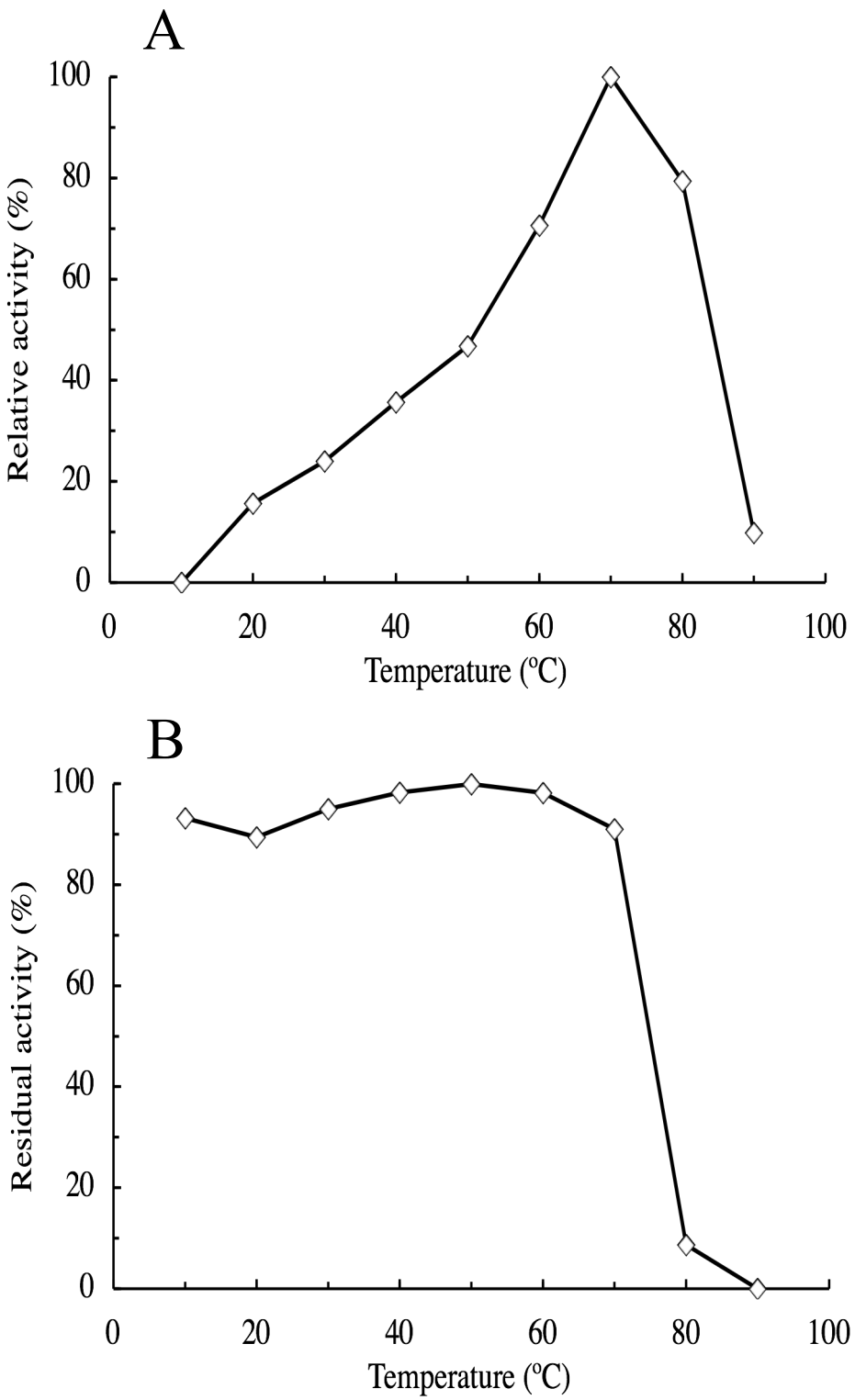

Fig. 3-3. Effect of temperature on activity (A) and stability (B) of purified xylanase from *A. pullulans* ATCC 20524.

The reaction conditions are described in the text (see *1-2-5*). Relative and residual activities were expressed as percentage of the highest activity and the initial activity, respectively.

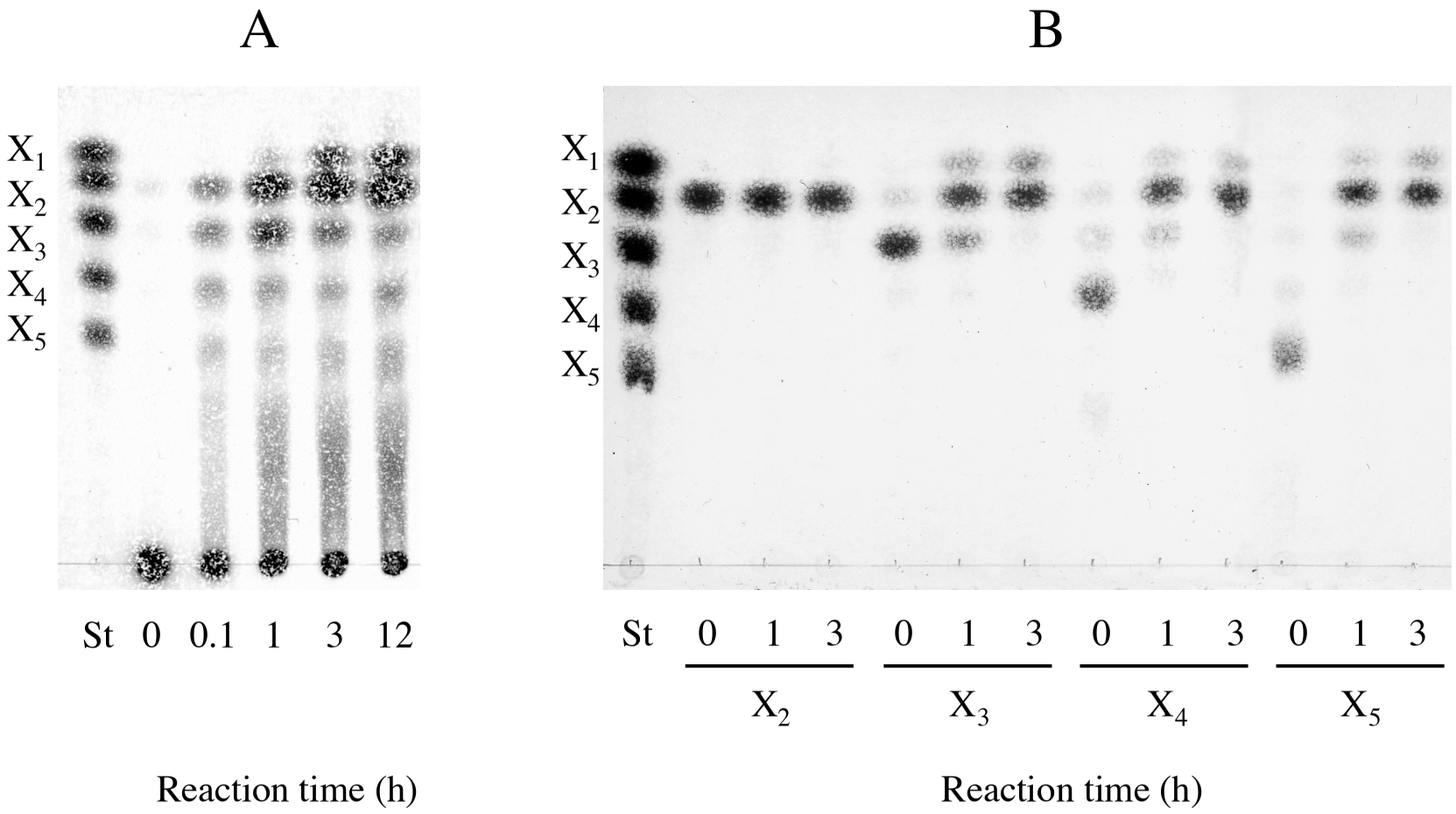

Fig. 3-4. Thin-layer chromatogram of hydrolysis products from birch-wood xylan (A) and xylooligosaccharides (B) by purified xylanase from *A. pullulans* ATCC 20524.

The enzyme reaction was done as described in the text (see *3-2-5*). Xylose (X_1), xylobiose (X_2), xylotriose (X_3), xylotetraose (X_4), and xylopentaose (X_5) were used as standards (St).

3-3-2. Cloning of the xylanase gene

The nucleotide sequence of the 152-bp fragment amplified from the *A. pullulans* genomic DNA (see *3-2-7*) showed that the deduced amino acid sequence included the N-terminal and internal sequences used for design of degenerate primers. Southern blots of the genomic DNA digested with various restriction enzymes were probed with the DIG-labeled 152-bp fragment. A hybridized 9.0-kbp *Eco*RI DNA fragment containing the *xynII* gene was cloned into the *Eco*RI site of pUC18 to generate a plasmid pXYN204. The 3.8-kbp *Xba*I-*Kpn*I fragment from pXYN204 was subcloned into pUC18 to generate pXYN205.

3-3-3. Nucleotide sequences of the xynII gene and its cDNAs

The 3.8-kbp *Xba*I-*Kpn*I insert in pXYN205 was sequenced for the first 3,293-bp from the *Kpn*I site. The 3,293-bp sequence contained a complete *xynII* ORF and its flanking regions (Fig. 3-5). The first in-flame ATG downstream of the transcription start points (see below) was the deduced start codon, which had a consensus A residue at the –3 position (Kozak 1989). A comparison of the *xynII* genomic and cDNA sequences showed that the regions encoding the signal sequence and the mature protein were interrupted by introns of 56 bp and 73 bp, respectively. Both introns fitted the GT/AG rule for 5′ and 3′ splicing sites (Gurr *et al*. 1987).

Two transcription start points were present at nt –60 (A) (three clones) and –54 (A) (three clones) as determined by sequence analysis of six independent cDNA clones of 5′ RACE products. The *xynII* 5′-noncoding region did not contain the TATAAA and CCAAT

motifs. A consensus binding site for the CreA repressor (5′-SYGGRG-3′), which mediates carbon catabolite repression in *Aspergillus nidulans* (Cubero and Scazzocchio 1994), was present at nt –294 (GTGGGG). In addition, consensus and near-consensus binding sites for the zinc finger transcription factor PacC (5′-GCCARG-3′), which mediates gene expression by the ambient pH in *A. nidulans* (Pañalva and Arst 2002), were present at nt –832 (GCCAAG) and –1136 (GCCATG of the complementary strand). However, the binding motif 5′-GGCTAA-3′ for the transcriptional activator XlnR of the xylanolytic system in *Aspergillus niger* (van Peij *et al.* 1998) was absent in the *xynII* promoter. Eight cDNA clones obtained by 3′ RACE were polyadenylated at three different positions, 114 bp (two clones), 119 bp (four clones), and 138 bp (two clones) downstream of the stop codon. The consensus sequence AATAAA preceding the polyadenylation sites was present 44 bp downstream of the stop codon.

3-3-4. Modulation of the xynII mRNA levels by ambient pH

To investigate whether the *xynII* expression was regulated by the ambient pH, *A. pullulans* was grown for 72 h with pH control by 0.1 M phosphate buffer of pH 6.0 or 8.0 and without pH control. The initial pH 6.0 decreased to 2.7 without pH control, and the culture showed abundant growth and became black due to dark hyphae. The initial pH 6.0 or 8.0 remained constant under pH-controlled conditions, and the culture showed delayed growth from that observed for the pH-uncontrolled culture and remained yellow or cream. Quantitative real-time PCR showed that the transcription levels at pH 6.0 and pH 8.0 were 8-fold and 22-fold higher, respectively, than that at pH 2.7 reached in the culture without pH control.

3-3-5. Deduced amino acid sequence and enzymatic activity of the xynII gene product

The *xynII* gene encoded a precursor protein (XynII) of 361 amino acids with a calculated M_r of 39,937. The XynII contained sequences identical to the N-terminal and two internal amino acid sequences from the purified protein (Fig. 3-5), indicating that the signal peptide of 26 amino acids was cleaved off during secretion. The XynII mature protein consisted of 335 amino acids with a calculated M_r of 37,344 and a deduced p*I* of 8.44. The calculated M_r was smaller than 39,000 as estimated by SDS–PAGE, probably because the xylanase was a glycoprotein. In this regard, there were two potential *N*-linked glycosylation sites (Asn-X-Thr) in the deduced amino acid sequence (Fig. 3-5). The deduced p*I* was consistent with the p*I* of 8.9 found by IEF. Four Cys residues were present at positions 110, 152, 304, and 310.

To verify the identity of the *xynII* as a xylanase gene and to produce the recombinant enzyme in high yields, the yeast *P. pastoris* was chosen as a suitable host system for heterologous expression of *xynII* cDNA because of the lack of xylanase activity and its high secretion efficiency (Cregg 1999). The pXYN207 transformant grown for 3 days showed xylanase activity of 0.12 U/ml in the culture supernatant, whereas the control strain transformed with the vector pPIC3.5 was devoid of the extracellular enzyme activity. Elution profile of the extracellular proteins from a SP-Sepharose column revealed two xylanase peaks, P-I and -II, and pooled fractions from each peak were purified individually by a Superdex 75 pg column. SDS–PAGE analysis showed that the M_r of the purified recombinant xylanase P-I was slightly larger than that of the P-II enzyme (Fig. 3-1). N-terminal amino acid sequence of P-II was identical to that of the native protein, while P-I contained additional 6 amino acid

residues preceding the native cleavage site. Concentrations of the recombinant xylanases, P-I and -II, in the culture media were estimated to be 6.5 mg/*l* and 36 mg/*l*, respectively, on the basis of their specific activities. The results show that most of the XynII precursor protein was correctly recognized and processed by the *P. pastoris* secretory pathway.

3-3-6. Sequence comparisons with other xylanases

A BLAST search of *A. pullulans* XynII in the protein sequence database found significant degree of identity to the following family-10 xylanases of fungal and bacterial origin that can hydrolyze xylan and/or cellulose (Gilkes *et al*. 1991): 46% for *Penicillium funiculosum* (accession no. AJ635947) and *Humicola grisea* (Iikura *et al*. 1997); 43% for the basidiomycete fungus *Agaricus bisporus* (De Groot *et al*. 1998) and the bacterium *Cellulomonas fimi* (O'Neill *et al*. 1986); 42% for the actinomycete *Thermobifida alba* (Blanco *et al*. 1997); 41% for *A. nidulans* (MacCabe *et al*. 1996); 39% for *Aspergillus kawachii* (Ito *et al*. 1992) and *Penicillium simplicissimum* (Schmidt *et al*. 1998); 38% for *Penicillium chrysogenum* (Haas *et al*. 1993); 37% for the fungal pathogen *Magnaporthe grisea* (Wu *et al*. 1995). The alignment of the homologous sequences showed eight conserved regions (I to VIII) as previously described for family-10 xylanases (Fig. 3-6; Baba *et al*. 1994; Fukumura *et al*. 1995), suggesting that the XynII would be the first xylanase from *A. pullulans* belonging to family 10. The Glu-160 in region III (WDVVNE) and Glu-276 in region VI (TELD) of *A. pullulans* XynII could be involved in catalytic reaction as an acid-base and as a nucleophile, respectively (Tull *et al*. 1991).

3-3-7. Phylogenetic positions of fungal family-10 xylanases

To determine the phylogenetic position of the family-10 xylanase from *A. pullulans* among the homologous xylanases of microbial origin, the alignment of their catalytic domain sequences shown in Fig. 3-6 was used to construct a neighbor-joining tree (Fig. 3-7).

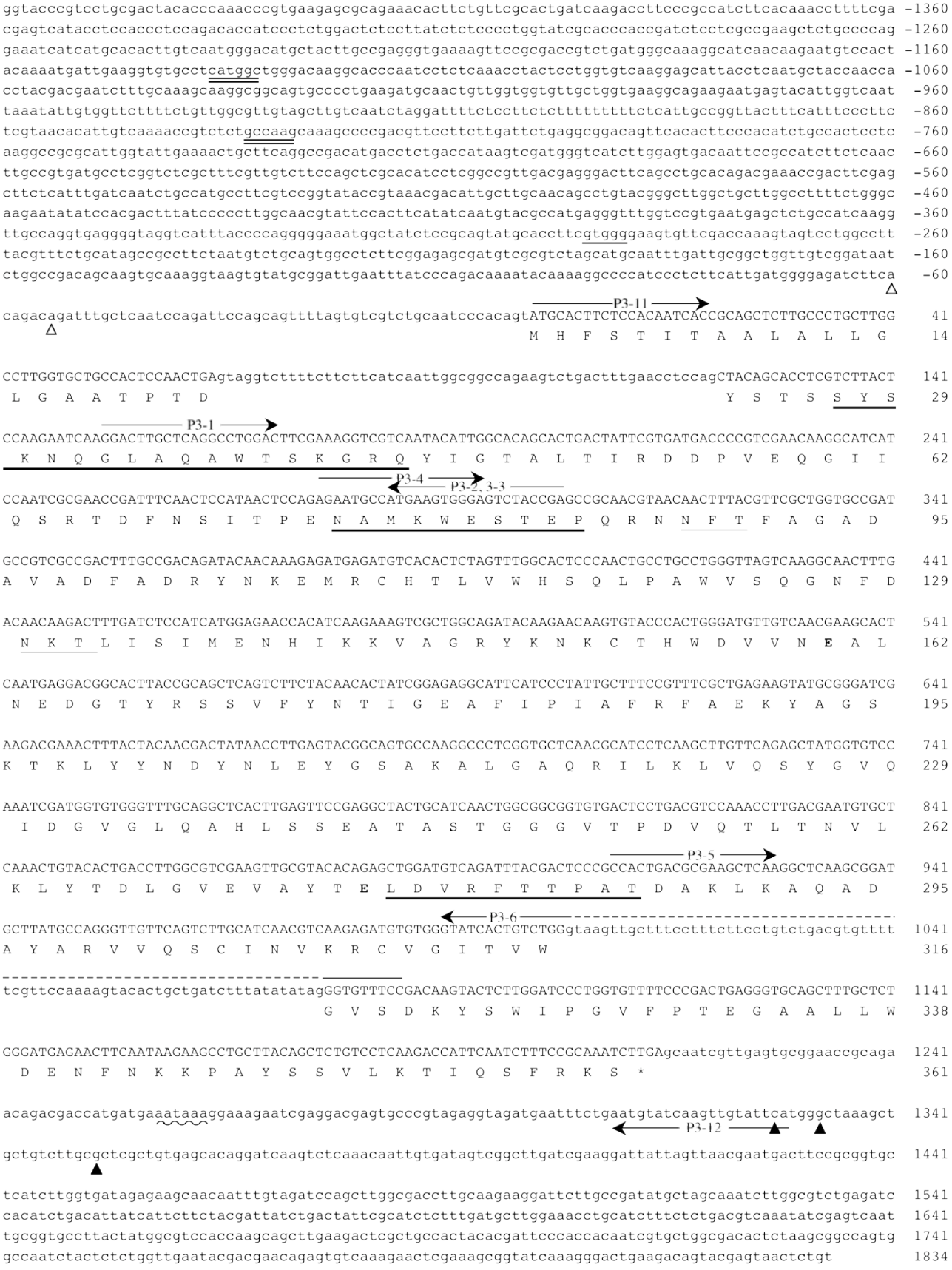

Fig. 3-5. Nucleotide sequence of *A. pullulans xynII* gene and its flanking regions and deduced amino acid sequence.

The non-coding sequences, including introns, are shown by lower-case letters. Two transcription start points and three polyadenylation sites are indicated by open and solid arrowheads, respectively. Two putative PacC binding sites in the *xynII* promoter region and a putative polyadenylation signal are double and wavy underlined, respectively. Amino acid sequences underlined by thick line were identical to those found for the purified protein. The putative catalytic Glu residues are indicated by bold letters. Potential sites for *N*-linked glycosylation are underlined. The positions of gene-specific primers, P3-1 to P3-12 (excluding primers P3-7 to -10 using for the quantitative real-time PCR), are indicated by horizontal arrows above the sequence.

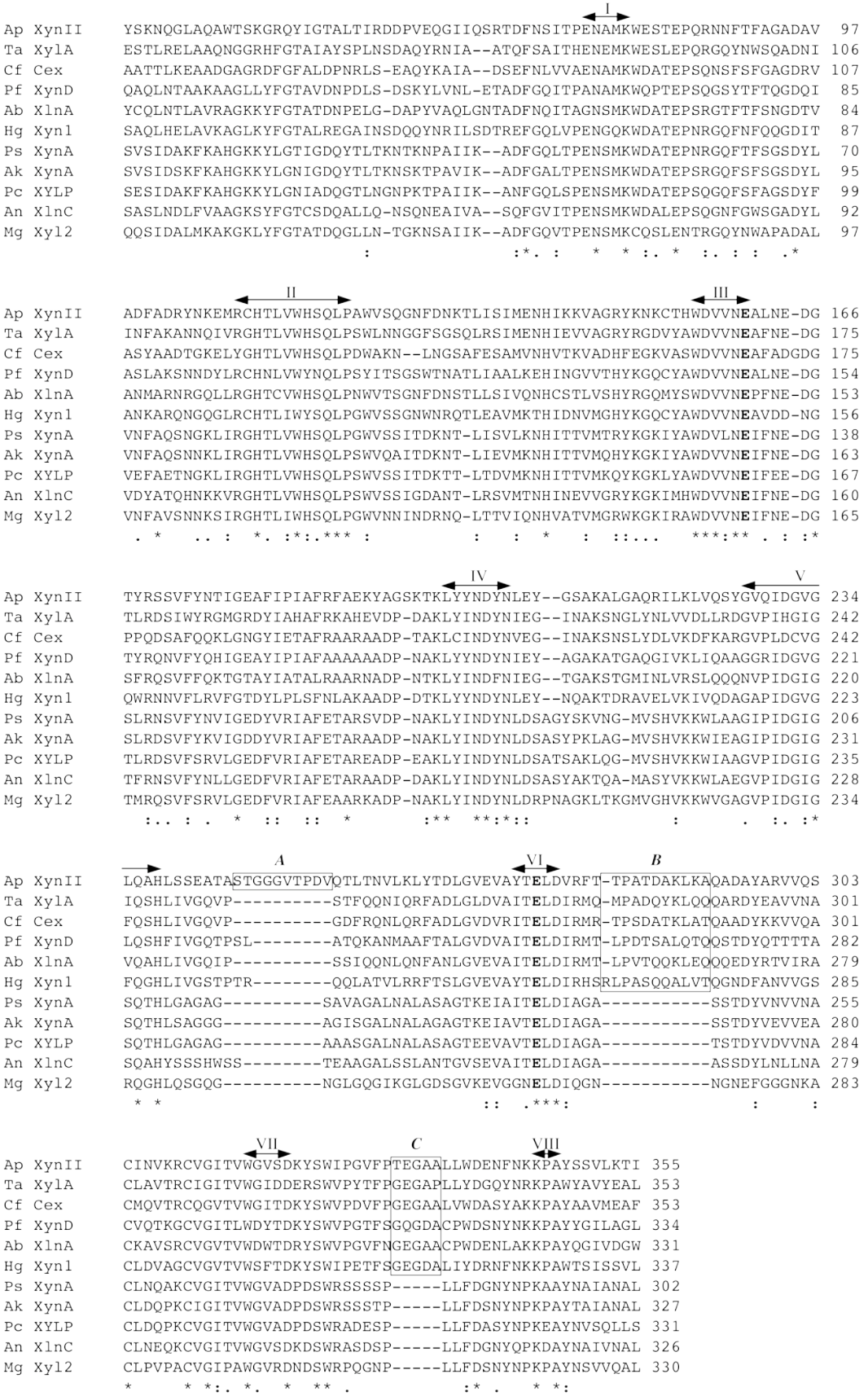

Fig. 3-6. Amino acid sequence alignment of the catalytic domain of *A. pullulans* XynII and other homologous xylanases.

Ap, *A. pullulans* (this study); Ta, *T. alba* (Z81013); Cf, *C. fimi* (M15824); Pf, *P. funiculosum* (AJ634957); Ab, *A. bisporus* (Z83310); Hg, *H. grisea* (AB001030); Ps, *P. simplicissimum* (AF070417); Ak, *A. kawachii* (D14847); Pc, *P. chrysogenum* (M98458); An, *A. nidulans* (Z49894); Mg, *M. grisea* (L37530). Numbering of the amino acids starts at the N-termini of the proteins. The alignment was done using the ClustalW program (version 1.81). Gaps were introduced for optimal alignment and are indicated by dashes. Asterisks indicate identity, and single and double dots indicate semiconservative and conservative replacements. Conserved regions, I to VIII, are indicated by horizontal arrows. Inserted region *A* in *A. pullulans* xylanase and conserved regions *B* and *C* in xylanases of cluster I (see Fig. 3-7) are boxed. The bold type amino acids are described in the text.

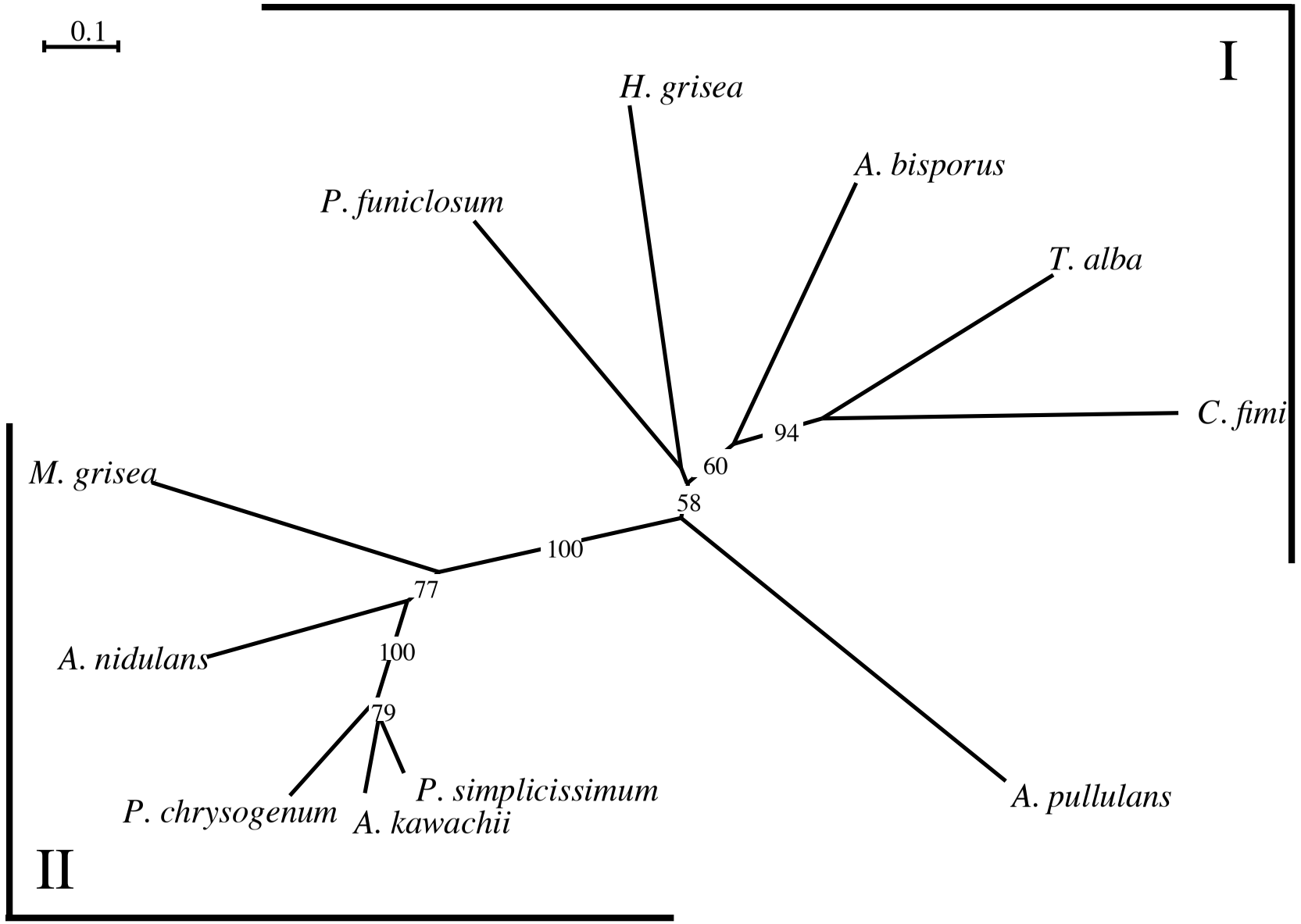

Fig. 3-7. Unrooted tree showing phylogenetic relationships of catalytic domains between *A. pullulans* XynII and other homologous xylanases.

Numbers on the branch represent the percentage of bootstrap confidence values based on 1,000 replications (values below 50 are not shown). The scale bar corresponds to 0.1 amino acid substitutions per site. For sources of sequence data, see the legend to Fig. 3-6.

3-4. Discussion

When *A. pullulans* was grown on xylan as a sole carbon source under the control at pH 6.0, the family-10 xylanase (XynII) was secreted into the culture medium. The purified enzyme XynII produced xylooligosaccharides of various DP as intermediates of xylan hydrolysis. It released mainly xylobiose and xylose as end products from xylan but did not hydrolyzed xylobiose. These results indicate that the enzyme XynII is an endo-1,4-β-xylanase. Family-10 xylanases exhibit lower substrate specificity than family-11 enzymes (Biely *et al*. 1997). The *A. pullulans* enzyme showed the weak activity toward *p*NP-β-D-xylopyranoside. The family-10 xylanase was free of activity toward carboxymethyl cellulose and this substrate specificity is advantageous for bleaching of pulps where purified cellulose is required.

The preferential transcription of the *xynII* gene at alkaline pH coincided with the presence of two PacC consensus sequences in the 5′-noncoding region. In contrast, the *xynI* gene encoding an acidophilic family-11 xylanase from the *A. pullulans* strain described in Chapter I was expressed at pH 2.7 but not or weakly expressed under the conditions of pH control at 6.0 or 8.0. Likewise, the *A. nidulans xlnA* encoding a neutral xylanase and possessing two consensus PacC binding sites was preferentially expressed at alkaline ambient pH, while the *xlnB* gene encoding an acidic xylanase from the same strain was preferentially expressed at acidic ambient pH despite the presence of a single consensus PacC binding site (MacCabe *et al*. 1998). These results indicated that the PacC-like transcription factor participates in pH regulation of the *xynII* expression in *A. pullulans*. Thus, *A. pullulans* seems to have a regulatory system responsible for the high transcription level at the optimum pH for the enzyme activity of the gene product.

Unlike other homologous fungal xylanases, both the *A. pullulans xynI* and *xynII* genes encoding family-11 and -10 xylanases, respectively, had a single intron in the region encoding the secretory signal sequence. In addition, the *xynII* gene had a single intron in mature protein coding region. Typically several introns exist in fungal family-10 xylanase genes. Sato *et al.* (1999) showed that introns in family-10 xylanase genes play a key role in protein evolution as a mediator for module fusion and exon shuffling to facilitate slightly different substrate specificities to xylanases without changing the catalytic function (Sato *et al*. 1999).

As shown by Sato *et al*. (1999), the above-mentioned xylanases except the *A. pullulans* XynII were separated into two clusters I and II (Fig. 3-7). Cluster I included bacterial and fungal xylanases in spite of their evolutionary distances and may have evolved through lateral or horizontal gene transfer of the catalytic domains, while cluster II consisted of those from only filamentous fungi. Sequence alignment (Fig. 3-6) showed that cluster I xylanases and the XynII shared extra regions *B* and *C* as compared to those of cluster II and a further insertion of 10 amino acid sequences was found in the XynII (region *A* between conserved regions V and VI in Fig. 3-6). The XynII was phylogenetically located at an intermediate position between the two clusters. Although limited availability of closely related fungal xylanase sequences makes interpretation of the phylogenetic analysis difficult, the XynII seemed to be deviated from the cluster I xylanases and to be phylogenetically distant from cluster II xylanases.

In conclusion, this is the first description of the purification of a family-10 xylanase from *A. pullulans* as well as cloning and characterization of the encoding gene *xynII*. The *xynII* gene was preferentially expressed at alkaline ambient pH in contrast to the acid-expressed *xynI* gene encoding a family-11 xylanase from the same strain. Further

compilation of the relevant sequence data to be published might allow us to present a more complete picture of the evolutional relationship of the *A. pullulans* XynII with other family-10 xylanases.

Chapter IV
Purification and characterization of a family-11 xylanase from *Penicillium citrinum* and sequence analysis of the encoding gene

4-1. Introduction

Xylanases XynI and XynII were purified from *A. pullulans* and were classified into GH family-11 and -10, respectively, on the basis of their amino acid sequences as described in Chapters I and III. It is noteworthy that the XynI was acidophilic and had an optimum of pH 2.0. However, the ethanologenic strains *E. coli* KO11 and *Saccharomyces* yeasts are not suitable for growth and fermentation under such acidic conditions. For biomass-ethanol production, it is preferable to use the family-11 xylanase that shows maximum activity around neutral pH.

Filamentous fungi are the most common industrial sources of xylanases because of their high productivity. In particular, GH family-11 xylanases from *A. niger* and *Trichoderma reesei* have been extensively studied, and the 3D structures were shown to have the shape of a right hand (Törrönen and Rouvinen, 1995; Krengel and Dijkstra, 1996). In this chapter, the author purified and characterized a GH family-11 xylanase from a filamentous fungus *P. citrinum* FERM P-15944, which is the first *P. citrinum* xylanase to be reported. The author also cloned and sequenced genomic DNA and cDNAs encoding the enzyme to clarify the organization of the encoding gene and to define the phylogenetic position of the fungal enzyme among homologous xylanases.

4-2. Materials and methods

4-2-1. Strain and culture conditions

P. citrinum FERM P-15944 used in this study is a wild-type strain originally isolated from soil samples by Hayashi *et al*. (2000). The fungal strain was inoculated into 50 ml of medium (initial pH 6.5) containing 10 g/*l* of birch-wood xylan (Sigma), 10 g/*l* of yeast extract (Difco), 1 g/*l* of K_2HPO_4, 0.6 g/*l* of $MgSO_4 \cdot 7H_2O$, 0.5 g/*l* of KCl, 0.01 g/*l* of $FeSO_4 \cdot 7H_2O$, and 2 g/*l* of agar in 500-ml Erlenmeyer flasks. The precultures were grown on a rotary shaker (150 rpm) at 30ºC for 2 days. A 2-ml aliquot of the culture was used to inoculate 100 ml of main-culture medium (initial pH of 7.5) that contained 10 g/*l* of birch-wood xylan, 20 g/*l* of yeast extract, 2 g/*l* of K_2HPO_4, and 1 g/*l* of NaCl in 500-ml Erlenmeyer flasks. Liquid cultures were grown on a rotary shaker (150 rpm) at 30ºC for 3 days.

4-2-2. Enzyme and protein assays

The reaction mixture consisted of 0.3 ml of a 1.0% (w/v) suspension of birch-wood xylan in deionized water, 0.1 ml of an enzyme solution, and 0.1 ml of 0.3 M acetate buffer (pH 5.0). After incubation at 50ºC for 10 min, reducing sugars were determined by the Somogyi-Nelson method (Somogyi 1952; Nelson 1955). The unit definition is described in *1-2-2*. The *p*NP-glycoside degradation activity was assayed as described in *3-2-2*. Protein concentrations were measured as described in *1-2-2*.

4-2-3. Enzyme purification

All purification procedures were carried out at 4ºC. Submerged cultures were centrifuged at 2,000 × *g* for 30 min. The culture supernatant (2,620 ml) was concentrated to

570 ml in dialysis tubing surrounded by a thick layer of dry polyethylene glycol 20,000 (Wako). The concentrate was dialyzed for 2 days against several changes of distilled water, and then lyophilized. The lyophilized sample was dissolved in 30 ml of 20 mM acetate buffer (pH 6.0) and loaded to anion-exchange column of a DEAE-Cellulofine A-500 (Seikagaku Kogyo) column (2.6 × 45 cm) previously equilibrated with 20 mM acetate buffer (pH 6.0). The column was washed with the same buffer. The adsorbed proteins were eluted at a flow rate of 1.0 ml/min with a linear gradient of 0 to 0.6 M NaCl in the same buffer. The fractions exhibiting the enzyme activity were pooled and then chromatographed on a Superdex 75 pg (Amersham Biosciences) column (1.6 × 60 cm) at a flow rate of 0.5 ml/min with 10 mM acetate buffer (pH 6.0) containing 0.15 M NaCl.

4-2-4. SDS-PAGE, amino acid sequencing, and IEF

SDS–PAGE, IEF, and membrane transfer methods used in this chapter is described in *1-2-4*. N-terminal amino acid sequence was identified using a G1005A Hewlett-Packard protein sequencer.

4-2-5. Effect of pH and temperature on enzyme activity and stability

The optimal pH for xylanase activity was determined by performing assays at 50ºC for 10 min with the following buffers: 0.3 M acetate–HCl (pH 1.0 to 3.0), 0.3 M acetate (pH 3.0 to 6.0), 0.3 M phosphate (pH 6.0 to 8.0), and 0.3 M Tris–HCl (pH 8.0 to 10.0). The xylanase activity was assayed in a reaction mixture containing 0.1 ml of buffer of the desired pH, 0.3 ml of 1% (w/v) xylan suspension, and 0.1 ml of enzyme solution. Enzyme stability at different pH values was measured by the residual activity after the enzyme was incubated at

room temperature for 3 h at pH 1.0 to 10.0. The optimal temperature for xylanase activity was found under the standard assay conditions except that the reaction mixture was incubated at temperatures from 30ºC to 70ºC. Thermal stability was measured in terms of the residual activity after the enzyme was incubated in 10 mM acetate buffer (pH 6.0) at temperatures from 30ºC to 70ºC for 30 min.

4-2-6. Effect of metal ions on enzyme activity

The effect of metal cations on xylanase activity was determined at a final concentration of 1 mM. The reaction mixture containing 0.3 ml of 1% (w/v) xylan suspension, 0.1 ml of the enzyme solution, and 0.1 ml of 0.1 M piperazine-*N*,*N'*-bis(2-ethanesulfonic acid) (PIPES) buffer (pH 6.1) was incubated at 50ºC for 10 min. The xylanase activity without any added compound was assigned a value of 100.

4-2-7. TLC analysis

The reaction mixture (25 μl) consisting of equal volumes of a 1% (w/v) solution of xylooligosaccharide (xylobiose or xylotriose; Wako) or 10% (w/v) suspension of birch-wood xylan and the enzyme solution (6 U/ml) in 0.3 M acetate buffer (pH 5.0) was incubated at 50ºC. Hydrolysis was stopped by boiling for 20 min, and the hydrolysis products were analyzed by TLC on silica gel plates (Merck). The plate was developed under the conditions described in *3-2-5*.

4-2-8. DNA manipulations and analyses

DNA manipulations and analyses were carried out as described in *3-2-6*.

4-2-9. Construction of xylanase-specific DNA probe

A pair of degenerate 18-mer oligonucleotides was designed and synthesized according to the N-terminal and internal amino acid sequences of the purified enzyme (see Results): P4-1 (forward; 5′-YACYGGYACYWSYAAYGG-3′ derived from the STGTSNG in the N-terminus) and P4-2 (reverse; 5′-RTARGTRCCRAARTCYTC-3′ complementary to the nt sequence encoding the EDFGTY in a V8 peptide). The PCR was done with the primer pair using genomic DNA from *P. citrinum* FERM P-15944 as a template. The resultant 388-bp amplicon was cloned, sequenced, and labeled with DIG for use as a *xynA*-specific hybridization probe using the methods described in *1-2-8* to *-10*.

4-2-10. Isolation of poly(A)$^+$ RNA and cDNA cloning

Culture conditions and poly(A)$^+$ RNA isolation methods from mycelia used in this chapter is described in *3-2-8*.

To map the 5′ and 3′ ends of the *xynA* transcripts and to obtain the full-length cDNA sequences, the author did 5′ and 3′ RACE described in *1-2-11*, except that the P4-3 (reverse; 5′-GTG CCG AAG TCT TCG ACG ATG TAG-3′ complementary to nt 468 to 485 relative to the A of the ATG codon [see nt sequence in Fig. 4-5]) and the P4-4 (forward; 5′-CTT CCA GCT CGA CTG GAA CTA GCA ATG GC-3′ corresponding to nt 92 to 120) instead of the P1-4 and the P1-7, respectively.

4-2-11. Expression of P. citrinum xynA cDNA in P. pastoris

A *xynA* cDNA was expressed in the methylotrophic yeast *Pichia pastoris* GS115

(Invitrogen) using the integrative yeast expression vector pPIC3.5 (Invitrogen) according to the manufacturer's instructions. The vector pPIC3.5 contains the promoter and terminator of the alcohol oxidase I gene (*AOX1*) as an expression cassette and *HIS4* selectable marker. The entire *xynA* open reading frame, including the sequence for the 27 amino acid secretory signal (see *4-3-5*), was amplified from the first-strand cDNA as the template with P4-5 (forward; 5′-CGG GAT CCC GGA TTT TCC AAA **ATG CCG TCT**-3′) and P4-6 (reverse; 5′-CGG GAT CCC GCT CAA GCA TTA AT**C TAG CTA**-3′) (letters in bold type indicate the coding sequence). The primers contained additional sequences at their 5′ ends to generate *Bam*HI sites (underlined) in the amplified fragment at the 5′ and 3′ ends. The amplified 667-bp cDNA fragment was inserted into pPIC3.5 at the *Bam*HI site in the orientation of transcription from the *AOX1* promoter to generate pXYN303. The pXYN303 was linearized with *Sac*I. The *P. pastoris* strain was transformed with the resulting DNA fragment by electroporation as described in *2-2-4*. His^+ transformants were recovered on minimal dextrose medium plates. One of the resultant transformants was randomly selected and grown at 30ºC for 120 h in the buffered methanol-complex medium (pH 6.0) as described in *2-2-5*. The cells were removed by centrifugation at 10,000 × *g* for 10 min. The supernatant fluid was assayed for the xylanase activity as described in *4-2-2*.

4-2-12. Nucleotide sequence accession number

The nucleotide sequence of the 2,228-bp region containing the *xynA* gene has been deposited in the DDBJ/EMBL/GenBank nucleotide sequence databases with the accession number AB198065.

4-3. Results

4-3-1. Production, purification and partial amino acid sequences of P. citrinum xylanase

Microbial xylanases are usually inducible and secreted into culture media containing xylan. When *P. citrinum* FERM P-15944 was grown on xylan as the carbon source, the culture showed extracellular xylanase activity of 3.5 U/ml after a 72-h incubation. Table 4-1 summarizes the procedure for the purification of extracellular xylanase from the *P. citrinum*. Anion exchange chromatography of the adsorbed proteins on a DEAE-Cellulofine A-500 resulted in one major xylanase peak with a discernible shoulder. Xylanase was eluted from the Superdex 75 pg column as a single protein peak that coincided with the peak of enzyme activity. This protocol afforded 174-fold purification of the enzyme from the culture filtrate with a yield of 13.1%. The purified enzyme was homogeneous as judged by SDS–PAGE and IEF, which showed an apparent M_r of 20,000 and a p*I* below 3.5, respectively (Fig. 4-1). Thus, the enzyme is a low-M_r xylanase with an acidic p*I*. The purified xylanase had a specific activity of 303 U/mg. N-terminal amino acid sequencing of the purified enzyme identified the first 15 residues: E-S-Y-T-S-S-S-T-G-T-S-N-G-Y-Y. An internal sequence was determined for a peptide recovered after cleavage by V8 protease: F-Y-I-V-E-D-F-G-T-Y.

Table 4-1. Purification of extracellular GH family-11 xylanase from *P. citrinum* FERM P-15944.

Step	Total activity (U)	Total protein (mg)	Specific activity (U/mg)	Purification (fold)	Yield (%)
Culture supernatant	9120	5210	1.74	1.00	100
Concentrate	8090	2230	3.62	2.08	88.8
DEAE-Cellulofine	4130	72.8	56.7	32.6	45.3
Superdex 75 pg	1190	3.92	303	174	13.1

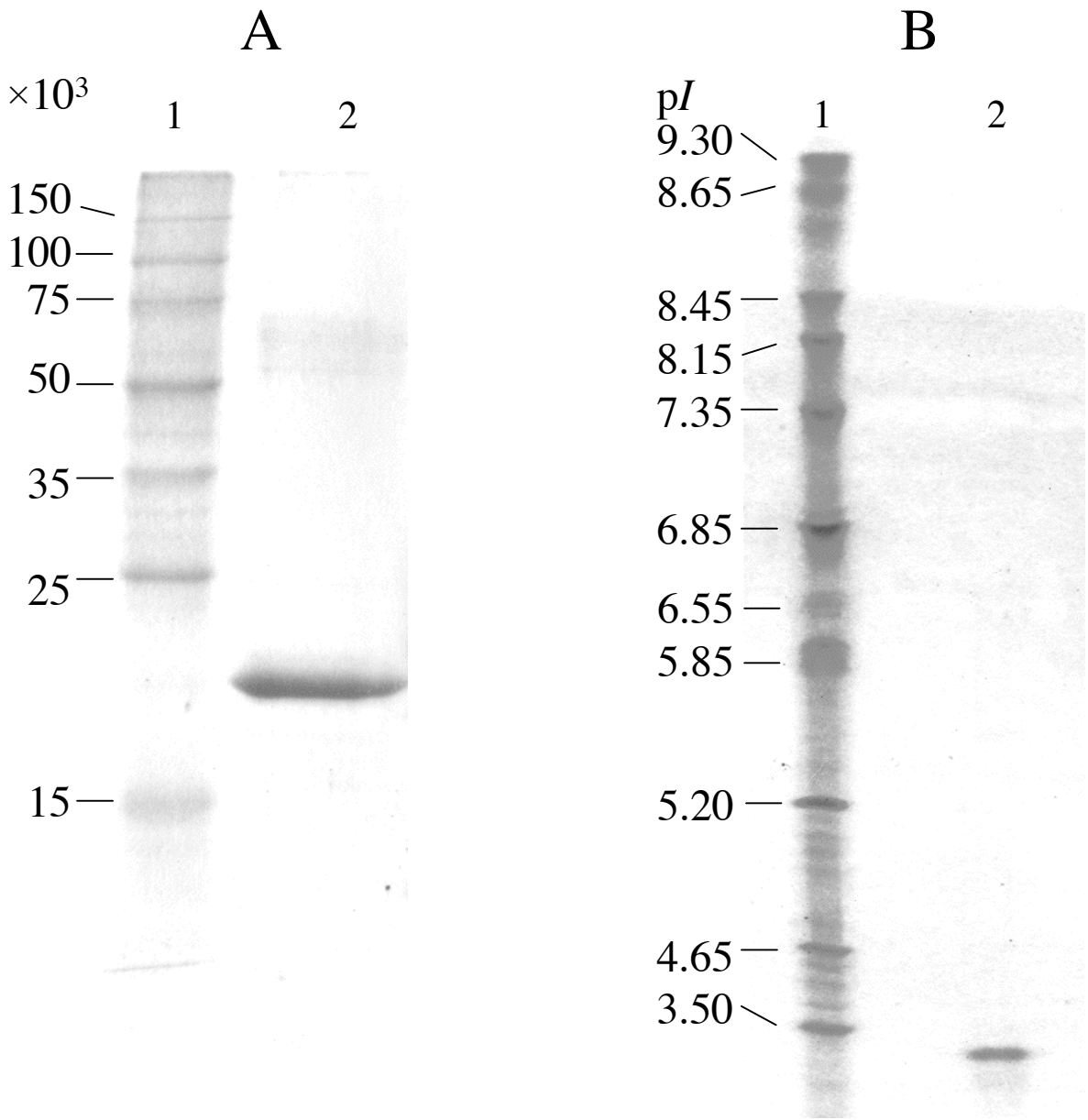

Fig. 4-1. SDS–PAGE (A) and isoelectric focusing (B) of purified xylanase from *P. citrinum* FERM P-15944.

Proteins were visualized by Coomassie Brilliant Blue R-250 staining. Lanes: 1, standard proteins; 2, purified xylanase (10 μg).

4-3-2. Enzymatic properties of the P. citrinum xylanase

The purified enzyme showed an optimum of pH 5.0 (Fig. 4-2A). The enzyme retained greater than 80% of the original activity between pH 2.0 and 10.0 (Fig. 4-2B). Thus, the xylanase was stable over a wide pH range. The optimal temperature for the enzyme activity was 55ºC (Fig. 4-3A). The enzyme remained stable up to 40ºC, but it lost activity at 80ºC (Fig. 4-3B). Fe^{2+} (114%), Cu^{2+} (109%), Mg^{2+} (90%), and Ni^{2+} (112%) showed no effects, but Co^{2+} (66%), Mn^{2+} (58%), Zn^{2+} (76%), and Cd^{2+} (68%) showed some inhibitory effects. TLC analysis showed that initial hydrolysis of birch-wood xylan by the xylanase yielded a series of oligosaccharides with a DP of two and above and the enzyme eventually released mainly xylose, xylobiose, xylotriose and xylotetraose (Fig. 4-4).

4-3-3. Cloning of the P. citrinum xylanase gene

Southern blots of the *P. citrinum* genomic DNA digested with various restriction enzymes were probed with the DIG-labeled 388-bp fragment (see *4-2-9*). A single hybridizing band was observed for digestion with *Bam*HI (5.0 kbp), *Hin*dIII (8.7 kbp), or *Sal*I (9.0 kbp), suggesting that the *xynA* gene exists as a single copy in the *P. citrinum* genome. A 5.0-kbp *Bam*HI fragment containing the *xynA* gene was cloned into pUC18, generating a plasmid pXYN302.

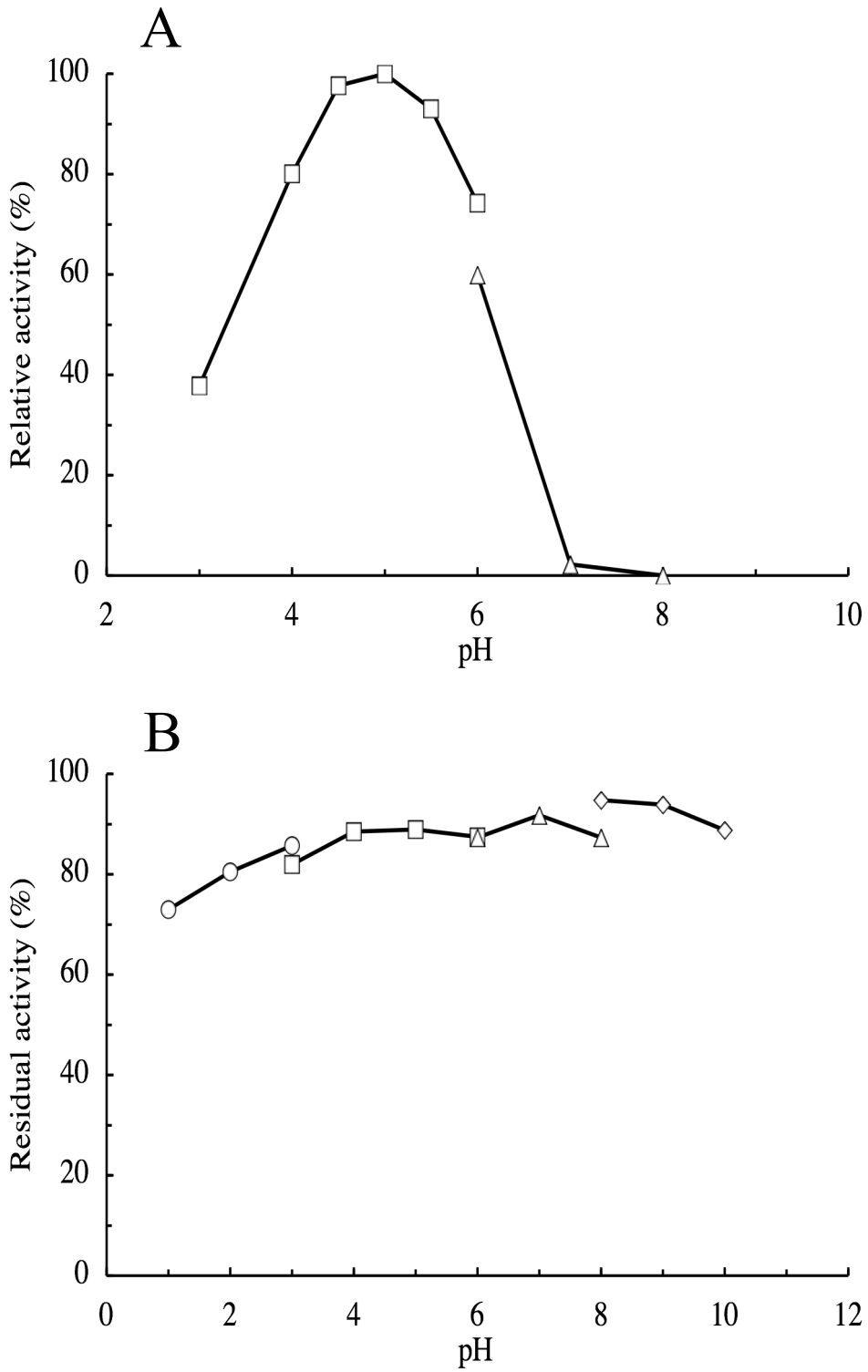

Fig. 4-2. Effect of pH on activity (A) and stability (B) of purified xylanase from *P. citrinum* FERM P-15944.

The reaction conditions are described in the text (see *4-2-5*). Relative and residual activities were expressed as percentage of the highest activity and the initial activity, respectively. Symbols: circles, sodium acetate-HCl buffer; squares, acetate buffer; triangles, phosphate buffer; diamonds, glycine-NaOH buffer.

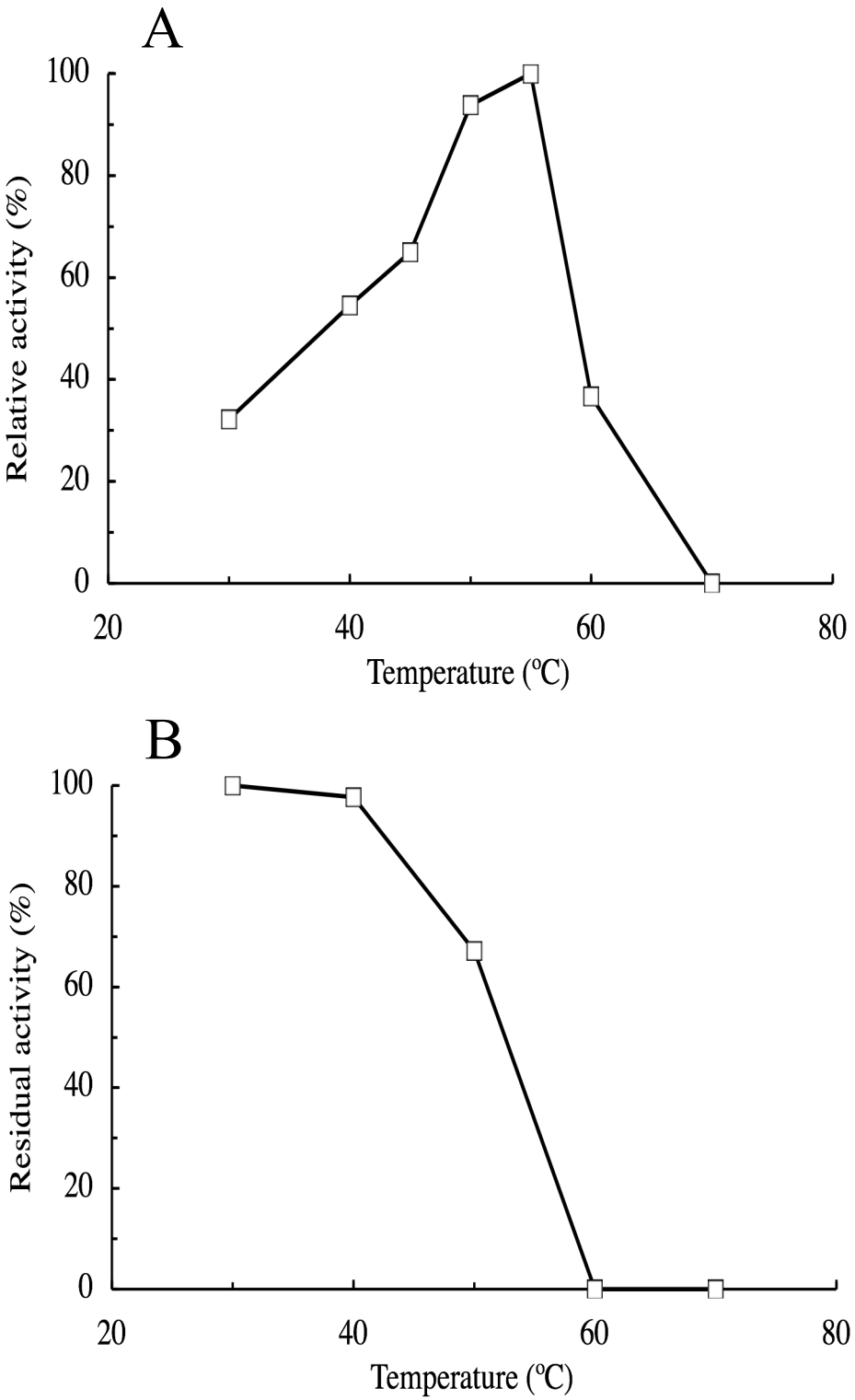

Fig. 4-3. Effect of temperature on activity (A) and stability (B) of purified xylanase from *P. citrinum* FERM P-15944.

The reaction conditions are described in the text (see *4-2-5*). Relative and residual activities were expressed as percentage of the highest activity and the initial activity, respectively.

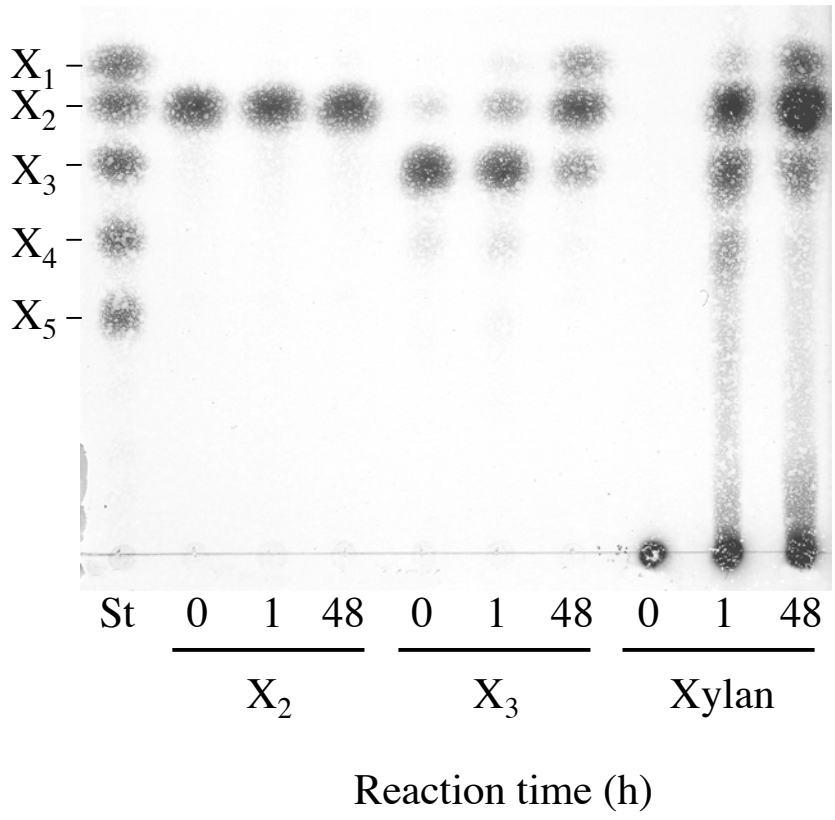

Fig. 4-4. TLC analysis for hydrolysis products of birch-wood xylan by purified xylanase from *P. citrinum* FERM P-15944.

The enzyme reaction was done as described in the text (see *4-2-7*). St, standards; X_1, Xylose; X_2, xylobiose; X_3, xylotriose; X_4, xylotetraose; X_5, xylopentaose.

4-3-4. Nucleotide sequences of the xynA gene and its cDNAs

The 5.0-kbp *Bam*HI insert in pXYN302 was sequenced for the first 2,228 bp from one of the *Bam*HI sites. The 2,228-bp sequence encompassed an entire *xynA* coding region of 657 bp and its flanking regions (Fig. 4-5). The first in-frame ATG downstream of the transcription start points (see below) was the deduced start codon, which had a consensus A residue at the –3 position (Kozak 1989). Although GH family-11 fungal xylanase genes typically contain single introns, the *P. citrinum xynA* coding region was interrupted by two introns of 65 and 55 bp as revealed by a comparison of the genomic and cDNA sequences. Both the introns matched the GT/AG rule for 5′ and 3′ splicing sites (Gurr *et al.* 1987).

The 5′-noncoding region of the *xynA* gene included promoter elements of a putative TATA box at nt –66 (TATAAA) and a putative CCAAT motif at nt –221 from the start codon. Carbon catabolite repression in *A. nidulans* is known to be mediated via the transcriptional repressor CREA (Cubero and Scazzocchio 1994). Three consensus binding sites for the CREA repressor (5′-SYGGRG-3′) were present further upstream in the *xynA* promoter region at nt –483 (CTGGAG), –565 (GTGGAG), and –588 (GTGGGG). van Peij *et al.* (1998) have shown that the sequence 5′-GGCTAA-3′ is the binding site for a transcriptional activator XlnR of the xylanolytic system in *A. niger*. The *P. citrinum xynA* promoter included two potential XlnR-binding sites, 5′-GGCTAA-3′at nt –304 and its complement 5′-TTAGCC-3′ at –276.

Sequence analysis of five independent cDNA clones of 5′ RACE products showed that three distinct transcription start points of the *xynA* gene were present at nt –20 (A) (two clones), –31 (A) (one clone), and –36 (A) (two clones) from the start codon. Six different

cDNA clones obtained by 3′ RACE were polyadenylated at three different positions, 87 bp (four clones), 88 bp (one clone), and 130 bp (one clone) downstream of the stop codon.

4-3-5. Deduced amino acid sequence and enzymatic activity of xynA gene product

The *xynA* gene encoded a precursor protein (XynA) of 217 amino acid residues (Fig. 4-5). The N-terminal and internal amino acid sequences of the mature protein purified from the culture filtrate matched the deduced sequences of Glu-28 to Tyr-42 and Phe-114 to Tyr-123, respectively. A potential leader sequence of 27 amino acid residues at the N-terminus of the XynA precursor protein possessed the characteristic features of secretory signal prepropeptides containing a long hydrophobic region preceding the dibasic residues Lys-Arg. There is a potential signal peptidase recognition site within the prepropeptide between Ser-19 and Ala-20 on the basis of the parameters described by von Heijne (1986) and a secondary cleavage site after Arg-27 by the *Penicillium* equivalent of yeast *KEX2* endopeptidase.

The *P. citrinum* XynA mature protein consisted of 190 amino acids with a calculated M_r of 20,674 and a deduced p*I* of 4.39. The calculated M_r was consistent with 20,000 as measured by SDS–PAGE, indicating the virtual absence of carbohydrate. In this regard, there was no Asn-X-Ser/Thr sequence required for *N*-linked glycosylation in the XynA. Cys residues were not present in the XynA protein. The deduced p*I* was higher than the p*I* of purified xylanase found by isoelectric focusing. The difference in p*I* may be due to the particular configuration of this protein.

To prove the identity of the *xynA* as a xylanase gene, we studied the expression of the *xynA* cDNA in *P. pastoris* GS115. The pXYN303-derived transformant carrying *xynA* cDNA

and the control strain transformed with the vector pPIC3.5 showed similar growth curves in shake-flask cultures. The pXYN303 transformant showed xylanase activity of 17 U/ml in the culture supernatant after 120 h of incubation, which was five-fold higher than that shown above for the culture filtrate of *P. citrinum* FERM P-15944. The control transformant had no detectable extracellular xylanase activity. These results suggested that the signal prepropeptide of *P. citrinum* XynA directed the efficient secretion of the recombinant xylanase in *P. pastoris*.

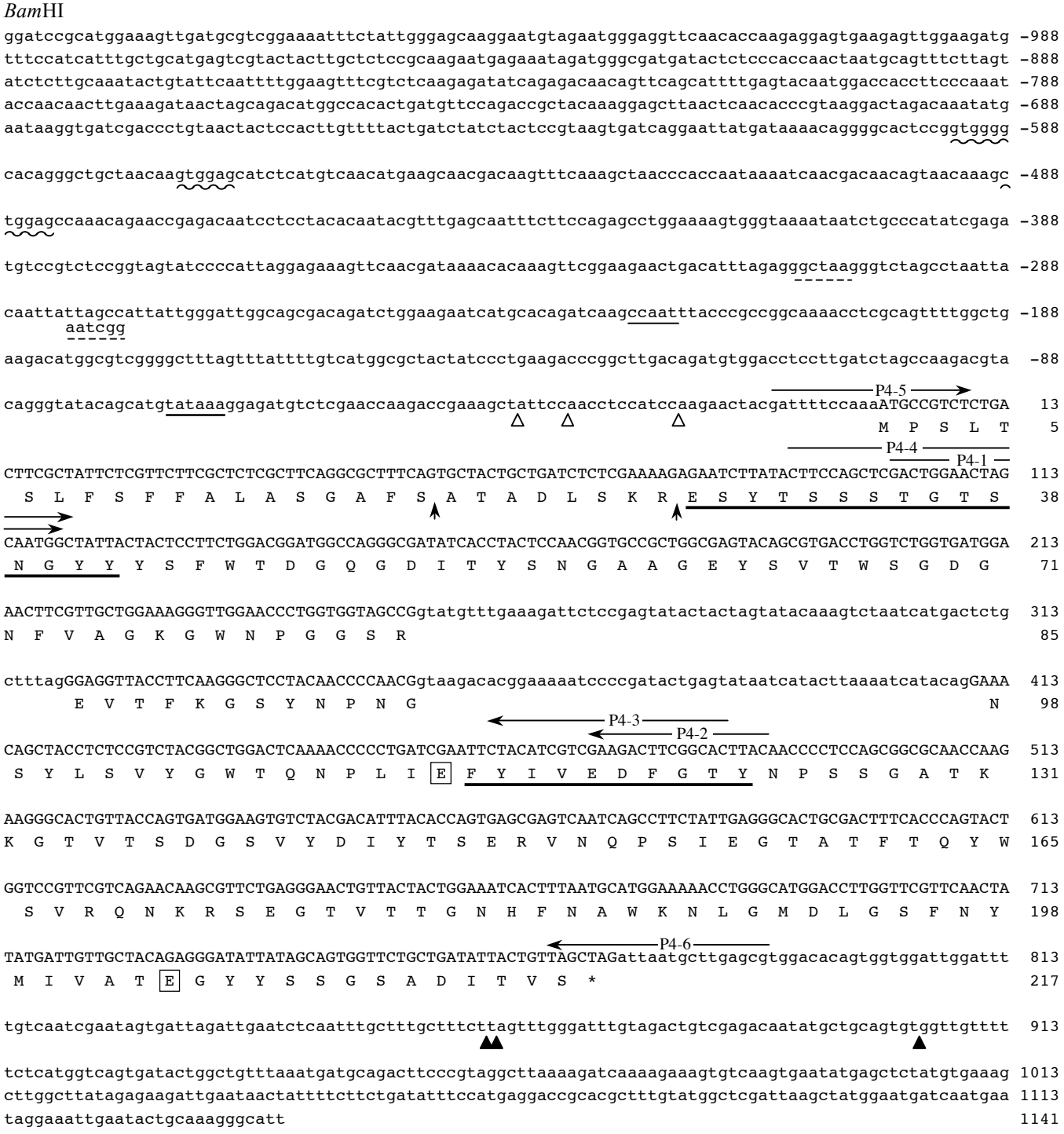

Fig. 4-5. Nucleotide and deduced amino acid sequences of *xynA* gene encoding xylanase from *P. citrinum* FERM P-15944.

The non-coding sequences, including introns, are shown in lower-case letters. The predicted TATA box and CAAT motif are underlined. Three putative CREA-binding sites (5′-SYGGRG-3′) and two putative XlnR-binding sites (5′-GGCTAA-3′) are indicated by wavy and dotted underlines, respectively. Underlined amino acid sequences were identical to those found for the purified protein and its peptide. Putative recognition sites for the signal peptidase and *KEX2*-like endopeptidase in the XynA signal peptide are shown by upward arrows. Putative catalytic residues Glu-113 and -204 are boxed. The stop codon is indicated by an asterisk. Open and solid upward arrowheads indicate transcription start points and polyadenylation sites, respectively. The positions of gene-specific primers, P4-1 to P4-6, are indicated by horizontal arrows.

4-3-6. Sequence comparisons with other xylanases

A BLAST search for *P. citrinum* XynA in the protein sequence databases found high degrees of identity to the following GH family-11 xylanases of fungal origin: 69% for *T. reesei* XYN2 (la Grange *et al.* 1996); 63% for *A. niger* XynNB (Kinoshita *et al.* 1995); 71% for *Aspergillus tubigensis* XlnB (accession no. A39368); 57% for *Chaetomium gracile* CgXB (Yoshino *et al.* 1995); 56% for *Penicillium funiculosum* XYNC (Furniss *et al.* 2002); 71% for *Penicillium* sp. strain 40 XynA (Kimura *et al.* 2000); 71 and 68% for *A. nidulans* XlnA and XlnB, respectively (Pérez-González *et al.* 1996; Fernández-Espinar *et al.* 1996). Lower sequence identity was found with other GH family-11 fungal xylanases such as *Aureobasidium pullulans* XynA (Li and Ljungdahl 1994) and XynI (see Chapter I), *Aspergillus kawachii* XynC (Ito *et al.* 1992), *A. tubigensis* XlnA (de Graaff *et al.* 1994), and *Penicillium purpurogenum* XynB (Díaz *et al.* 1997). The alignment of some representatives of these homologous sequences is given in Fig. 4-6. The presence of an Arg residue prior to the cleavage site by the signal peptidase is common to GH family-11 fungal xylanases and raises the possibility of a two-step processing in the formation of mature proteins as described above. Two of the conserved regions in GH family-11 xylanases, [PSA]-[LQ]-x-E-Y-Y-[LIVM](2)-[DE]-x-[FYWHN] and [LIVMF]-x(2)-E-[AG]-[YWG]-[QRFGS]-[SG]-[STAN]-G-x-[SAF], are known as active site signatures 1 and 2, respectively (http://www.expasy.org/prosite/). Glu residues centered in the active site signatures have been identified as catalytic residues using *Bacillus pumilus* xylanase on the basis of 3D model and mutational analysis (Ko *et al.* 1992). The corresponding residues Glu-113 and -204 in *P. citrinum* XynA could be involved in catalysis

as a nucleophile and as a proton donor to the glycosidic oxygen, respectively. However, the middle Y of the sequence E-Y-Y in the signature 1 was conservatively replaced by F in the *P. citrinum* XynA.

4-3-7. Phylogenetic position of the P. citrinum xylanase

To determine the phylogenetic position of the *P. citrinum* xylanase among the homologous xylanases of filamentous fungi, the multiple alignment of their full-length amino acid sequences shown in Fig. 4-6 was used to construct a neighbor-joining tree (Fig. 4-7). All branches of the tree were supported by the bootstrap confidence values ranging from 75 to 100%.

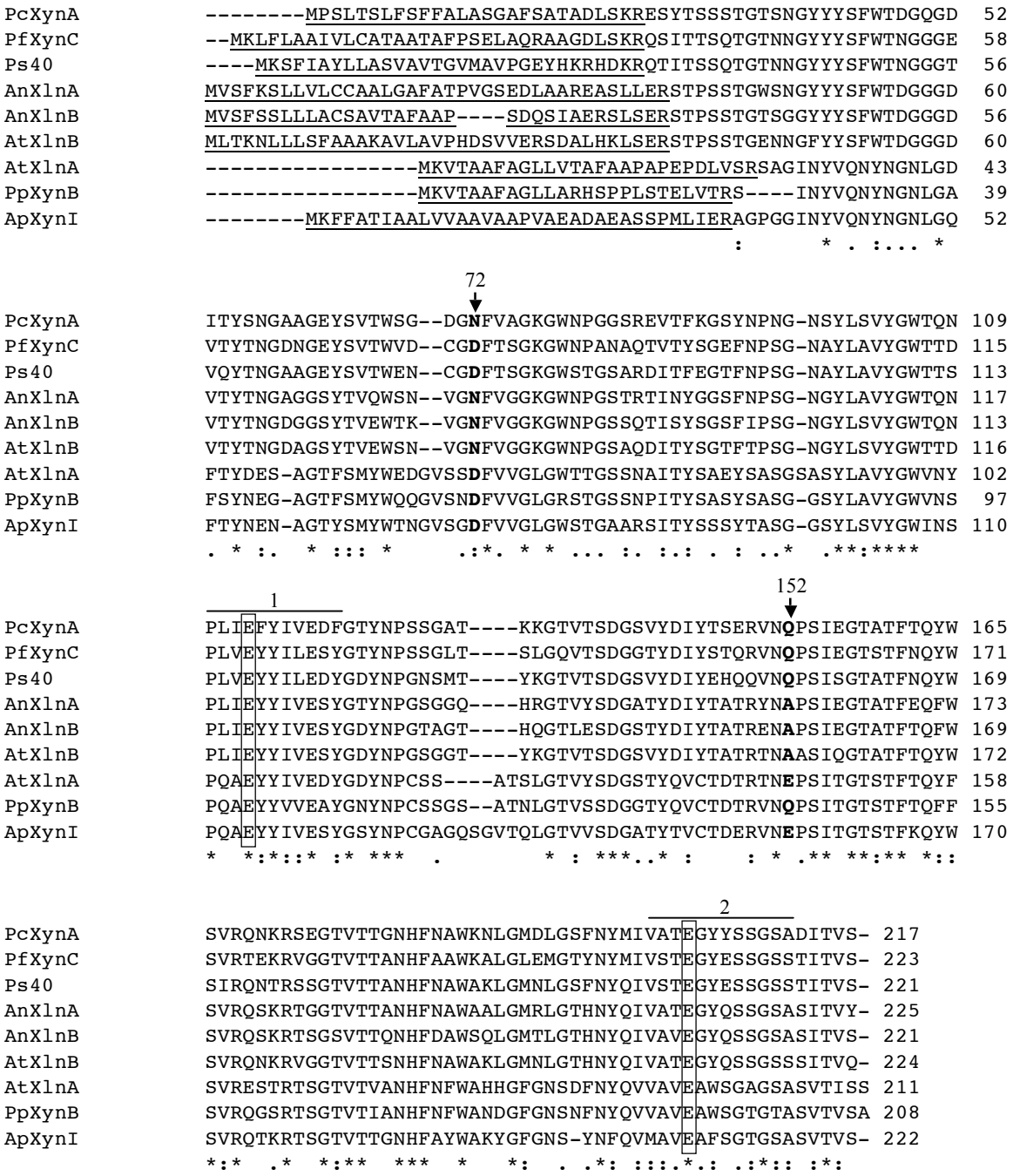

Fig. 4-6. Alignment of amino acid sequences of *P. citrinum* XynA and other homologous GH family-11 xylanases.

Pc, *P. citrinum*; Pf, *P. funiculosum*; Ps, *Penicillium* sp. strain 40; An, *A. nidulans*; At, *A. tubigensis*; Pp, *P. purpurogenum*; Ap, *A. pullulans*. Dashes indicate gaps introduced during the alignment process. Asterisks indicate identity, and single and double dots indicate semiconservative and conservative replacements, respectively. Numbering of the amino acids starts at the N-termini of the proteins. Active site signatures 1 and 2 are overlined and the putative catalytic Glu residues are boxed. The predicted secretory prepropeptides are underlined. Bold typed residues are described in the text.

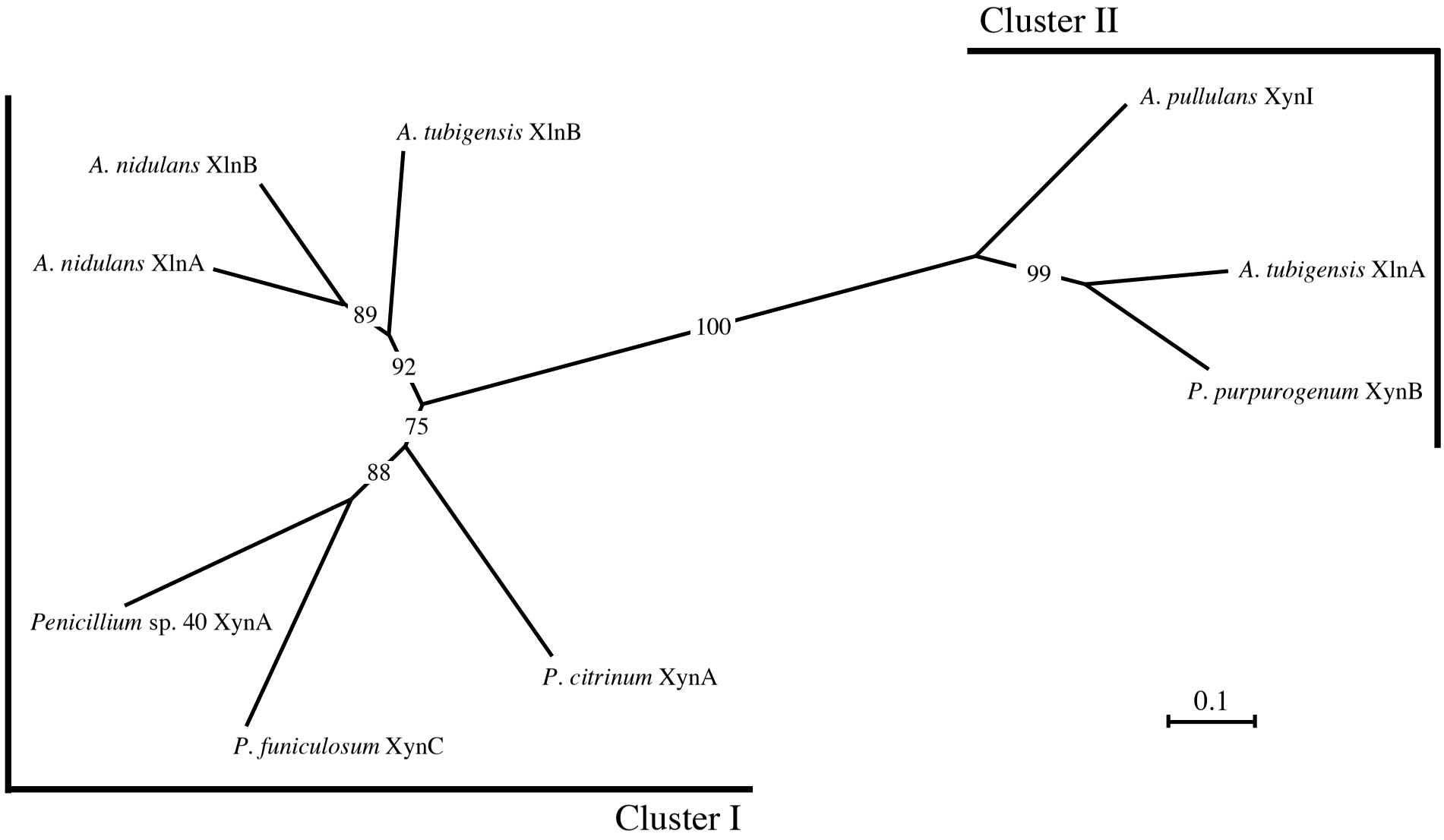

Fig. 4-7. Unrooted tree showing phylogenetic relationships between *P. citrinum* XynA and homologous xylanases.

The sequence alignment in Fig. 4-6 was used for drawing the phylogenetic tree. Numbers on the branches represent the bootstrap confidence values (%) based on 1,000 replications. The scale bar denotes 0.1 amino acid substitutions per site. Sources of sequence data (accession numbers are given in parentheses): *P. citrinum xynA* (this study), *A. pullulans* xynI (AB053298), *A. tubigensis xlnA* (L26988) and *xlnB* (A39368), *P. purpurogenum xynB* (Z50050), *A. nidulans xlnA* (Z49892) and *xlnB* (Z49893), *Penicillium* sp. strain 40 *xynA* (AB035540), and *P. funiculosum xynC* (AJ278385).

4-4. Discussion

The purified enzyme produced xylooligosaccharides of various DP as intermediates of xylan hydrolysis. It released mainly xylobiose and xylose as end products from xylan. In addition, the xylanase had no detectable activity toward carboxymethyl cellulose and *p*-nitrophenyl-β-D-xylopyranoside. These findings confirmed that the enzyme was an endo-1,4-β-xylanase. Furthermore, the deduced amino acid sequence of XynA had two significant conserved regions, the *P. citrinum* XynA belongs to GH family 11.

The author proposed a plausible 3D model for the *P. citrinum* XynA using Swiss-Model (Peitsch 1995; Guex and Peitsch 1997; Schwede *et al.* 2003). The overall structure of the XynA has the shape of right hand in common with family-11 xylanases xylanases (Krengel and Dijkstra 1996; Fushinobu *et al.* 1998; Törrönen *et al.* 1994). The 3D model and mutational analysis of the *A. kawachii* XynC (Fushinobu *et al.* 1998) and the *A. pullulans* XynI (see Chapter II) have shown that Asp and Glu residues located at the upper and lower edges of the active site cleft, respectively, play an important role in their low pH optima. Instead, the *P. citrinum* XynA had Asn-72 and Gln-152 at the corresponding positions. This observation may explain the reason why the XynA showed a higher pH optimum of 5.0.

As shown by phylogenetic analysis in Chapter I of this thesis, nine sequences from homologous xylanases were separated into two major clusters, I and II. *Aspergillus* and *Penicillium* xylanases were both located in clusters I and II, implying that orthologous and paralogous genes are contained in the tree. To explain the evolutionary relationships between the two clusters, the author imagines that duplication of an ancestral xylanase gene occurred before species divergence. Six xylanase sequences within cluster I were further separated into

two subgroups: *Aspergillus* xylanases such as *A*. *nidulans* XlnA and XlnB, and *A*. *tubigensis* XlnB; *Penicillium* xylanases of *Penicillium* sp. strain 40, *P*. *funiculosum*, and *P*. *citrinum*.

In conclusion, this is the first description of the purification of a family-11 xylanase from *P. citrinum* as well as cloning and characterization of the encoding gene *xynA*. Because the XynA has the activity in the range of pH 4 to 6, it is expected that the XynA is available for application to biomass-ethanol production using ethanologenic strain *E. coli* KO11.

Chapter V.

Expression and secretion of fungal xylanases in *Escherichia coli*

5-1. Introduction

E. coli is the best-characterized host with many expression systems available for the production of recombinant proteins. However, *E. coli* cannot produce some proteins containing complex disulfide bond, or eukaryotic proteins that require post-translational modification for their activity. A variety of techniques have been developed to solve these problems, including co-expression of molecular chaperones, and secretion of proteins into the periplasm or culture medium (Choi and Lee 2004).

Recombinant strains of *E. coli* B have been engineered which produce ethanol efficiently from all sugar constituents of lignocellulose by using the *Z. mobilis* genes encoding the pyruvate-to-ethanol pathway (*pdc* and *adhB*) (Ingram *et al.* 1987; Ohta *et al.* 1991). However, this strain could not directly convert ligneous materials to ethanol, because *E. coli* has no ligneous degradation enzymes. Therefore, Burchhardt and Ingram (1992) tried to develop improved ethanologenic biocatalysts, which supply ligneous degradation enzymes needed for the direct microbial conversion of ligneous materials into ethanol. Because a two-stage process was needed for direct conversion of xylan into ethanol, the use of secretory expression systems in *E. coli* is expected to solve the problem.

This chapter describes the use of the signal sequence from *A. pullulans* XynI for protein secretion in *E. coli*. In addition, ethanologenic strain *E. coli* KO11 was transformed with fusion gene encoding the signal sequence from *A. pullulans* XynI and mature protein region of XynA from *P. citrinum*.

5-2. Materials and methods

5-2-1. Strains and culture conditions

The ethanologenic bacteria *E. coli* KO11 (Ohta *et al.* 1991) and standard strain *E. coli* JM109 (Takara Bio) were used in this study. Cultures were grown in Luria-Bertani (LB) broth (10 g/*l* of tryptone [Wako], 5 g/*l* of yeast extract [Wako], 5 g/*l* of sodium chloride [Wako]) or LB with 5% birch-wood xylan (Sigma). Ampicillin (100 mg/ml) and chloramphenicol (150 mg/ml) were added as appropriate for selection.

5-2-2. Enzyme assay

The method for enzyme assay used in this chapter is described in *3-2-2*.

5-2-3. DNA manipulations and analyses

DNA manipulations and sequence analyses were carried out as described in *3-2-6*.

5-2-4. Construction of E. coli expression plasmids

A full-length cDNA of the xylanase gene *xynI* from *A. pullulans* strain ATCC 20524 and *xynA* from *P. citrinum* strain FERM P-15944 were cloned into pUC18 as described in Chapters I and IV, respectively. The *xynI* and *xynA* cDNA were used for construction of the following series of *E. coli* expression plasmids.

Plasmid containing or not containing the xynI secretory signal On the basis of the nucleotide sequence of *xynI* (see *1-3-5*), the following PCR primers were designed to amplify

the precursor or mature protein region of *xynI* cDNA (letters in bold type indicate the *xynI* coding sequence): 5′-CCG GAA TTC C**AT GAA GTT CTT CGC CAC TAT**-3′ (P5-1; forward) and 5′-TCC CCC GGG GGA TGA CAT CTA **AGA GAC AGT AAC GCT**-3′ (P5-2; reverse) containing *Eco*RI and *Sma*I sites (underlined) for expression of the precursor protein with its own signal sequence; 5′-CCG GAA TTC C**GC CGG CCC CGG TGG CAT CAA**-3′ (P5-3; forward) and P5-2-reverse containing *Eco*RI and *Sma*I sites (underlined) for the mature protein without its own signal sequence. These two amplified *xynI* cDNA fragments were digested with the appropriate endonucleases and cloned into pUC18 to yield pEXN102 and pEXN101, respectively.

The xynA expression plasmid On the basis of the nucleotide sequence of *xynA* (see *4-3-4*), the following PCR primers were designed to amplify the precursor protein region of *xynA* cDNA (letters in italic and bold type indicate the *xynI* and *xynA* coding sequence, respectively): 5′-GGG GTA CCC **ATG CCG TCT CTG ACT TC**-3′ (P5-4; forward) and 5′-GCT CTA GAG C**CT AGC TAA CGA TAA TAT CAG**-3′ (P5-5; reverse) containing *Kpn*I and *Xba*I sites (underlined) for expression of the precursor protein with its own signal sequence; the internal fusion primers 5′-*TAT CGA GCG T***GA ATC TTA TA**-3′ (P5-6; forward) and 5′-**TAT AAG ATT C***AC GCT CGA TA*-3′ (P5-7; reverse), and the external primers (P5-1 and P5-5) for the expression of the *xynA* precursor protein with the *xynI* signal sequence. The fused technique was performed using the overlap extension PCR method as described in *2-2-3*. The amplified *xynA* cDNA fragment and fused fragment were digested with the appropriate endonucleases and cloned into pUC18 to yield pEXN301 and pEXN401, respectively.

5-2-5. Transformation of E. coli strains

The resulting plasmids were used to transform the *E. coli* JM109 and KO11 by chemical competent cell method (Takara Bio) and electroporation according to the manufacturer's instructions, respectively. The electroporation was done using a Gene Pulser II with Pulse Controller (Bio-Rad) under the conditions that pulsed at 12.5 kV/cm, 25 μF, and 200 Ohms. After pulsing, 500 μl of SOC medium, pH 7.0 (20 g/*l* of tryptone, 5 g/*l* of yeast extract, 0.5 g/*l* of NaCl, 0.186 g/*l* of KCl, 2.033 g/*l* of $MgCl_2 \cdot 6H_2O$, 3.6 g/*l* of glucose) was added to the cuvettes immediately, and the cells were grown on an orbital shaker (60 rpm) at 37ºC for 1 h. Then, the transformants were recovered on LB plates contained ampicillin and chloramphenicol. As the corresponding controls, *E. coli* cells were also transformed with the vector pUC18 using the same method.

5-2-6. Media and culture conditions for E. coli transformants

E. coli transformants were inoculated into 5 ml of LB medium in 20-ml test tube. The pre-cultures were grown on an orbital shaker (60 rpm) at 37°C for 16 h. The 50-μl portions of the culture were added to 5 ml of LB medium in 20-ml test tube. The cultures were grown at 37°C under the same aerobic conditions to an A_{660} of 0.2. To enable induction of the *lac* promoter, 0.5 mM of Isopropyl-β-D-thiogalactopyranoside (IPTG) was added into the media. The growth of transformants was monitored by measuring the A_{600} periodically. Culture aliquots were withdrawn and cells were collected by centrifugation at 1,500 × *g* for 10 min. The cells were homogenized using French press 5501-MF (Ohtake Seisakusho, Tokyo). The lysates were centrifuged at 8,000 × *g* for 3 min and supernatant fluids were assayed for the xylanase activity as described *5-2-2*.

5-2-7. TLC analysis

The liquid cultures of *E. coli* KO11 (pUC18) and *E. coli* KO11 (pEXN401) after grown for 0 h, 12 h and 24 h were treated at 98ºC for 30 min to inactivate the xylanase activity. The cultures were centrifuged at 8,000 × *g* for 3 min. The equal volume of absolute ethanol was added to the culture supernatants to remove contaminants, and then centrifuged at 10,000 × *g* for 10 min at 4ºC. The 15-µl portions of supernatants were spotted onto the TLC plate (Merck AG). TLC development and staining were done as described in *3-2-5*.

5-3. Results

5-3-1. Xylanase activities of XynI and XynA expressed in E. coli JM109

The pEXN101-derived transformant carrying *xynI* cDNA without its own signal sequence and the control strain transformed with the vector pUC18 showed similar growth curves (Fig. 5-1). The cell lysate of the pEXN101-derived transformant showed xylanase activity of 38 mU/ml after 4 h of induction, while the culture supernatant had no detectable xylanase activity (Table 5-1). The pEXN102-derived transformant carrying *xynI* cDNA containing the signal sequence and the control transformant showed different growth rates (Fig. 5-1). However, the pEXN102-derived transformant showed xylanase activity of 80 mU/ml in the culture supernatant but no detectable activity in the cell lysate after 4 h of induction (Table 5-1). The pEXN301-derived transformant with its own signal sequence showed xylanase activity of 10 mU/ml in the cell lysate, but xylanase activity was not detectable in the culture supernatant (Table 5-1). When the *xynA* mature region was fused

with the *xynI* secretory signal sequence, the transformant harboring pEXN401 containing the fused gene showed xylanase activity of 60 mU/ml in the culture supernatant (Table 5-1).

Table 5-1. Xylanase activities of recombinant xylanase expressed in *E. coli* transformants.

Transformants	Xylanase activities (mU/ml)	
	Cell lysate	Culture supernatant
E. coli JM109 (pEXN101)[1]	38	ND
E. coli JM109 (pEXN102)[1]	ND	80
E. coli JM109 (pEXN301)[1]	10	ND
E. coli JM109 (pEXN401)[1]	44	60
E. coli KO11 (pEXN101)[2]	8	ND
E. coli KO11 (pEXN102)[2]	7	88
E. coli KO11 (pEXN401)[2]	55	64

ND, not detected; 1, Xylanase activities were assayed after 4 hours of induction using IPTG; 2, Xylanase activities were assayed after 8 hours incubation.

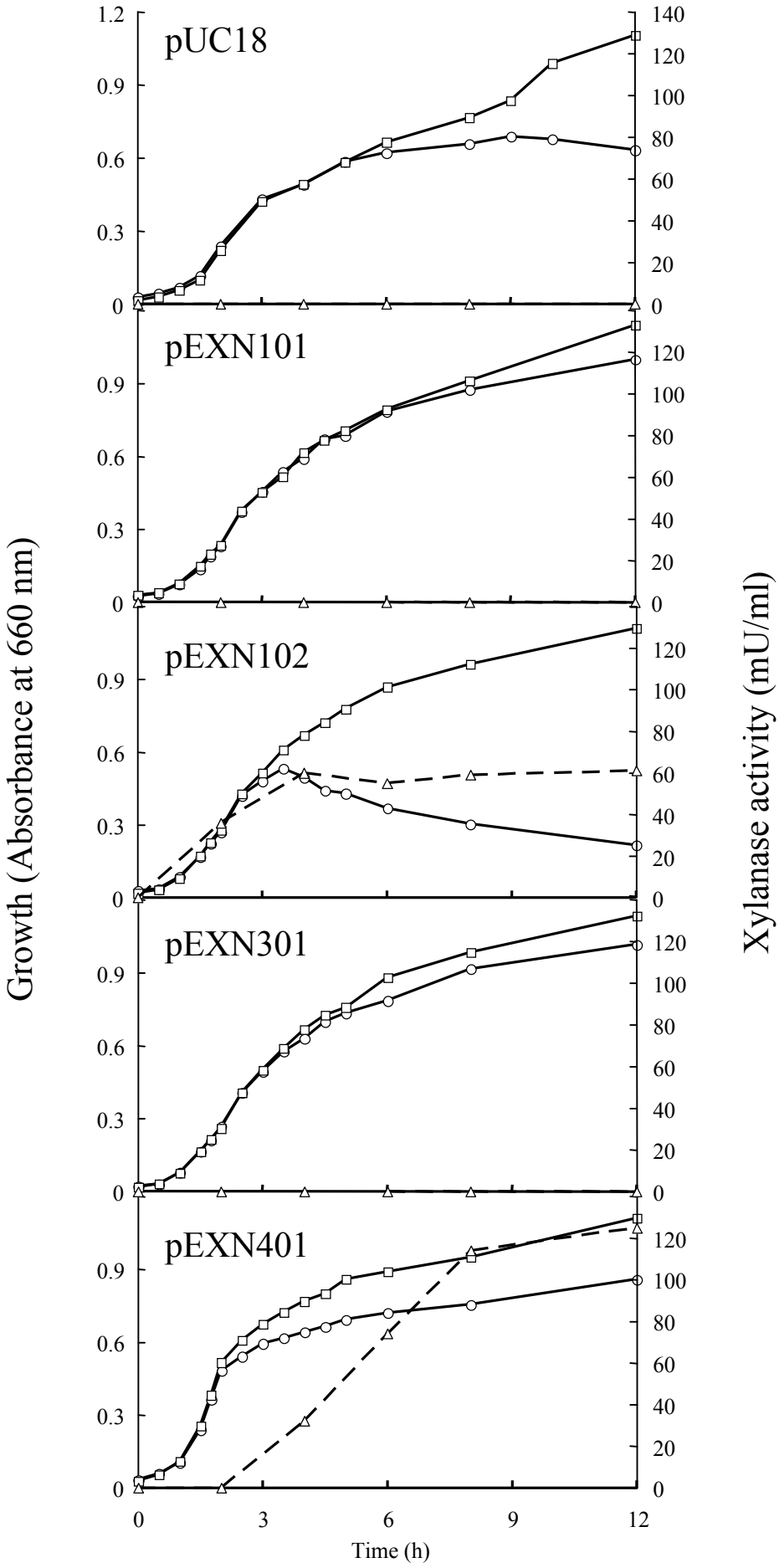

Fig. 5-1. Growth curves and xylanase activity in culture supernatant of *E. coli* transformants.

The transformants were generated with each plasmids. Symbols: squares, growth curve of not induced; circles, growth curve of induced; broken-line, xylanase activity in culture supernatant.

5-3-2. Xylanase activities of XynI and XynA expressed in E. coli KO11

The pEXN101-derived transformant carrying *xynI* cDNA without its own signal sequence and the control strain transformed with the vector pUC18 showed similar growth curves. The pEXN101-derived transformant showed xylanase activity of 8 mU/ml in the cell lysate after 8 hours incubation, while the culture supernatant had no detectable xylanase activity (Table 5-1). The pEXN102-derived transformant carrying *xynI* cDNA containing the signal sequence and the control strain showed different growth rates. However, the pEXN102-derived transformant showed xylanase activity of 88 mU/ml in the culture supernatant as well as 7 mU/ml in the cell lysate after 8 hours incubation (Table 5-1). When the *xynA* mature region was fused with the *xynI* secretory signal sequence, the transformant harboring pEXN401 containing the fused gene showed xylanase activity of 64 mU/ml in the culture supernatant (Table 5-1). TLC analysis revealed that oligosaccharides with a DP of two and above mainly remained in the culture media (Fig. 5-2).

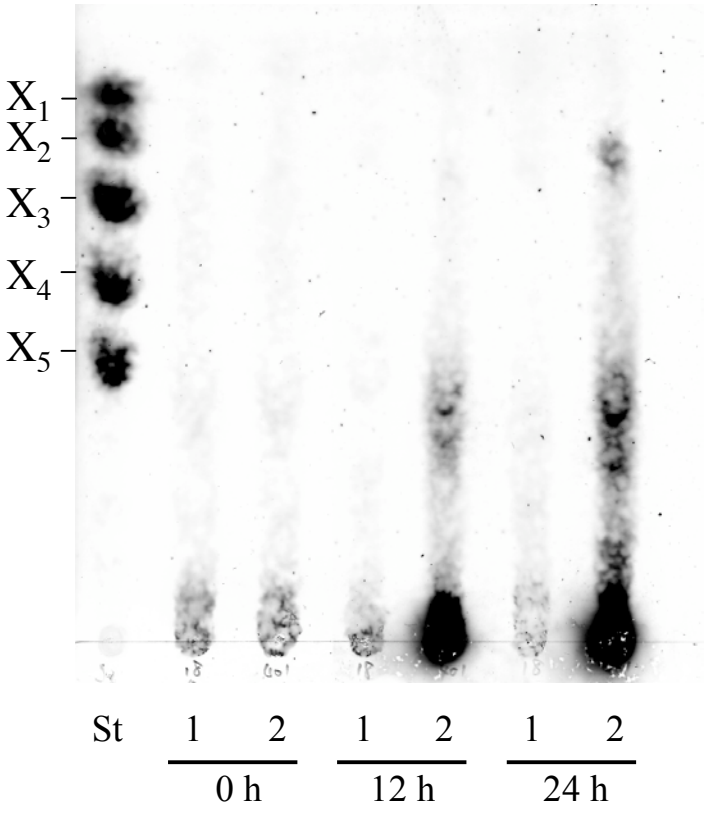

Fig. 5-2. Thin-layer chromatogram of the *E. coli* transformants culture medium contained birch-wood xylan.

The conditions were described in *5-2-7*. St, standards; X_1, xylose; X_2, xylobiose; X_3, xylotriose; X_4, xylotetraose; X_5, xylopentaose; 1, *E. coli* KO11(pUC18); 2, *E. coli* KO11(pEXN401).

5-4. Discussion

One of the protein secretion systems in gram-negative bacteria involves a two-step process in which a premature protein containing a signal sequence is exported to the periplasmic space using the Sec pathway and processed into a mature protein (Pugsley 1993). Although heterologous proteins are often exported to the periplasm by the common Sec system, extracellular secretion of target proteins depends on the characteristics of signal sequences and proteins. Typical signal sequences are composed of positively charged short N-domain, hydrophobic H-domain, and usually less hydrophobic C-domain that contains a recognition site, Ala-X-Ala box, of the signal peptidase I (Pugsley 1993; Choi and Lee 2004). The secretory signal sequence of *xynI* from *A. pullulans* nearly fitted the rules; it had three potential cleavage sites, Ala-20 to Ala-22, Ala-22 to Ala-24 and Ala-24 to Ala-26 (see Fig. 1-6). The pEXN102 transformant with the secretion signal sequence showed xylanase activity in the culture supernatant, although the pEXN101 transformant without the secretion signal showed no detectable activity. To determine whether or not the secretion depends on the *xynI* signal sequence, the author constructed two transformants derived from pEXN301 or pEXN401. The pEXN301-derived transformants that contain *xynA* precursor sequence form *P. citrinum* had no detectable activity in the culture supernatant. While the pEXN401-derived transformants that contain the fused sequence of *xynI* signal sequence and *xynA* mature protein region showed the xylanase activity in the culture supernatant. These results showed that the secretory signal sequence from *A. pullulans* XynI might play a role for Sec system in *E. coli*. To our knowledge, this is the first report of the secretory signal sequence involved in Sec system of *E. coli* from eukaryote.

The ethanologenic strain *E. coli* KO11 was transformed with pEXN401. The neutral xylanase gene *xynA* was expressed and the gene product was successfully secreted to the culture medium using the XynI secretory signal sequence. Although the XynI had potential to yield xylose and xylobiose as degradation products (see Chapter I), the TLC analysis revealed that there was no xylose in the culture medium. The result showed that xylose might be metabolized by *E. coli* KO11, however ethanol was not detected using a gas chromatography in the culture supernatant (data not shown). On the other hand, *E. coli* KO11 harboring pEXN401 still had the ability to produce ethanol. These finding suggested that it is possible to construct a microorganism which has the ability of direct conversion of xylan into ethanol, if a xylosidase activity is applied to *E. coli* KO11 using the secretory signal sequence. Further research is needed to acquire xylosidases and successful expression into the culture medium.

Conclusion

Biomass fuels are gaining increasing attention as an effective material to curb emissions of greenhouse effect gases. Japan has abundant ligneous resources, which are supplied as architectural scraps and woods from thinning, and it is important to use these biomasses for biomass fuel production. The major composition of these ligneous biomasses is cellulose, hemicellulose and lignin. Enzymes, such as cellulases and xylanases, are gaining significance because of their biotechnological application in degradation of ligneous materials. In this doctoral thesis, endo-1,4-β-xylanases were studied in detail.

Major findings in the present study can be summarized as follows: (1) the identification of key amino acid residues responsible for low pH optimum of the acidophilic xylanase XynI; (2) the different expression levels of two xylanases (XynI and XynII) from *A. pullulans* at alkaline pH; (3) the function of the XynI secretory signal peptide in *P. pastoris* and *E. coli*.

Three extracellular xylanases were purified from *A. pullulans* var. *melanigenum* ATCC 20524 and *P. citrinum* FERM P-15944, and their enzymatic properties were characterized. Moreover, all the fungal xylanase genes were cloned and sequenced. The XynI (M_r of 24,000 and p*I* of 6.7) and XynA (M_r of 20,000 and p*I* below 3.5) from *A. pullulans* and *P. citrinum*, respectively, were classified into GH family 11, while the XynII (M_r of 39,000 and p*I* of 8.9) from *A. pullulans* was classified into family 10. Xylanase activity of the XynI was optimum at pH 2.0. Nonetheless, the deduced amino acid sequence showed 94% identity with that of a previously reported equivalent gene (*xynA*) encoding a xylanase with an optimum pH of 4.8 from a color variant strain, NRRL Y-2311-1 of *A. pullulans*. The

construction of a 3D model and mutational analysis of the XynI helped in finding differences in optimal pH between XynI and XynA. It has facilitated identification of key amino acid residues responsible for its low pH optimum, along with their locations; it was found that Glu-157 as well as previously described Asp-73 at the edge of the active site cleft play an important role in its acidophilicity.

These cloned xylanase genes were expressed in methylotrophic yeast *P. pastoris* using its own secretory signal sequence. In subsequent experiment, the efficiency of xylanase secretion directed by the XynI signal peptide in *P. pastoris* was compared with those directed by the signal peptides of *S. cerevisiae* α-MF and *P. pastoris* PHO1. These results revealed that the amount of recombinant xylanase secreted into the medium by the XynI signal peptide (178 mg/*l*) was comparable to that by the α-MF signal peptide and two-fold higher than that by the PHO1 peptide. It was also higher than the previously reported 60 mg/*l* value for the *A. niger* xylanase secreted from *P. pastoris* using the 19 amino acid signal peptide of the *S. cerevisiae* invertase (Berrin *et al.* 2000). In addition, the XynI signal peptide has the function of protein secretion in *E. coli*. Accordingly, the signal sequence might be useful for heterologous secretory expression in bacterial cells as well as fungal cells.

The family-10 xylanase (XynII) was purified from the *A. pullulans* culture with pH control and the encoding gene was cloned, whereas the family-11 xylanase (XynI) was purified from the fungal culture without pH control. To investigate whether the *xynII* was regulated by the ambient pH, the expression levels were quantified by using real-time PCR analysis. These results showed that *A. pullulans* seems to have a regulatory system responsible for the high transcription level at the optimum pH for the enzyme activity of the gene product.

Finally, it was attempted to create the ethanologenic derivative of *E. coli* KO11 that ferment xylan directly using the secretory signal peptide of XynI from *A. pullulans* and the xylanase XynA from *P. citrinum*. Although, the resulting transformant was not able to produce detectable ethanol in the culture supernatant, these results would be promising for constructing a microorganism that has the ability of direct conversion of xylan into ethanol.

References

Alcocer, M. J., Furniss, C. S., Kroon, P. A., Campbell, M. and Archer, D. B. (2002) Comparison of modular and non-modular xylanases as carrier proteins for the efficient secretion of heterologous proteins from *Penicillium funiculosum*. Appl. Microbiol. Biotechnol. 60, 726–732.

Altschul, S. F., Madden, T. L., Schaffer, A. A., Zhang, J., Miller, W. and Lipman, D. J. (1997) Gapped BLAST and PSI-BLAST: a new generation of protein database search programs. Nucleic Acids Res. 25, 3389–3402.

Baba, T., Shinke, R. and Nanmori, T. (1994) Identification and characterization of clustered genes for thermostable xylan-degrading enzymes, β-xylosidase and xylanase, of *Bacillus stearothermophilus* 21. Appl. Environ. Microbiol. 60, 2252–2258.

Barry, V. C. and Dillon, T. (1940) The occurrence of xylan in marine algae. Nature (London) 146, 620.

Belancic, A., Scarpa, J., Peirano, A., Díaz, R., Steiner, J. and Eyzaguirre, J. (1995) *Penicillium purpurogenum* produces several xylanases: purification and properties of two of the enzymes. J. Biotechnol. 41, 71–79.

Berrin, J.-G., Williamson, G., Puigserver, A., Chaix, J.-C., McLauchlan, W. R. and Juge, N. (2000) High-level production of recombinant fungal endo-β-1,4-xylanase in the methylotrophic yeast *Pichia pastoris*. Protein Express. Purif. 19, 179–187.

Biely, P., Vršanská, M., Tenkanen, M. and Kluepfel, D. (1997) Endo-β-1,4-xylanase families: differences in catalytic properties. J. Biotechnol. 57, 151–166.

Blanco, J., Coque, J. J. R., Velasco, J. and Martín, J. F. (1997) Cloning, expression in *Streptomyces lividans* and biochemical characterization of a thermostable endo-β-1,4-xylanase of *Thermomonospora alba* ULJB1 with cellulose-binding ability. Appl. Microbiol. Biotechnol. 48, 208–217.

Burchhardt, G. and Ingram, L. O. (1992) Conversion of xylan to ethanol by ethanologenic strains of *Escherichia coli* and *Klebsiella oxytoca*. Appl. Environ. Microbiol. 58, 1128–1133.

Chaves, R., Almarza, C., Schachter, K., Peirano, A., Bull, P. and Eyzaguirre, J. (2001) Structure analysis of the endoxylanase A gene from *Penicillium purpurogenum*. Biol. Res. 34, 217–226.

Choi, J. H. and Lee, S. Y. (2004) Secretory and extracellular production of recombinant proteins using *Escherichia coli*. Appl. Microbiol. Biotechonol. 64, 625–635.

Cleveland, D. W., Fischer, S. G., Kirschner, M. W. and Laemmli, U. K. (1977) Peptide

mapping by limited proteolysis in sodium dodecyl sulfate and analysis by gel electrophoresis. J. Biol. Chem. 252, 1102–1106.

Coughlan, M. P. and Hazlewood, G. P. (1993) β-1,4-D-xylan-degrading enzyme systems: biochemistry, molecular biology and applications. Biotechnol. Appl. Biochem. 17, 259–289.

Coutinho, P. M. and Henrissat, B. (1999) The modular structure of cellulases and other carbohydrate-active enzymes. In: Ohmiya, K., Hayashi, K., Sakka, K., Kobayashi, S., Karita, S. and Kimura, T. (eds) Genetics, Biochemistry and Ecology of Cellulose Degradation. Uni Publishers Co., Tokyo, pp. 15–23.

Cregg, J. M. (1999) Expression in the methylotrophic yeast *Pichia pastoris*. In: Fernandex, J. M. and Hoeffler, J. P. (eds) Gene expression systems. Academic Press, Harcourt Brace & Company, London, pp. 157–191.

Cubero, B. and Scazzocchio, C. (1994) Two different, adjacent and divergent zinc finger binding sites are necessary for CREA-mediated carbon catabolite repression in the proline gene cluster of *Aspergillus nidulans*. EMBO J. 13, 407–415.

De Groot, P. W. J., Basten, D. E. J., Sonnenberg, A. S. M., Van Griensven, L. J. L. D., Visser, J. and Schaap, P. J. (1998) An endo-1,4-β-xylanase-encoding gene from *Agaricus bisporus* is regulated by compost-specific factors. J. Mol. Biol. 277, 273–284.

DeHoog, G. A. and McGinnis, M. R. (1987) The expanding realm of yeast-like fungi: proceedings of an international symposium on the perspective of taxonomy, ecology, and phylogeny of yeasts and yeast-like fungi. Elsevier Sci. Publ., Amsterdam, pp. 187.

Dekker, R. F. H. and Richards, G. N. (1976) Hemicelluloses: their occurrence, purification, properties, and mode of action. Adv. Carbohydr. Chem. Biochem. 32, 277–352.

Deshpande, M. S., Rale, V. B. and Lynch, J. M. (1992) *Aureobasidium pullulans* in applied microbiology: A status report. Enzyme Microb. Technol. 14, 514–527

Domsch, K. H., Gams, W. and Anderson, T.-H. (1980) Compendium of soil fungi. Academic Press, London, pp. 130–134.

Díaz, R., Sapag, A., Peirano, A., Steiner, J. and Eyzaguirre, J. (1997) Cloning, sequencing and expression of the cDNA of endoxylanase B from *Penicillium purpurogenum*. Gene 187, 247–251.

Felsenstein, J. (1985) Confidence limits on phylogenies: an approach using the bootstrap. Evolution, 39, 783–791.

Fernández-Espinar, M. T., Piñaga, F., Sanz, P., Ramón, D. and Vallés, S. (1993) Purification and characterization of a neutral endoxylanase from *Aspergillus nidulans*. FEMS Microbiol. Lett. 113, 223–228.

Fernándex-Espinar, M. T., Vallés, S., Piñaga, F., Pérez-González, J. A. and Ramón, D. (1996) Construction of an *Aspergillus nidulans* multicopy transformant for the *xlnB* gene and its use in purifying the minor X_{24} xylanase. Appl. Microbiol. Biotechnol. 45, 338–341.

Fujii, N. and Shinohara, S. (1987) Isolation of the microbial producing agglutinating substance. Bull. Fac. Agric., Miyazaki Univ. 34, 213–219 (in Japanese).

Fukumura, M., Sakka, K., Shimada, K. and Ohmiya, K. (1995) Nucleotide sequence of the *Clostridium stercorarium xynB* gene encoding an extremely thermostable xylanase, and characterization of the translated product. Biosci. Biotech. Biochem. 59, 40–46.

Furniss, C. S. M., Belshaw, N. J., Alcocer, M. J. C., Williamson, G., Elliott, G. O., Gebruers, K., Haigh, N. P., Fish, N. M. and Kroon, P. A. (2002) A family 11 xylanase from *Penicillium funiculosum* is strongly inhibited by three wheat xylanase inhibitors. Biochim. Biophys. Acta, 1598, 24–29.

Fushinobu, S., Ito, K., Konno, M., Wakagi, T. and Matsuzawa, H. (1998) Crystallographic and mutational analyses of an extremely acidophilic and acid-stable xylanase: biased distribution of acidic residues and importance of Asp37 for catalysis at low pH. Protein Engineering 11, 1121–1128.

de Graaff, L. H., van den Broeck, H. C., van Ooijen, A. J. J. and Visser, J. (1994) Regulation of the xylanase-encoding *xlnA* gene of *Aspergillus tubigensis*. Mol. Microbiol. 12, 479–490.

la Grange, D. C., Pretorius, I. S. and van Zyl, W. H. (1996) Expression of a *Trichoderma reesei* β-xylanase gene (*XYN2*) in *Saccharomyces cerevisiae*. Appl. Environ. Microbiol. 62, 1036–1044.

Gerard, C. (1990) Purification of glycoproteins. Methods Enzymol. 182, 529–539.

Gilkes, N. R., Henrissat, B., Kilburn, D. G., Miller, R. C. JR and Warren, R. J. (1991) Domains in microbial β-1,4-glycanases: sequence conservation, function, and enzyme families. Microbiol. Rev. 55, 303–315.

Guex, N. and Peitsch, M. C. (1997) SWISS-MODEL and the Swiss-Pdb Viewer: an environment for comparative protein modeling. Electrophoresis 18, 2714–2723.

Gurr, S. J., Unkls, S. E. and Kinghorn, J. R. (1987) The structure and organization of nuclear genes of filamentous fungi. In: Kinghorn, J. R. (eds) Gene structure in eukaryotic microbes. IRL Press, Oxford, United Kingdom, pp. 93–139.

Haas, H., Friedlin, E., Stöffler, G. and Redl, B. (1993) Cloning and structural organization of a xylanase-encoding gene from *Penicillium chrysogenum*. Gene 126, 237–242.

Hayashi, S., Yoshiyama, T., Fujii, N. and Shinohara, S. (2000) Production of a novel syrup containing neofructo-oligosaccharides by the cells of *Penicillium citrinum*. Biotechnol.

Lett. 22, 1465–1469.

von Heijne, G. (1986) A new method for predicting signal sequence cleavage sites. Nucleic Acids Res. 14, 4683–4690.

Henrissat, B. (1991) A classification of glycosyl hydrolase bnased on amino acid sequence similarities. Biochem. J. 280, 309–316.

Henrissat, B. and Bairoch, A. (1993) New families in the classification of glycosyl hydrolases based on amino acid sequence similarities. Biochem. J. 293, 781–788.

Hermanides-Nijhof, E. J. (1977) Aureobasidium and allied genera. Stud. Mycol. 15, 141–177.

Hessing, J. G. M., van Rotterdam, C., Verbakel, J. M. A., Roza, M., Maat, J., van Gorcom, R. F. M. and van den Hondel, C. A. M. J. J. (1994) Isolation and characterization of a 1,4-β-endoxylanase gene of *A. awamori*. Curr. Genet. 26, 228–232.

Ho, S. N., Hunt, H. D., Horton, R. M., Pullen, J. K. and Pease, L. R. (1989) Site-directed mutagenesis by overlap extension using polymerase chain reaction. Gene 77, 51–59.

Iefuji, H., Chino, M., Kato, M. and Iimura, Y. (1996) Acid xylanase from yeast *Cryptococcus* sp. S-2: purification, characterization, cloning, and sequencing. Biosci. Biotechnol. Biochem. 60, 1331–1338.

Iikura, H., Takashima, S., Nakamura, A., Masaki, H. and Uozumi, T. (1997) Cloning of a gene encoding a putative xylanase with a cellulose-binding domain from *Humicola grisea*. Biosci. Biotech. Biochem. 61, 1593–1595.

Ingram, L. O., Conway, T., Clark, D. P., Sewell, G. W. and Preston, J. F. (1987) Genetic engineering of ethanol production in *Escherichia coli*. Appl. Environ. Microbiol. 53, 2420–2425.

Innis, M. A., Holland, M. J., McCabe, P. C., Cole, G. E., Wittman, V. P., Tal, R., Watt, K. W. K., Gelfand, D. H., Holland, J. P. and Meade, J. H. (1985) Expression, glycosylation, and secretion of an *Aspergillus* glucoamylase by *Saccharomyces cerevisiae*. Science 228, 21–26.

Ito, K., Ikemasu, T. and Ishikawa, T. (1992) Cloning and sequencing of the *xynA* gene encoding xylanase A of *Aspergillus kawachii*. Biosci. Biotech. Biochem. 56, 906–912.

Ito, K., Iwashita, K. and Iwano, K. (1992) Cloning and sequencing of the *xynC* gene encoding acid xylanase of *Aspergillus kawachii*. Biosci. Biotech. Biochem. 56, 1338–1340.

Kaiser, C., Michaelis, S. and Mitchell, A. (1994) Lithium acetate yeast transformation. In: Methods in yeast genetics: a Cold Spring Harbor Laboratory course manual, 1994 ed. Cold Spring Harbor Laboratory Press, Cold Spring Harbor, New York, pp. 133–134.

Kimura, T., Ito, J., Kawano, A., Makino, T., Kondo, H., Karita, S., Sakka, K. and Ohmiya, K. (2000) Purification, characterization, and molecular cloning of acidophilic xylanase from

Penicillium sp.40. Biosci. Biotechnol. Biochem. 64, 1230–1237.

Kinoshita, K., Takano, M., Koseki, T., Ito, K. and Iwano, K. (1995) Cloning of the *xynNB* gene encoding xylanase B from *Aspergillus niger* and its expression in *Aspergillus kawachii*. J. Ferment. Bioeng. 79, 422–428.

Ko, E. P., Akatsuka, H., Moriyama, H., Shinmyo, A., Hata, Y., Katsube, Y., Urabe, I. and Okada, H. (1992) Site-directed mutagenesis at aspartate and glutamate residues of xylanase from *Bacillus pumilus.* Biochem. J. 288, 117–121.

Kozak, M. (1989) The scanning model for translation: an update. J. Cell Biol. 108, 229–241.

Krengel, U. and Dijkstra, B. W. (1996) Three-dimensional structure of endo-1,4-β-xylanase I from *Aspergillus niger*: molecular basis for its low pH optimum. J. Mol. Biol. 263, 70–78.

Laemmli, U. K. (1970) Cleavage of structure proteins during the assembly of the head of bacteriophage T4. Nature 227, 680–685.

Leathers, T. D. (1989) Purification and properties of xylanase from *Aureobasidium*. J. Ind. Microbiol. 4, 341–348.

Li, S., Cullen, D., Hjort, M., Spear, R. and Andrews, J. H. (1996) Development of an oligonucleotide probe for *Aureobasidium pullulans* based on the small-subunit rRNA gene. Appl. Environ. Microbiol. 62, 1514–1518.

Li, X.-L. and Ljungdahl, L. G. (1994) Cloning, sequencing, and regulation of a xylanase gene from the fungus *Aureobasidium pullulans* Y-2311-1. Appl. Environ. Microbiol. 60, 3160–3166.

Li, X.-L. and Ljungdahl, L. G. (1996) Expression of *Aureobasidium pullulans xynA* in, and secereton of the xylanase from, *Saccharomyces cerevisiae*. Appl. Environ. Microbiol. 62, 209–213.

Li, X.-L., Zhang, Z.-Q., Dean, J. F. D., Eriksson, K.-E. L. and Ljungdahl, L. G. (1993) Purification and characterization of a new xylanase (APX-II) from the fungus *Aureobasidium pullulans* Y-2311-1. Appl. Environ. Microbiol. 59, 3212–3218.

Liu, W. and Saint, D. A. (2002) A new quantitative method of real time reverse transcription polymerase chain reaction assay based on simulation of polymerase chain reaction kinetics. Anal. Biochem. 302, 52–59.

Lowry, O. H., Rosebrough, N. J., Farr, A. L. and Randall, R. J. (1951) Protein measurement with the Folin phenol reagent. J. Biol. Chem. 193, 265–275.

MacCabe, A. P., Fernández-Espinar, M. T., de Graaff, L. H., Visser, J. and Ramón, D. (1996) Identification, isolation and sequence of the *Aspergillus nidulans xlnC* gene encoding the 34-kDa xylanase. Gene 175, 29–33.

MacCabe, A. P., Orejas, M., Pérez-González, J. A. and Ramón, D. (1998) Opposite patterns of expression of two *Aspergillus nidulans* xylanase genes with respect to ambient pH. J. Bacteriol. 180, 1331–1333.

Miller, G. L. (1959) Use of dinitrosalicylic acid reagent for determination of reducing sugar. Anal. Chem. 31, 426–428.

Nelson, N. J. (1955) Colorimetric analysis of sugar. Methods Enzymol. 3, 85–86.

Ohta, K., Beall, D. S., Mejia, J. P., Shanmugam, K. T. and Ingram L. O. (1991) Genetic improvement of *Escherichia coli* for ethanol production: chromosomal integration of *Zymomonas mobilis* gene encoding pyruvate decarboxylase and alcohol dehydrogenase II. Appl. Environ. Microbiol. 57, 893–900.

O'Neill, G., Goh, S. H., Warren, R. A. J., Kilburn, D. G. and Miller, R. C. Jr (1986) Structure of the gene encoding the exoglucanase of *Cellulomonas fimi*. Gene 44, 325–330.

Pañalva, M. A. and Arst, H. N. Jr (2002) Regulation of gene expression by ambient pH in filamentous fungi and yeast. Microbiol. Mol. Biol. Rev. 66, 426–446.

van Peij, N. N. M. E., Gielkens, M. M. C., de Vries, R. P., Visser, J. and de Graaff, L. H. (1998) The transcriptional activator XlnR regulates both xylanolytic and endoglucanase gene expression in *Aspergillus niger*. Appl. Environ. Microbiol. 64, 3615–3619.

Peitsch, M. C. (1995) Protein modeling by e-mail. Biotechnology (N. Y.) 13, 658–660.

Pell, G., Szabo, L. Charnock S. J., Xie, H., Gloster, T. M., Davies, G. J. and Gilbert, H. J. (2004) Structure and biochemical analysis of *Cellvibrio japonicus* xylanase 10C. J. Biol. Chem. 279, 11777–11788.

Pitt, J. I. (1979) The genus *Penicillium* and its teleomorphic states *Eupenicillium* and *Talaromyces*. Academic Press, London, pp. 291–295.

Pugsley, A. P. (1993) The complete general secretory pathway in gram-negative bacteria. Microbiol. Rev. 57, 50–108.

Puls, J. and Schuseil, J. (1993) Chemistry of hemicelluloses: relationship between hemicellulose structure and enzymes required for hydrolysis. In: Coughlan M. P. and Hazlewood G. P. (eds) Hemicellulose and Hemicellulases. Portland Press, London, pp. 1–27.

Pérez-González, J. A., de Graaff, L. H., Visser, J. and Ramón, D. (1996) Molecular cloning and expression in *Saccharomyces cerevisiae* of two *Aspergillus nidulans* xylanase genes. Appl. Environ. Microbiol. 62, 2179–2182.

Reilly, P. J. (1981) Xylanases: structure and function. In: Hollaender, A. and Rabson, R. (eds) Trends in the biology of fermentations for fuels and chemicals. Plenum Press, New York, pp. 111–129

Saitou, N. and Nei, M. (1987) The neighbor-joining method: a new method for reconstructing phylogenetic trees. Mol. Biol. Evol. 4, 406–425.

Sambrook, J. and Russell, D. W. (2001) Molecular cloning: a laboratory manual, 3rd ed. Cold Spring Harbor Laboratory Press, Cold Spring Harbor, New York.

Sato, Y., Niimura, Y., Yura, K. and Gō, M. (1999) Module-intron correlation and intron sliding in family F/10 xylanase genes. Gene 238, 93–101.

Schmidt, A., Schlacher, A., Steiner, W., Schwab, H. and Kratky, C. (1998) Structure of the xylanase from *Penicillium simplicissimum*. Protein Sci. 7, 2081–2088.

Schwede, T., Kopp, J., Guex, N. and Peitsch, M. C. (2003) SWISS-MODEL: an automated protein homology-modeling server. Nucleic Acids Res. 31, 3381–3385.

Somogyi, M. (1952) Notes on sugar determination. J. Biol. Chem. 195, 19–23.

Strauss, M. L., Jolly, N. P., Lambrechts, M. G. and Rensburg, P. (2001) Screening for the production of extracellular hydrolytic enzymes by non-*Saccharomyces* wine yeasts. J. Appl. Microbiol. 91, 182–190.

Tahir, T. A., Berrin, J.-G., Flatman, R., Roussel, A., Roepstorff, P., Williamson, G. and Juge, N. (2002) Specific characterization of substrate and inhibitor binding sites of a glycosyl hydrolase family 11 xylanase from *Aspergillus niger*. J. Biol. Chem. 277, 44035–44043.

Thompson, J. D., Higgins, D. G. and Gibson, T. J. (1994) CLUSTAL W: improving the sensitivity of progressive multiple sequence alignment through sequence weighting, position-specific gap penalties and weight matrix choice. Nucleic Acids Res. 22, 4673–4680.

Tull, D., Withers, S. G., Gilkes, N. R., Kilburn, D. G., Warren, R. A. and Aebersold, R. (1991) Glutamic acid 274 is the nucleophile in the active site of a “retaining” exoglucanase from *Cellulomonas fimi*. J. Biol. Chem. 266, 15621–15625.

Törrönen, A. and Rouvinen, J. (1995) Structural comparison of two major endo-1,4-xylanases from *Trichoderma reesei*. Biochemistry 34, 847–856.

Törrönen, A., Harkki, A. and Rouvinen, J. (1994) Three-dimensional structure of endo-1,4-β-xylanase II from *Trichoderma reesei*: two conformational states in the active site. EMBO J. 13, 2493–2501.

Van de Peer, Y. and De Wachter, R. (1994) TREECON for Windows: a software package for the construction and drawing of environment. Comput. Applic. Biosci. 10, 569–570.

Wickerham, L. J. and Kurtzman, C. P. (1975) Synergistic color variants of *Aureobasidium pullulans*. Mycologia 67, 342–361.

Wu, S.-C., Kauffmann, S., Darvill, A. G. and Albersheim, P. (1995) Purification, cloning and characterization of two xylanases from *Magnaporthe grisea*, the rice blast fungus. Mol.

Plant-Microbe Interact. 8, 506–514.

Wymelenberg, A. V., Cullen, D., Spear, R. and Andrews, J. (1999) Regulated expression of green fluorescent protein under the control of *Aureobasidium pullulans* xylanase gene *xynA*. FEMS Microbiol. Lett. 181, 205–209.

Yanisch-Perron, C., Vieira, J. and Messing, J. (1985) Improved M13 phage cloning vectors and host strains: nucleotide sequences of the M13mp18 and pUC19 vectors. Gene 33, 103–119.

Yoshino, S., Oishi, M., Moriyama, R., Kato, M. and Tsukagoshi, N. (1995) Two family G xylanase genes from *Chaetomium gracile* and their expression in *Aspergillus nidulans*. Curr. Genet. 29, 73–80.